Osteopontin protects from autoimmunity-driven diffuse large B cell lymphoma development

Thesis

The Open University
Milton Keynes, United Kingdom

Affiliated Research Centre
Fondazione IRCCS Istituto Nazionale dei Tumori
Milano, Italia

Osteopontin protects from autoimmunity-driven diffuse large B cell lymphoma development

Thesis presented for the degree of Doctor of Philosophy
The Open University, Milton Keynes (UK)

School of Life, Health and Chemical Sciences

Celeste Rizzello
Personal Identifier: G4459242

October 2021

DECLARATION

The data presented in this thesis are original, were not previously used for any other PhD degree and were originated by myself and by the cited below collaborators. During my PhD I worked in the Molecular Immunology Unit, Department of Research, at the Fondazione IRCCS Istituto Nazionale dei Tumori. My director of studies was Dr. Claudia Chiodoni (PhD) and my Supervisors were Dr. Mario Paolo Colombo (PhD) and Prof. Claudio Tripodo (MD, PhD).

This work was supported by the Italian Ministry of Health (project RF-2016-02364121, PI Dr. Mario Paolo Colombo)

The histopathological evaluation of murine spleens was performed by Prof. Claudio Tripodo (MD, PhD) and Dr. Valeria Cancila (PhD), Tumor Immunology Unit, Department of Health Sciences, University of Palermo.

Immunohistochemistry and immunofluorescence on murine tissues included in this thesis were performed by myself with the help of Prof. Claudio Tripodo's group, when I was hosted in his laboratory in Palermo.

Immunohistochemistry on human tissues were performed by the group of Prof. Claudio Tripodo.

Immunofluorescence on cytospin preparations were performed with the support of Dr. Sabina Sangaletti (PhD), Staff Scientist of Molecular Immunology Unit.

Bioinformatic analyses were performed by Dr. Matteo Milani, bioinformatician of Molecular Immunology Unit.

All in vivo experiments were performed with the support of Dr. Laura Botti, the technician specialized in the animal manipulation and surgery.

The results collected in this thesis are included in a manuscript in preparation.

LIST OF ABBREVIATION

ABC: activated B cell

ADCC: antibody-dependent cell-mediated cytotoxicity

AIRE: autoimmune regulator gene

ALL: acute lymphoblastic leukemia

ALPS: autoimmune lymphoproliferative disorder

APS1: autoimmune polyendocrinopathy syndrome type 1

BAFF: B cell activating factor

BCR: B cell receptor

BLIMP1: B lymphocyte-induced maturation protein 1

BM: bone marrow

BSA: Bovine serum albumin

BTK: Bruton's Tyrosine Kinase

COO: cell of origin

CTLA4: Cytotoxic T Lymphocyte Antigen 4

CSR: class switch recombination

DCs: dendritic cells

DEG: differentially expressed genes

DEL: double expressor lymphoma

DHL: double hit lymphoma

DLBCL: Diffuse large B cell lymphoma

ds-DNA: double strand DNA

DZ: dark zone

ECM: extracellular matrix

ELISA: enzyme linked immunosorbent assay

EMT: epithelial to mesenchymal transition

FBS: fetal bovine serum

FcR: Fc receptor

FDC: follicular dendritic cell

FDR: false discovery rate

FFPE: formalin-fixed paraffin-embedded

FOB: follicular B

GC: germinal center

GEP: gene expression profile

GFP: green fluorescent protein

HDAC: histone deacetylase

HLA: human leucocyte antigens

HS: housekeeping

IF: immunofluorescence

IFN: Interferon

Ig: immunoglobulin

IHC: immunohistochemistry

iOPN: intracellular OPN

IRES: internal ribosome entry site

IRF: Interferon regulatory factor

LYN: LCK/YES novel tyrosine kinase

LN: lymph node

LPR: lymphoproliferation

LPS: lipopolysaccharide

LZ: light zone

MHC: major histocompatibility complex

MS: multiple sclerosis

MMP: metalloproteinase

MRL: Murphy Roths Large

MYD88: myeloid differentiation primary response

MZB: marginal zone B

MZM: marginal zone macrophages

NHL: Non-Hodgkin Lymphoma

OPN: Osteopontin

PBS: phosphate buffered saline

pDC: plasmacitoid dendritic cell

Poly I:C: polycytidylic-inosinic acid potassium salt

PRDM1: PR Domain Zinc Finger Protein 1

RA: rheumatoid arthritis

R-CHOP: Rituximab, cyclophosphamide, doxorubicin, vincristine, prednisone

RGD: arginine-glycine-aspartate

SHM: somatic hypermutation

shRNA: short hairpin RNA

siRNA: small interfering RNA

SLE: systemic lupus erythematosus

SLO: secondary lymphoid organs

sOPN: secreted OPN

SPP1: Secreted phosphoprotein 1

ss-DNA: single strand DNA

STAT: signal transducer and activator of transcription

T conv: conventional T cells

Tfh: T follicular helper

TLR: Toll-like receptor

TM: tumour

TNF: tumour necrosis factor

Treg: T regulatory cells

VDJ: variable, diversity, joining

WB: Western Blot

Table of Contents

ABSTRACT

Several studies have highlighted the association between certain autoimmune diseases and increased occurrence of hematological malignancies, such as Systemic lupus erythematosus (SLE). Patients affected by SLE have indeed a high risk of developing non-Hodgkin lymphoma (NHL), mostly diffuse large B cell lymphoma (DLBCL). Osteopontin (OPN) has been associated with SLE pathogenesis, as SLE patients have increased serum levels of OPN and often polymorphisms in *SPP1,* the gene encoding for OPN.

To study the role of this molecule in autoimmunity-associated lymphomagenesis, the $Fas^{lpr/lpr}$ mutation of the autoimmunity-prone mouse strain has been transferred onto a OPN-deficient background. Interestingly, OPN-/-$Fas^{lpr/lpr}$ mice showed a significantly higher incidence of splenic B cell lymphomas in comparison to $Fas^{lpr/lpr}$ mice. Indeed, in OPN-deficient autoimmune mice we observed an expansion of mature CD19+IgM-CD23-CD21/35- cells, which showed the typical signature of the activated type of DLBCL (ABC-DLBCL), BCL6-, BCL2+, c-MYC+, IRF4+, $Ki67^{hi}$, and a striking activation of the STAT3 pathway. Additionally, OPN-deficient autoimmune CD19+ B cells showed a baseline hyper-activation of Toll-like receptor 9 (TLR9)-dependent MYD88 signaling pathway, and were more activated when stimulated with the TLR9 agonist CpG 1826, which mimics double strand-DNA circulating in autoimmune conditions. Immunohistochemistry on splenic tissues and immunofluorescence staining on CD19+ cells showed that CD19+ B cells from $Fas^{lpr/lpr}$ mice express the intracellular isoform of OPN at the endosomal surface, where TLR9 is also located. To gain mechanistic insights, I genetically modified ABC-DLBCL cell lines, derived from lymphomatous spleens of OPN-/- mice, to over-express either the soluble (sOPN) or the intracellular isoform of OPN (iOPN). Remarkably, *in vitro* experiments showed that iOPN was able to prevent the CpG-mediated activation of STAT3 and, partially, of NFkB pathway, suggesting a negative regulatory role for iOPN in this setting. Additionally, when injected *in vivo*, while the over-expression of sOPN conferred a growth advantage over control cells, iOPN-expressing cells were less tumorigenic.

Interestingly, other than B cell-intrinsic, the molecular mechanisms at the basis of the aggressive lymphomagenesis observed in OPN-/-$Fas^{lpr/lpr}$ mice were also likely stroma-related. Indeed, mainly myeloid cell subsets of the splenic microenvironment of OPN-deficient autoimmune mice expressed more *Tnfsf13B* (encoding for BAFF) and *Il6*, both key factors for B cell survival and proliferation, in comparison with OPN-competent

counterparts. Interestingly, in lymphomatous areas of the spleen from OPN-deficient mice, a high number of infiltrating CD8+ T cells with an activated morphology was notable. However, their analysis by flow cytometry showed markers of exhaustion (TIM3 and PD1), suggesting that, despite being recruited at the tumour site, they were likely dysfunctional and unable to contrast tumour expansion.

The translational relevance of these findings comes from the analysis of ABC-DLBCL biopsies that expressed a lower *SPP1*/OPN level than GC-DLBCL counterparts, suggesting how a diminished expression of B-cell intrinsic OPN may be associated with the development of the most aggressive DLBCL. However, the existence of a specific intracellular form and/or localization of OPN in humans remains to be investigated.

Altogether, my data suggest that B cell-intrinsic iOPN is contrasting autoimmunity-driven ABC-DLBCL development, also in concert with microenvironment-related dynamics, which in an OPN-competent host seem to contribute in preventing lymphomagenesis.

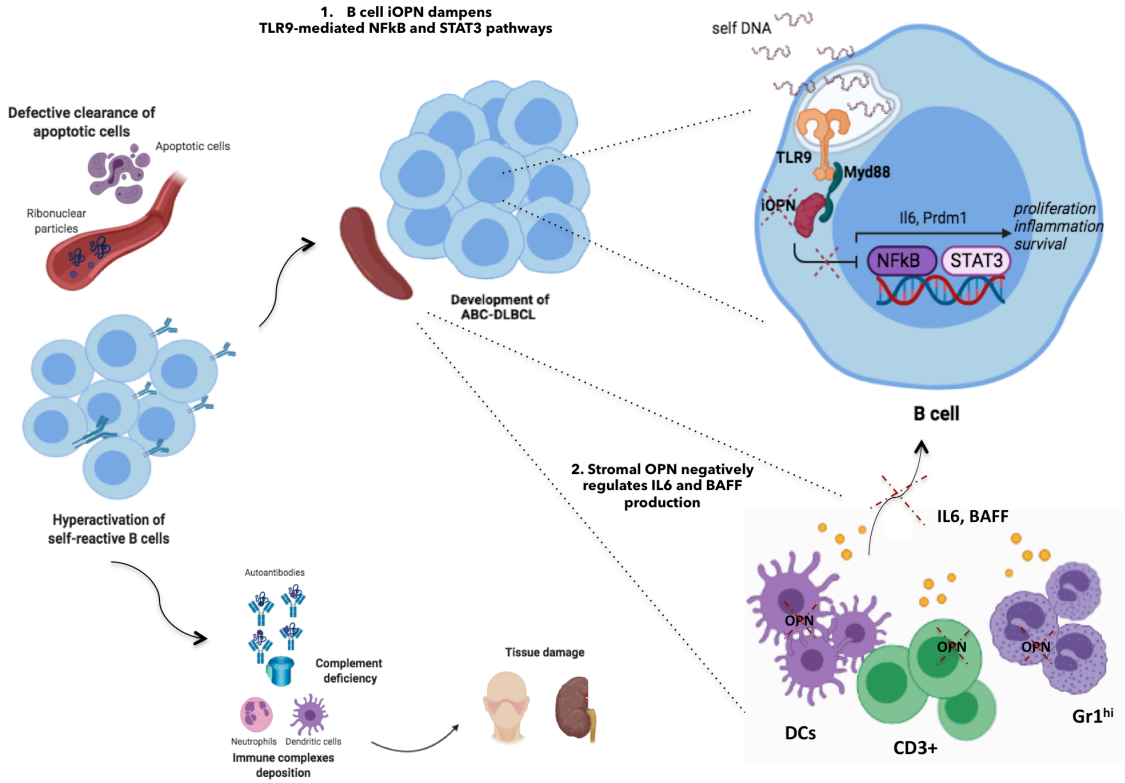

1. INTRODUCTION

1.1 Autoimmune disorders

Autoimmune disorders affect 5-8 % of the population worldwide, with approximately 75 % of patients being women [1]. So far, there have been described more or less one hundred distinct autoimmune diseases, characterized by different causes, symptoms and molecular features.

At the basis of the pathogenesis of all disorders there is a breach in the so-called "immunological tolerance", which is the ability of the immune system to prevent itself from targeting self molecules, cells or tissues. The impairment of this process leads, at the end, to tissue damage at certain sites. Indeed, according to the organs involved, autoimmune diseases are classified into organ specific (i.e. Graves' hyperthyroidism) when a single organ is interested, or systemic (i.e. Systemic lupus erythematosus), in case multiple organs are damaged.

The effector mechanisms of tissue destruction in autoimmune diseases are essentially the same of those acting in protective immunity and in hypersensitivity diseases [2]. Autoimmune disorders can be classified, according to their immune effector pathways, in type II (antibody-mediated), type III (immune complex-mediated), and type IV (T cell-mediated) diseases.

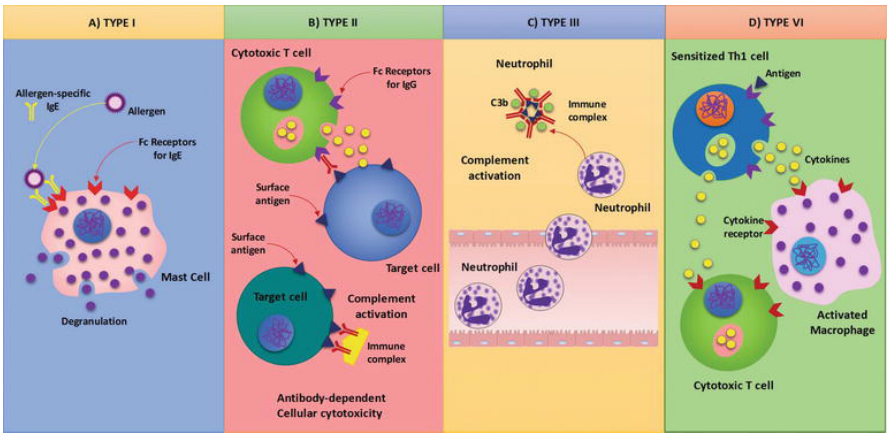

Figure 1. Immunological mechanisms of hypersensitivity diseases [2].

A common feature of autoimmune diseases is the presence of autoantibodies, whose mechanism of action is the cytotoxic destruction of cells by cell surface binding and

lysis. In this process, complement activation and/or antibody-dependent cell-mediated cytotoxicity (ADCC) are the most common pathways of destruction. As an example, in autoimmune hemolytic anemia, patients produce IgG or IgM that bind the Rh self-antigen on red cells. These cells are then rapidly cleared from the circulation by phagocytes, that interact, through their own Fc receptor, with the Fc constant region of Ig) and, through their own complement receptor, with complement system tied to IgM. Alternatively, the autoantibody-bound red cells are lysed by formation of the membrane-attack complex of complement [2].

Immune complexes are formed whenever an antibody binds to a soluble antigen. In physiological conditions, immune complexes are efficiently phagocytized by cells bearing Fc receptors and/or complement receptors, thus causing little damage. However, the immune complexes clearance could fail when a large amount of antigens, and the subsequent immune-complex deposition in blood vessels and organs, overwhelm the activity of the mononuclear phagocytic system. This is the case of systemic lupus erythematosus (SLE), an autoimmune disease caused by chronic IgG antibody production directed at ubiquitous self-antigens exposed on dead and dying cells and released from injured tissues. This leads to a continuous formation of immune-complexes, that, deposited in blood vessels and renal glomerulus, cause vasculitis and glomerulonephritis, respectively [2].

The third type of effector mechanism of damage in autoimmune diseases is mediated by effector T cells, that are specific for auto-antigens expressed through self MHC-I. As an example, in type 1 diabetes insulin-producing pancreatic beta cells are destroyed by cytotoxic T cells, that recognize insulin as non self, even though it is not the exclusive identified antigen in the pathogenesis of the disease [2,3].

Most autoimmune disorders are multifactorial diseases, as both genetic and environmental factors converge in their development. Among the rare monogenic autoimmune diseases, autoimmune polyendocrinopathy syndrome type 1 (APS1) is driven by a defect in the autoimmune regulator (AIRE) gene [4], encoding for the homonym transcription factor, which normally orchestrates the so-called “thymic education” [5]. Specifically, AIRE, expressed by the medullary thymic epithelial cells, allows them to express organ-specific proteins and to present them to thymocytes, the precursors of T cells, that, in turn, will be tolerant against these self-epitopes once they will reach the periphery. Indeed, in case of genetic abnormalities in the AIRE gene, people develop APS1, a very severe syndrome with clinical manifestations of

hypothyroidism, pernicious anaemia, type 1 diabetes, hepatitis, gastritis and alopecia [6].

The majority of autoimmune disorders are not monogenic, but rather they involve multiple genetic factors that contribute in causing the disease and that often codify for molecules playing a role in innate or in adoptive immunity. A variety of studies have shown that numerous genetic variants of the major histocompatibility complex (MHC) are associated with autoimmune diseases [7]. MHC locus encodes for molecules, termed human leucocyte antigens (HLAs), involved in antigen presentation and therefore critical in distinguishing self from non-self. To make some examples, variants of HLA-B27 are associated with ankylosing spondylitis and acute anterior uveitis, while altered sequences in HLA-DR3 can promote Graves' disease and SLE, and HLA-DR4 allele variants are risk factors for rheumatoid arthritis. Other than mutations in MHC sequence, also genetic defects in other genes with functions in immune processes can cause specific autoimmune diseases, such as mutations in genes encoding for the complement system (C3, CR4 and CR1Q units), the critical pathway for removing immune-complexes and apoptotic cells from the circulation, that are associated with SLE [8].

Additionally, also defects in Cytotoxic T-Lymphocyte Antigen 4 (CTLA-4), a receptor that switches off their inflammatory status to restore homeostasis, once they have exerted their functions, are risk factors for rheumatoid arthritis, SLE and Type 1 diabetes [9].

Remarkably, an impaired apoptosis of lymphocytes, caused by mutations in the TNF (tumor necrosis factor) family death receptor Fas and/or in its ligand FasL, can sustain the autoimmune lymphoproliferative disorder (ALPS) and SLE [10] [11]. Interestingly, a loss of function mutation in the gene encoding Fas represents the genetic basis of the syndrome of lymphoproliferation and autoimmunity characteristic of the *lpr* mouse strain, which has always been used as model for human SLE [12].

Autoimmunity can be also modulated by epigenetic mechanisms, that control gene packaging and expression independently from alterations in the DNA sequence. As an example, insulin DNA hypermethylation is associated with type 1 diabetes [13], while global acetylation of histones H3 and H4 in active CD4 T cells is a risk factor for SLE. [14].

Surprisingly, the concordance rate of autoimmune disease in monozygotic twins ranges from 12 % to 67 %, suggesting that, other than genetic dynamics, also factors environment-related are involved [15]. Environmental factors could include nutrition, microbiota, infectious agents, tobacco smoke, use of pharmaceutical drugs and heavy metals. To explore the connection between infections and autoimmunity, the example of acute rheumatic fever is very exhaustive. Genetically susceptible people may develop this disease following exposure to *Streptococcus pyogenes* [16]. The phenomenon at the basis of this pathogenesis is the so-called "molecular mimicry", in which microorganism antigens resemble host epitopes. In the specific case of acute rheumatic fever, the bacterial M protein has an amino acid sequence very similar to the human lysoganglioside, a protein expressed in kidney and heart, causing an autoimmune response and chronic damages to these organs.

The molecular mimicry is connected with another important mechanism, the "epitope spreading" [17]. This process occurs when, in such inflammatory scenario, cells damaged by virus infections and inflammatory milieu start to expose secondary self-antigens. This switch from the "dominant" epitope to neo-epitopes gives rise to the so-called "bystander activation" [18], through which it is generated an activation cascade of lymphocytes that start fighting the new antigens, fostering autoimmunity.

Additionally, smoking is by far one of the most important risk factors for rheumatoid arthritis [19] as well as for SLE [20], since cigarettes contain several Toll-like receptor (TLR)-stimulating molecules, including lipopolysaccharide (LPS), a TLR4 agonist that can elicit an innate immune response.

At present, a therapy that completely cures an autoimmune disease does not exist. Patients are usually treated with immunosuppressive drugs: glucocorticoids that suppress the whole immune system [21], methotrexate that inhibits the metabolism of folic acid in T and B cells [22], purine analogues that inhibits DNA synthesis [23], TNF and IL-6 inhibitors [24] [25] and rituximab (the anti-CD20 antibody that selectively depletes B cells) [26]. Of note, immunosuppressive drugs are known to promote severe adverse events, for example increased susceptibility to infection and augmented risk of malignancy [27].

1.1.1 Systemic lupus erythematosus

Systemic lupus erythematosus (SLE) is a rare systemic autoimmune disease with women being 9 times more susceptible than men [28]. Patients show a wide variety of

symptoms, including fatigue, fever, joint and muscle pain and the most known skin problems. Among the latter, the red “butterfly rash” across the cheeks is the most common, but also vasculitis and the development of tiny red spots (petechiae) may occur. Affected individuals could also have alopecia and ulcerations in the mucosae of the mouth, nose, or, less commonly, the genitals.

As mentioned before, SLE is a pathology mediated by immune complexes and, like all autoimmune disorders, a dysfunction of both innate and adoptive immunity is at the basis of its pathogenesis. Self-antigens (nucleic acids and their binding proteins) complexed with their cognate autoantibodies, directly contribute to the activation of both innate immune cells via Fc receptor (FcR)-mediated uptake of complexes, and B cells, through an initial engagement of the B cell receptor (BCR). Then, the nucleic acid component of these complexes engages intracellular TLRs, promoting inflammatory pathways with a subsequent activation of other innate cells and lymphocytes [2].

Although cases of monogenic lupus, caused by mutations of complement component 1q (C1q), three-prime repair exonuclease 1 (TREX1), or deoxyribonuclease 1-like 3 (DNASE1L3), do exist [29], in most cases this pathology results from a combination of multiple genetic abnormalities. Several human allelic variants have been identified as risk factors for SLE [30]. TREX1, DNASE1, autophagy related 5 (ATG5), and RAD51B encode for proteins functionally related to mechanisms of apoptosis, DNA degradation, and clearance of cellular debris, all processes involved at autoantigen formation and release. TLR7, TLR8, TLR9, Interferon regulatory factor 5 (IRF5), IRF7 and signal transducer and activator of transcription 4 (STAT4), are involved in nucleic acid sensing and type I interferon (IFN-I) production by antigen-presenting cells, events that generate a pro-inflammatory environment. Other human mutations associated with SLE affect proteins involved in T and B cell function and signaling, and include non-receptor type protein tyrosine phosphatase 22 (PTPN22), TNFSF4 (tumor necrosis factor superfamily member 4) and LCK/YES novel tyrosine kinase (LYN), molecules that decrease the activation threshold of CD4+ T and B cells upon auto-antigen encounter [31].

Interestingly, also epigenetic modifications have been linked to SLE. In particular, in T cells from SLE patients, autoimmunity-related genes, normally suppressed by DNA methylation, undergo hypomethylation, leading to protein over-expression. Among these genes, interleukin (IL)-6, IL-10, CD40L and IRF7 are noteworthy to be mentioned [32] [33]. Of note, also hypoacetylation of H3 and H4 histones have been identified in

lymphocytes from MRL/lpr lupus-prone mice [34] and in CD4+ T cells from SLE patients [14]. As an example, in human SLE T cells, which are defective in the production of IL-2, IL-2 gene is silenced by the histone deacetylase 1 (HDAC1), that, once recruited to the IL-2 promoter, acts via histone H3K18 deacetylation [35].

A deregulation in either the number or function of different immune cell populations is a well-recognised feature of SLE [36]. CD4+ T cells, for example, show compromised effector capacities, due to a severe defect in IL-2 production. On the other hand, IL-17, is massively released by CD4+, T helper (Th) 17 and autoreactive CD4-CD8-CD3+B220+ T cells, thus increasing the inflammatory response mostly via recruitment of neutrophils. A dynamic subset of T helper cells, T follicular helper (Tfh) cells, play a crucial role in SLE, since they produce IL-21, which drives B cell maturation and high-affinity autoantibodies production. Remarkably, in SLE patients and mouse models, an uncontrolled expansion of these cells, characterized by CXCR5+PD1+OX40+ICOS+ expression, is observed [37], and their abundancy in the circulation correlates with plasmablast B cell number and anti-DNA autoantibodies in patients [38]. Additionally, both human and mice affected by this disease show multiple B cell abnormalities, including B cell lymphopenia and B cell hyperactivity. In B cells from SLE patients, indeed, a pronounced activation of the BCR is observed, as a result of a strong phosphorylation of SYK and BTK [39]. Both kinases, of note, other than belonging to the BCR cascade, mediate a crass talk between BCR and TLRs, as well as BCR and JAK/STAT3 pathway.

Interestingly, another protein important for B cell activation contributing to SLE pathogenesis is MYD88, an adaptor molecule involved in TLR signaling cascades. Notably, B cells from MRL/lpr mice are dependent on MYD88 for autoantibody production [40].

Among the different innate immune populations, a reduced phagocytic activity was observed in neutrophils, despite their strong infiltration in tissues. Importantly, their presence has been linked to lupus damage via the extrusion of neutrophil extracellular trap (NETs), source of double strand DNA auto-antigens [41].

In addition, a specific subpopulation of dendritic cells, namely plasmacytoid dendritic cells (pDCs), existing both in humans and mice, play a pivotal role in SLE pathogenesis. Specifically, pDCs produce a large amount of type I interferon (IFN-I), known to directly promote T cell activation and survival [42] [43], and B cell response [44]. This IFN-α/β “signature”, indeed, is often observed in SLE patients [45].

Least but not last, a particular class of splenic macrophages, called "marginal zone macrophages" (MZMs), harboring a unique capacity to clear apoptotic cells and induce tolerogenic signals via TGF-β and IL-10, show a reduced phagocytic capacity and survival in SLE patients and lupus-prone mice [36].
From a clinical point of view, due to the heterogeneity of symptoms and pathologic processes, SLE has been one of the most challenging diseases to understand and treat and, unfortunately, most of all clinical trial have so far failed to show efficacy [46].

1.1.2 $Fas^{lpr/lpr}$ mice, a model of SLE-like syndrome

FAS, also known as apoptosis antigen 1 (APO-1), cluster of differentiation 95 (CD95) or tumor necrosis factor receptor superfamily member 6 (TNFRSF6) is a protein that is encoded by *FAS* gene, located on chromosome 10 in humans and on chromosome 19 in mice. After crosslinking with its ligand FASL, FAS receptor promotes the extrinsic pathways of programmed cell death (apoptosis) via the activation of caspase-8.
The mutation of the mouse *Fas* gene was described for the first time in 1978 by Andrews et al. [47], who, while establishing the autoimmune-prone Murphy Roths Large (MRL) mouse strain, discovered a mouse mutant showing splenomegaly and lymph-adenopathy. The identified autosomal recessive mutation was defined as *lpr* (for lymphoproliferation) and mice were termed MRL/lpr.
Interestingly, a phenotype similar to that observed in MRL/lpr mice was discovered few years later [48] and the autosomal recessive mutation responsible, termed *gld* (for generalized lympho-proliferative disease) was found to be located in *FasL* gene. The fact that severe autoimmune disorders are caused by these mutations highlights the importance of FAS-FASL interaction in lymphocyte homeostasis.
The *lpr* mutation results from the insertion of an early transposable element (ETn), similar to an endogenous retrovirus, into the intron 2 of the gene encoding *Fas* [49]. Since this ETn carries two poliA adenylation sites, transcription of *Fas* prematurely terminates in intron 2, leading to an inhibition of its expression.
The FAS defect causes an aberrant expansion in the secondary lymphoid organs (SLO), spleen and lymph nodes, of the so-called "double negative" T cells, since they do not express neither CD4 nor CD8, while retaining CD3 and B220 markers. The expansion of this population is due to an impaired "thymic education" of the auto-reactive thymocytes, that, lacking FAS, do not die through apoptosis, but survive and accumulate in the periphery [140].

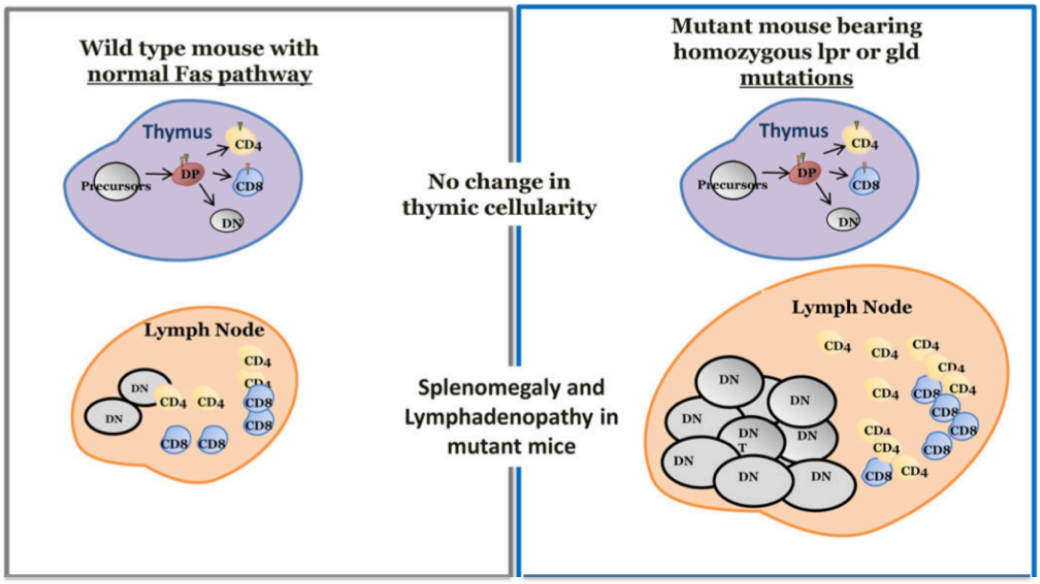

Figure 2. **Consequences of Fas mutation in Fas$^{lpr/lpr}$ mice**. [edited, 140]

It is not surprising that similar genetic defects and phenotype characterize autoimmune disorders in humans. As an example, the autoimmune lymphoproliferative syndrome (ALPS) is a consequence of mutations of FAS, FASL or other apoptosis-related molecules such as caspase 10 [50]. Interestingly, splenomegaly, lymph adenopathy, thymic enlargement and splenic infiltration of double negative (DN) T cells are hallmarks of ALPS.

MRL/lpr mouse strain is one of the best-studied models for spontaneous lupus, since these mice show many of the features observed in SLE patients. Lupus-prone mice exhibit serum autoantibodies against self-nucleic acids at about 6 weeks of age, while initial lymph-adenopathy is observed starting at 12 weeks [51].

Importantly, other than promoting SLE-like syndrome, the *lpr* mutation predisposes mice to malignant lymphomas later in life, in particular B cell malignancies [52]. This reflects the well-known and widely documented association between autoimmune disorders and hematological malignancies in humans, and allowed us study the early stages of B cell lymphomagenesis in Fas$^{lpr/lpr}$ mice, otherwise very difficult to investigate.

1.2 The association between autoimmune disorders and haematological malignancies

Over the years, several studies have pointed out that certain autoimmune and chronic inflammatory conditions, including rheumatoid arthritis, Sjögren's syndrome, SLE, psoriasis and celiac disease are associated with an increased occurrence of lymphoma [53].

As an example, in a pooled analysis of nearly 30000 patients with non-Hodgkin lymphoma (NHL) [54], SLE and Sjogren's syndrome were associated with a 2.7- and a 6.5-fold increase risk of B cell NHL, respectively. On the other hand, T-cell mediated autoimmune disorders, such as celiac disease and psoriasis, were associated with increased risk of T-cell NHL [54].

According to Smedby et al. [55], the risk of developing diffuse large B cell lymphoma (DLBCL), a specific subtype of NHL, was elevated among patients with rheumatoid arthritis, Sjögren syndrome, SLE or celiac disease. Specifically, in the case of SLE, patients affected by this disorder showed a 4.6-fold increase in all NHL and a 6-fold increase in DLBCL.

However, despite all the studies considered a huge number of patients and clearly support a link between autoimmunity and lymphomagenesis, values describing the increased risk for each disease vary considerably among studies. In addition, it is not so clear whether the risk of developing tumours concerns equally all individuals affected by a specific autoimmune disorder or changes according to phenotype and treatment. More robust, is the observation that the existing link may be related only to specific subtypes of NHL [56].

Expectedly, immunosuppressive therapies used in the treatment of autoimmune diseases have long been suspected to play a role in the development of lymphomas in these individuals, but epidemiologic studies have failed to demonstrate this "cause and effect" relationship [57]. More recently it has been investigated whether the new biological agents, especially those targeting TNF, could be the cause of the high incidence of lymphomas. While very few studies converged on this idea [58], large population-based studies have failed to demonstrate an increased risk with the use of anti-TNF drugs [59]. Indeed, the prevailing opinion is that immunomodulatory biologic agents seem not to increase the risk of lymphoma development.

About the possible mechanisms for progression of autoimmune diseases to lymphomas, the first consideration is that proliferative processes of lymphocytes in both

autoimmunity and hematologic malignancies are similar. The most prominent example is the finding that *FAS* mutations, as already mentioned, are associated with both autoimmune diseases and lymphomas in mice and in humans. Importantly, autoimmune disorders are characterized by a chronic inflammatory state due to the persisting presence of auto-antigens, leading to a massive T and B cells activation. Thus, the high proliferative rate of these cells, along with the consistent amount of cytokines secreted by the whole immune system, increase the possibility of transforming events.
Furthermore, such an inflammatory scenario induces, in the SLO microenvironment, modifications in the number, distribution, and phenotype of immune cell populations, as well as a remodeling of tissue architecture. These articulate mechanisms could be crucial in sustaining autoimmune proliferation.

1.3 B cell lymphomas

Lymphomas are a heterogeneous class of tumours generated from B cells (80 %) and less frequently from T cells (20 %) [60]. Such difference is due to the occurrence of aberrant processes, namely class switch recombination (CSR), somatic hyper-mutation (SHM) and receptor editing, involving genic alteration during B cell development, thus increasing the possibility of transforming events.
B cell development starts in the bone marrow, where lymphoid progenitors will become immature B cells, following a precise sequence of stages aimed at exposing a correct and functional B cell receptor (BCR) on the cell surface [61]. The assembly of genes for the variable region of both heavy and light chain is mediated by a process called V(D)J recombination. Specifically, the variable region of the heavy chain is formed by assembling the V (variable), D (diversity) and J (joining) segments, while those of the light chain (that can be k o λ) are assembled from V and J segments.
During the first phase, pro B cells, which do not exhibit any gene rearrangement and therefore immunoglobulin expression, become pre-B cells, characterized by the exposure of the pre-BCR, composed by a constant region associated with the surrogate light chains. Pre-B cells, after undergoing V-J rearrangement of the light chains, become immature B cells with a complete BCR. At the end, only cells that have rearranged BCR with the correct open reading frame, as well as cells with a BCR insensitive to self-antigens, survive. Indeed, newly formed B cells expressing auto-reactive BCR are removed through apoptosis or “edit” their receptor with a secondary

V(D)J rearrangement, a process termed “receptor editing” [62].

At this point, immature B cells leave the bone marrow and reach the secondary lymphoid organs (spleens, lymph nodes, mucosa-associated lymphoid tissue) where, after encountered an antigen, will definitely become mature [61]. Driven by antigen stimulation through BCR and the CD40-CD40L-mediated interaction with T cells, B cells enter the germinal center (GC) microenvironment, where they proliferate and undergo clonal expansion. In order to generate high-affinity antibodies, single-base changes are introduced by a mechanism termed SHM into the variable regions of the immunoglobulin. Concurrently, with the goal of generating a variety of antibodies with different effector properties, the immunoglobulin constant region undergoes a series of recombinations known as CSR, whereby different subclasses of antibodies (IgG, IgA or IgE) are produced. Finally, the proliferating B cells, referred as centroblasts, that produce high-affinity antibodies, either differentiate into plasma cells to suddenly secrete large quantities of antibodies, or become memory B cells, programmed to recognize antigens after future exposures.

Altogether, these processes occur in specific follicle structures, the germinal centers (GC), which are compartmentalized in two anatomically distinct areas: the dark zone (DZ), close to the T cell zone, populated by rapidly dividing centroblasts, and the light zone (LZ), which is composed by smaller non-dividing centrocytes [63,65]. The master regulator of the GC reaction is BCL6, responsible for the proliferative status of GC cells, that allows the execution of SHM and CSR and prevents a premature differentiation of GC B cells by repressing BLIMP1. B cells leave the DZ to enter the LZ, enriched in follicular dendritic cells (FDC) and T follicular helper cells (Tfh), both playing a fundamental role in promoting B cell survival and response. Here, centrocytes display an activated phenotype, including a high expression of activation markers such as CD86 and CD83. Indeed, a series of signals like crosslinking of BCR by the antigen, CD40-CD40L interaction and stimulation of TLRs activate downstream signaling cascades, such as NF-κB pathway. This leads to the expression of IRF4, that represses *BCL6* transcription, thus restoring the expression of BLIMP1, which enables plasma cell differentiation. Together, the antigen encounter and the activated phenotype indicates that LZ is the site of selection of high-affinity SHM variants [65].

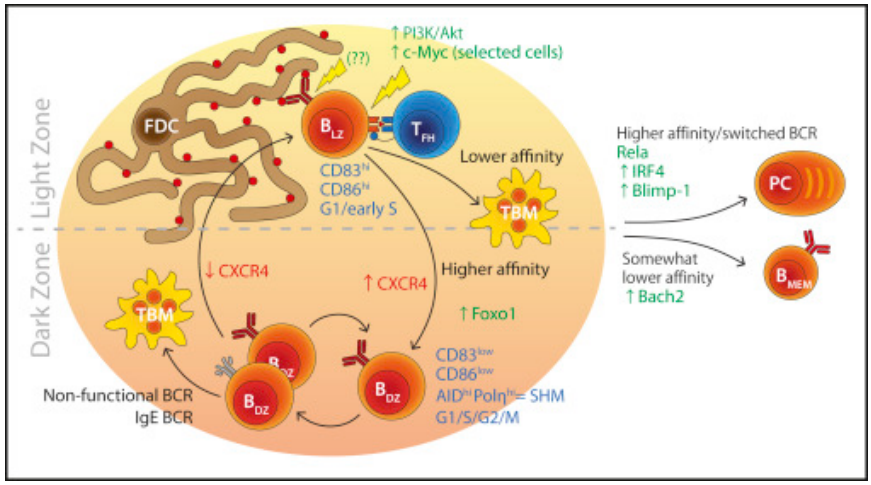

Figure 3. The dark and the light zone of the germinal center[65].

Disruption of steps in normal B cell differentiation, including V(D)J, SHM and CSR, can result in the genesis of B cell lymphomas. For example, the t(14;18) translocation involving the *IGH* and *BCL2* genes occurs from a mistake in VDJ process and results in the overexpression of BCL2 in follicular lymphoma [66]. Additionally, in Burkitt lymphoma SHM is likely involved in t(8;14) translocation of *IGH* and *c-MYC* [67], the latter brought under the control of the IG enhancer elements leading to its constitutive transcription. Furthermore, an aberrant switch recombination involving *BCL6* and *c-MYC* was found to be responsible for translocations in the activated type of DLBCLs [68].

1.3.1 Diffuse Large B cell lymphoma

B cell lymphomas comprise two categories of malignancies: the rare HL, characterized by the presence of Reed-Sternberg cells, and the more common and heterogeneous NHL.

DLBCL is the most common type of NHL worldwide, comprising 30-40 % of all new diagnoses [64]. Histologically, lymphomatous cells are large, with abundant cytoplasm and prominent round-ovoid nuclei with thick nuclear membrane and multiple nucleoli. Based on the cytological aspects, DLBCL can be divided into several variants. The most frequent variant is the centroblastic DLBCL (80 % of cases) where the cell population is composed of cells resembling the centroblasts of the GC; in the immunoblastic variant, which represents 10 % of the DLBCL, almost the entire neoplastic population is constituted by immunoblasts. Finally, in the anaplastic variant, cells are morphologically indistinguishable from anaplastic large cell lymphoma of T

cell type.

Although a substantial proportion of patients is cured by R-CHOP (Rituximab, cyclophosphamide, doxorubicin, vincristine, prednisone) immune-chemotherapy, about 40% of cases do not achieve durable remissions [64]. A reason for such a lack of success is the heterogeneity of this malignancy, both in terms of molecular pattern and clinical manifestations, other than the response to therapy. Interestingly, it was with the introduction of genome and transcriptome analysis, which allowed the recognition of multiple genetic and transcriptional signatures, that DLBCL could be classified according to different criteria, namely the cell of origin and the oncogene amplifications. Very recently, a new classification of DLBCL has been created, based on the mutational burden [69]. The most common classification refers to the cell of origin (COO), and, according to this parameter, DLBCL are subdivided into germinal center B cell-like (GCB) and activated B cell-like (ABC) subtypes, while about 15 % of cases are unclassifiable [64].

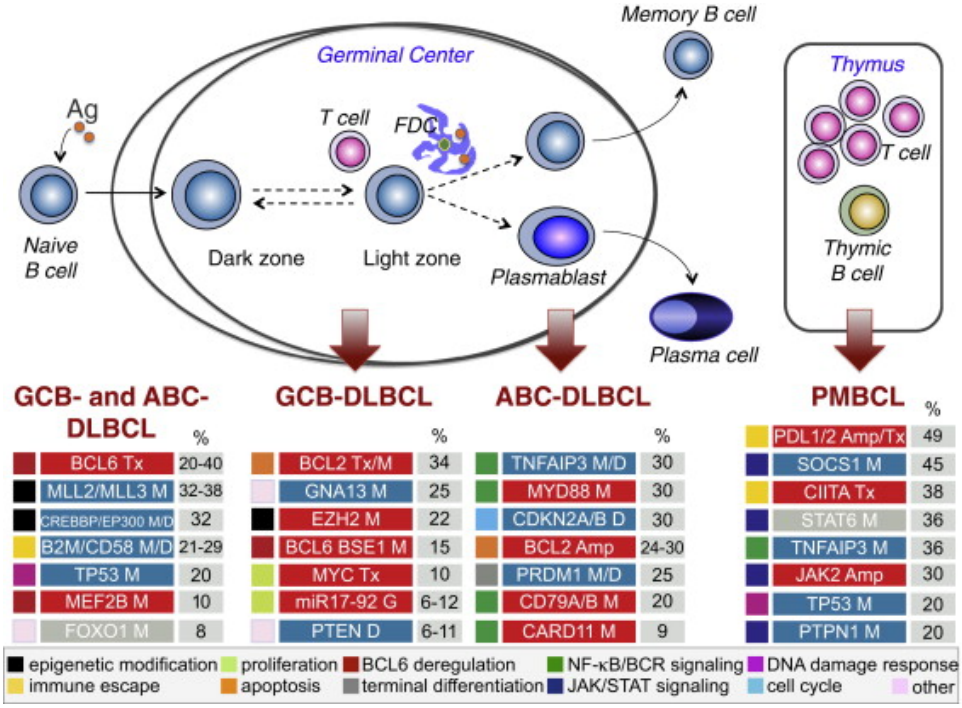

Figure 4. The genetic landscape of GC- and ABC-DLBCL [64].

The GC-DLBCL seems to be more related to light zone GC B cells [70], while ABC-DLBCL is transcriptionally more reminiscent of plasmablasts [71,72]. Specifically, GCB-DLBCLs display high-level expression of CD10 and BCL6 and harbor hyper-mutated immunoglobulin genes with ongoing SHM, while ABC-DLBCLs show

activation of NFkB and BCR signaling pathways, and an up-regulation of genes, such as IRF4, required for plasmacytic differentiation.

Although GC- and ABC-DLBCL have a distinct genetic landscape, the two subtypes may share some abnormalities [64]. As an example, 30 % of cases, with some preference for GC-DLBCLs, harbor mutations and/or deletions inactivating the acetyltransferase CREBBP, while about one third of DLBCLs show mutations in the MLL2 gene, which encodes for the homonym methyltrasferase. Notably, chromosomal rearrangements of the BCL6 locus characterize as many as 35 % of DLBCL, with ABC-DLBCL patients being from two to three times more susceptible. Furthermore, in more or less 30 % of cases, the beta-2-microglobulin (B2M) gene, encoding for a subunit of the HLA- I complex, is mutated or deleted, as a mechanism of immune surveillance escape [64].

As concern genetic lesions specific for the GC type of DLBCL, about 40% and 10-14 % of patients harbor the chromosomal translocations of BCL2 and MYC, respectively. In addition, 10 % of GC-DLBCL patients show deletion of the tumor suppressor PTEN, while in about 22 % of cases mutations in the histone methyltransferase EZH2 have been reported [64].

Among the genetic aberrations characterizing ABC-DLBCL patients, it is not surprising that mutations leading to a chronic activation of both BCR and NFkB signaling pathways are very common. In particular, CD79A is mutated in 20 % of ABC-DLBCL patients, as well as CD79B, to a lesser extent. Of note, in about 9 % of ABC-DLBCL, activation of BCR and NF-κB is sustained by oncogenic mutations of the CARD11 gene, the major component of the “signalosome” complex [64]. Importantly, also the adaptor molecule MYD88, which participates in the signal transduction of most TLRs, is affected by gain-of-function mutations in its TIR domain (L265P substitution) in one third of ABC-DLBCLs. Least but not last, more or less 25 % of patients have lost BLIMP1 due to mutations or deletions of its gene (PRDM1), or because of the constitutively active, translocated BCL6 gene [64].

A further method for classifying DLBCL is based on BCL2 and C-MYC gene expression. Specifically, DLBCL are referred as “double hit” lymphomas (DHLs) when rearrangements of both genes are present, while in the so called “double expressor” lymphoma (DELs) BCL2 and C-MYC are overexpressed at protein level, without genetic translocations [73].

The C-MYC-related t(8;14) translocation is classically associated with Burkitt

lymphoma, a very aggressive and fast-growing lymphoma, whereas the BCL2-related t(14;18) translocation is the genetic hallmark of follicular lymphoma and leads to a drug-resistant phenotype with increased cancer cell survival. However, these translocations are not specific. Rearrangement of C-MYC also occurs in about 25–30 % of DLBCL, whereas that of BCL2 appears in 10-15 % of patients affected by this disease. “Double hit” DLBCLs, in which both rearrangements coexist, account for approximately 5-7 % of all DLBCL cases and are characterized by a refractory disease and short survival [73].

“Double expressor” DLBCL, on the other hands, accounting for one third of all DLBCL cases, are defined as lymphomas with increased expression of C-MYC and BCL2 proteins by immunohistochemistry, in the absence of detectable translocation by fluorescence in situ hybridization (FISH). They do not form a distinct clinicopathological entity in the World Health Organization (WHO) classification, but offer additional information about markers associated with a poor outcome. [74].

Additionally, the two described classifications, the COO-related and the oncogene amplification-based, somehow overlap, at least to some extent. Indeed, more DEL have gene expression profiles consistent with the activated B-cell subtype of DLBCL, whereas most DHLs are GC-DLBCL [73,74].

It is widely recognized that patients with the ABC subtype of DLBCL have significantly poorer outcomes to R-CHOP therapy than GC-DLBCL patients [75]. Efforts to improve treatment efficacy in patients affected by the ABC disease have been made by combining immune-chemotherapy with biologic agents targeting BCR and NFkB signaling pathways [76]. Examples are Ibrutinib, an irreversible inhibitor of Bruton's Tyrosine Kinase (BTK) belonging to the BCR cascade, and bortezomib, a proteasome inhibitor thought to prevent proteosomal degradation of IkB, inhibitor of NFkB.

In cases of relapsed diseases, especially of DHLs, the potent regiment of immune-chemotherapy R-EPOCH (Rituximab, etoposide, prednisone, vincristine, cyclophosphamide, and doxorubicin) is often beneficial and it may also be combined with autologous stem cell transplantation (ASCT) [77].

A new and more comprehensive understanding of DLBCL molecular aberrations was described in 2018 by Schmitz et al., who investigated 574 DLBCL biopsies using exosome and transcriptome sequencing, DNA copy-number analysis and targeted

amplicon resequencing [69]. Interestingly, authors identified four genetic subtypes of DLBCL, based on the patient mutational burden: MCD (with the co-occurrence of MYD88 L265P and CD79B mutations), BN2 (according to BCL6 fusions and NOTCH2 mutations), N1 (with NOTCH1 mutations) and EZB (characterized by EZH2 mutations and BCL2 translocations).

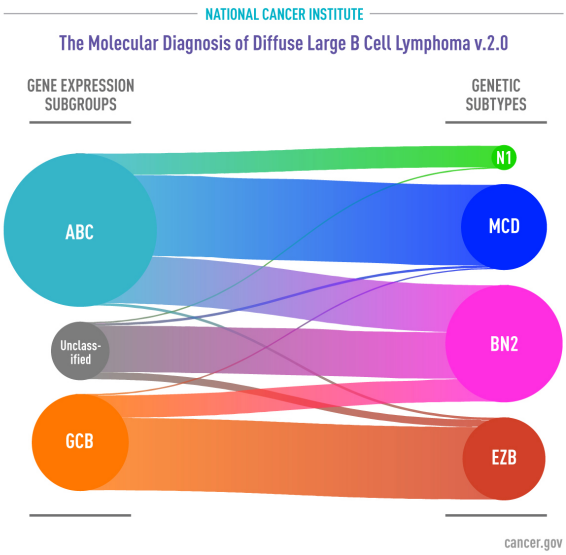

Figure 5. The mutational burden-based classification of DLBCL [69].

When combining this mutation-based classification with the classical one based on the cell of origin, MCD and N1 were primarily ABC DLBCLs, EZB comprised mostly GCB DLBCLs, and BN2 included ABC, GCB, and unclassified cases. Of note, the authors were able to better characterize unclassified DLBCL cases (neither GC- nor ABC-type). In line with the already described worst prognosis of ABC-DLBCL patients, better outcomes were found in the BN2 and EZB subtypes, while poorer outcomes in the MCD and N1 subtypes.

1.4 MYD88 and its role in SLE and lymphomas

To detect microbes and self-derived molecules released from damaged cells, the innate immune system uses the so-called "pattern-recognition receptors" (PRRs) that recognize "pathogen-associated molecular patterns" (PAMPs) and damage-associated molecules patterns (DAMPs) [78]. PRRs activate downstream signaling pathways that trigger an immediate innate immune response, as well as an antigen-specific adaptive immunity. Among the different classes of PRRs, Toll-like receptors were the first to be identified, and are therefore the best characterized. While some TLRs are located on the

cell surface, others show an intracellular (endosomal) compartmentalization. The TLR family includes 10 members (TLR1–TLR10) in human and 12 members (TLR1–TLR9, TLR11–TLR13) in mouse. The downstream signaling pathways of most TLRs are mediated by the adaptor molecule MYD88 (myeloid differentiation primary response 88) [79].

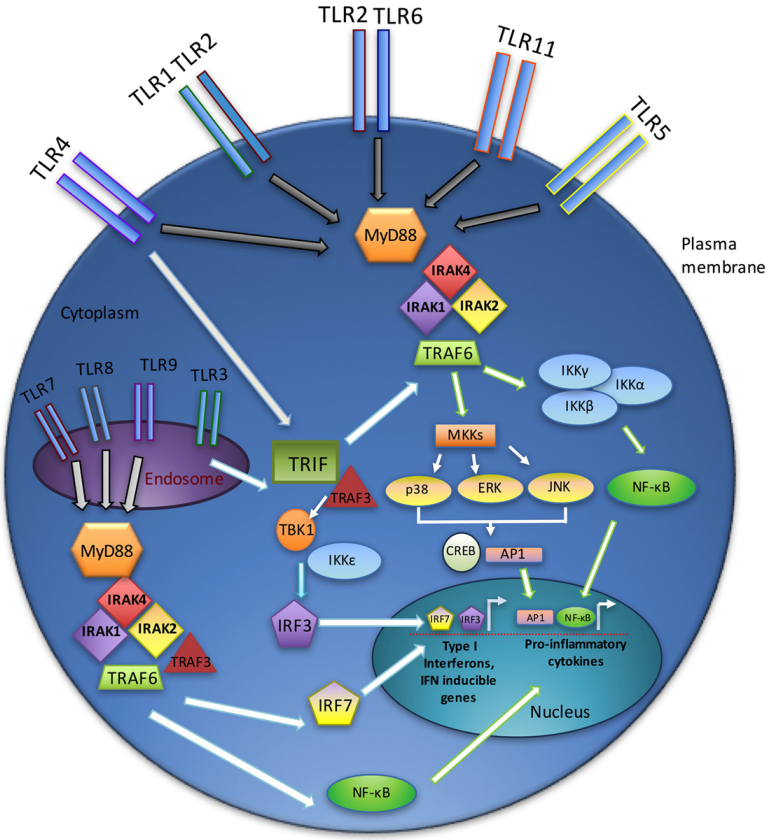

Figure 6. An overview of TLR signaling cascades [79].

MYD88 structure includes the C-terminal TIR (Toll IL-1R) domain, which mediates the interaction with other TIR domain-containing proteins (receptors or adaptors), and the N-terminal death domain (DD) that associates with the IRAK family members through homotypic DD interactions. An intermediate (INT) domain links the TIR and DD.

Except from TLR3, which requires TRIF as scaffold-protein for mediating its signaling, MYD88 mediates all TLR signaling cascades. After TLR engagement, MYD88 forms a complex with IRAK kinase family members, referred to as the Myddosome. During Myddosome formation, IRAK4 activates IRAK1, which is then autophosphorylated at several sites and released from MYD88. IRAK1 associates with the ubiquitin ligase TRAF6, that promotes polyubiquitination of both TRAF6 itself and the TAK1 protein kinase complex. TAK1 then activates two different pathways that lead to activation of the IKK complex-NF-κB pathway and -MAPK pathway. The IKK complex

phosphorylates the NF-κB inhibitory protein IκBα, which undergoes proteasome degradation, allowing NF-κB to translocate into the nucleus to induce proinflammatory gene expression. TAK1 also activates MAPK family members such as ERK1/2, p38 and JNK, which mediate activation of AP-1 family transcription factors. Among the transcribed genes, *IL-6*, *IL1β*, *TNF-α*, and *IFN-I* are worth noting [79].

Also, MYD88 plays a crucial role in physiological B cell response, as it is required for antibodies production [80]. More importantly, TLR9-MYD88 axis is highly active in the context of SLE, both in humans and mice. Firstly, the endosomal TLR9 recognizes unmethylated CpG sequences in DNA molecules, that are massively released by SLE patients, as well as by lupus-prone mice. Additionally, TLR9-MYD88 signaling promotes autoantibodies class switching to pathogenic IgG2a and 2b in patients [81] and lupus-prone mice lacking TLR9 developed a more severe clinical disease [82] [83].

As previously mentioned, gain-of-function mutations of MYD88 have been found to sustain lymphomagenesis, especially in the ABC type of DLBCL [84]. In particular, Staudt's group reported that 29 % of ABC DLBCL tumours harbored the same amino acid substitution, L265P, in the MYD88 TIR domain at an evolutionarily invariant residue in its hydrophobic core. MYD88-L265P promoted cell survival by spontaneously assembling a protein complex containing IRAKs, thus activating NF-κB signaling, JAK/STAT3 pathway and secretion of IL-6, IL-10 and interferon-β.

Importantly, it has been demonstrated that SYK, a component of the BCR signaling, co-localizes with MYD88 in MYD88-mutated B cell-lymphomas, driving pro-survival signals [85].

1.5 Blimp1 and human lymphomas

B-lymphocyte-induced maturation protein 1 (BLIMP1) is a transcriptional repressor encoded by PR Domain Zinc Finger Protein 1 (PRDM1) gene and its structure includes zinc finger DNA-binding domains, a proline-rich region (PR) and an acidic region [86].

BLIMP1 is essential for the terminal differentiation of B cells into plasma cells, as demonstrated by the fact that mice with B cell conditional knockout (KO) of PRDM1 failed to produce plasma cells and serum immunoglobulins [87]. While during the GC stage of B cell development its premature transcription is prevented by BCL6, a master regulator of the GC reaction, BLIMP1, in turn, orchestrates plasma cell differentiation through a controlled inhibition of a broad spectrum of GC-related molecules [88].

Among its targets, BLIMP-1 represses c-MYC, which explains the cessation of cell cycle in plasma cells, the MHC class II transactivator CIITA, leading to a downregulation of MHC-II in plasma cells, and PAX5, which is required for CSR in GCs.

Interestingly, the expression of BLIMP1 is known to be induced by MYD88-related pathways, as LPS-stimulated B cells from MYD88-/- mice show decreased expression levels of PRDM1 [89]. In line with this, BLIMP1 is transcriptionally regulated by NFkB [90]. Furthermore, BLIMP1 is a well-known target of STAT3 signaling pathway [91].

BLIMP1 is inactivated at gene level in nearly 25 % of ABC-DLBCL patients, who harbor PRDM1 homozygous deletions, truncating or missense mutations. However, BLIMP1 could be also transcriptionally repressed by constitutively active BCL6 [92]. Furthermore, *in vivo*, conditional deletion of *Blimp1* in mouse B cells promotes the development of lymphoproliferative disorders recapitulating critical features of the human ABC-DLBCL. In light of all these findings, BLIMP1 may be referred as a tumor suppressor and indeed its absence correlates with the upregulation of genes involved in B cell receptor signaling and cell proliferation (i.e. C-MYC), and with the poor prognosis of ABC-DLBCL patients [93].

Surprisingly, BLIMP1 expression was reported in a sizable fraction of DLBCL, which displayed more aggressive behavior and shorter failure-free survival [94]. These tumors, however, co-expressed BCL-6 and MUM1/IRF4, confirming that PRDM1 expression was insufficient to drive the full genetic program associated with plasmacytic differentiation.

A further study investigated *PRDM1* transcript variants in 82 DLBCL patients [95]. PRDM1 has two isoforms: PRDM1α and PRDM1β, generated from the same gene by alternative transcription. PRDM1β differs from PRDM1α by lacking the N-terminal 101 amino acids and having a disrupted PR domain, thus losing repressive function on multiple target genes. Notably, using laser micro-dissection combined with reverse transcription–polymerase chain reaction (RT-PCR) amplification, the authors found that both *PRDM1α* and *PRDM1β* transcripts were expressed in lymphoma cells only in the non-GC subtype of DLBCL. Of note, PRDM1β was correlated with short survival in non-GC patients treated with CHOP but not with R-CHOP. Indeed, *in vitro*, B lymphoma cells resistant to chemotherapy expressed PRDM1β, that was suppressed when treated with rituximab, concomitantly with NFkB inactivation.

1.6 Osteopontin

Osteopontin (OPN) is a glycosylated phosphoprotein that is expressed in a variety of cells, namely macrophages, neutrophils, dendritic cells, NK cells, T and B lymphocytes, as well as epithelial cells and fibroblasts [96]. It was originally identified as a bone matrix protein and subsequently identified as a cytokine (Eta-1) produced by activated T cells and transformed cell lines [96]. Additionally, OPN is a significant component of the extracellular matrix (ECM), where it interacts with specific elements including collagen, fibronectin and calcium (due to its Ca2+ binding sequence), thereby regulating matrix interactions and cell adhesion [97].

OPN is able to interact with ubiquitously expressed multiple cell surface receptors that mediate many physiological and pathological processes. Among these, OPN promotes cell survival, inflammation, adhesion, migration and, more generally, it has been associated with bone formation, wound healing, autoimmune disorders and tumorigenesis.

1.6.1 Osteopontin structure

OPN is a highly negatively charged protein lacking extensive secondary structure and it belongs to the SIBLING (Small Integrin-Binding Ligand, N-linked Glycoprotein) family. It is encoded by *SPP1* gene, located on chromosome 4 in humans and 5 in mice. OPN is a 33kDa protein, being composed by more or less 300 amino acids. However, a wide range of post-translational modifications, including phosphorylation, O-linked glycosylation, sulfation and sialylation, increase its molecular weight to around 44Kda [96].

Near the center of OPN sequence there is an arginine-glycine-aspartate (RGD) domain, a motif common to many extracellular matrix proteins and known to engage several integrins. OPN also contains an aspartate-rich region, two heparin-binding sites, proteolytic cleavage sites for thrombin and metalloproteinases, and, near the C-terminus, a region that binds CD44 [96]. Via the RGD sequence, OPN interacts with a variety of integrins, including αvβ1, αvβ3, αvβ5, αvβ6, and α5β1 [98]. The thrombin-mediated cleavage of OPN allows the exposure of a cryptic integrin binding site (SVVYGLR in human, SLAYGLR in mouse). The N-terminal fragment of OPN has been described to sustain processes like cell adhesion, spreading and migration, by

promoting the adherence of cells, mostly leukocytes, expressing α4β7 and α9β1 integrins.

Furthermore, OPN interacts with two specific variants of the receptor CD44, namely v6 and v7, mediating a loop which stimulates its own transcription and accumulation of the protein on the cell surface [96].

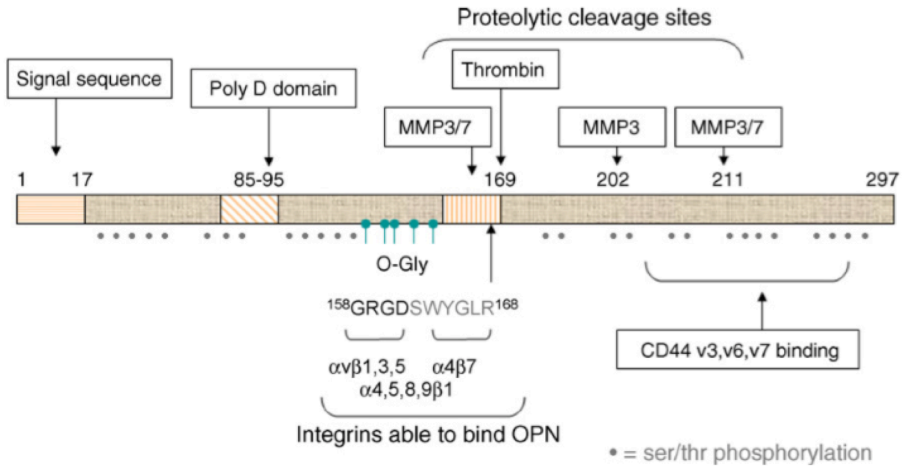

Figure 7. Osteopontin structure [96].

1.6.2 The secreted and the intracellular isoforms of OPN

OPN has always been studied as a secreted protein (sOPN), as it is released by the expressing cells into body fluids. However, recently it has been identified in mouse an intracellular isoform of the protein (iOPN), firstly described by Sodek's group in rat calvarial cells [99]. Using confocal microscopy, the authors found two patterns of OPN distribution: a perinuclear (Golgi reticulum) for sOPN, and a perimembrane distribution for iOPN. Surprisingly, iOPN was also found in cytoplasm [100] as well as in the nucleus, being associated to MYD88 [101] or BCL6 [102].

Importantly, the intracellular isoform of OPN does not derive from an alternative splicing of *Spp1* gene. Indeed, iOPN differs from sOPN because of its non-AUG translation start site, located downstream that of the full-length protein. Thus, in the structure of iOPN the sequence leading to the secretory vesicles is missing, so that cells do not secrete the protein in the extracellular space [103].

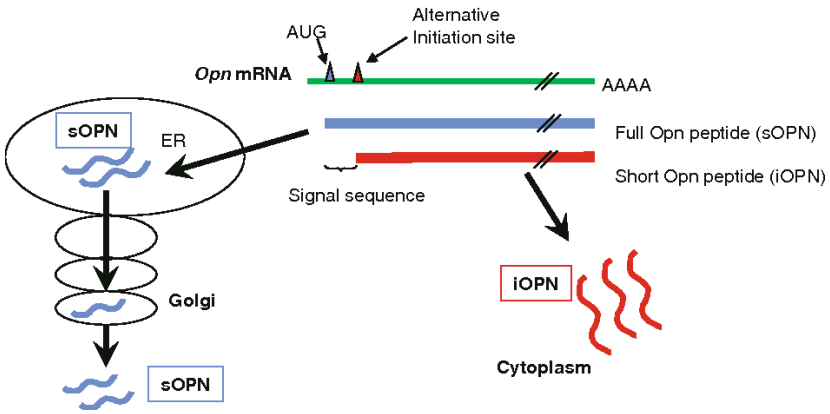

Figure 8. The secreted and the intracellular isoform of OPN [103].

Additionally, iOPN exists as an integral component of a CD44-ezrin/radixin/moesin (ERM) complex located in the internal region of the plasmatic membrane, being a player in cell motility and fusion [103].

The sOPN-integrin axis promotes NFkB activation via Ras and Src [104]. NFkB, on the other hand, regulates the expression of many inflammatory cytokines, including OPN [105]. Additionally, CD44 engagement by OPN mediates the activation of PI3K/AKT/β-catenin pathway [106] [107], that, in turns, promotes the transcription of *SPP1* gene.

Also, iOPN not only functions as an adaptor or scaffold protein in signal transduction pathways, but also stabilizes other intracellular proteins. Indeed, in T follicular helper and T follicular regulatory cells, Cantor's group discovered an ICOS-mediated interaction between p85α regulatory subunit of PI3K and iOPN, followed by nuclear translocation of the latter, its interaction with Bcl-6 and protection of Bcl-6 from ubiquitin-dependent proteasome degradation [102]. Interestingly, the co-localization of iOPN and the scaffold protein Myd88 has been described in different cell types and contexts, but with contradictory results: while iOPN was found to promote TLR9-mediated IFN-α production in plasmacitoid dendritic cells [108], overexpression of iOPN in OPN-deficient macrophages strongly suppressed production of NFkB-transcribed pro-inflammatory cytokines after stimulation with cellular debris [101]. Moreover, iOPN interacts with and stabilizes TRAF3, adaptor molecule belonging to the TLR3 signaling cascade, thus promoting IRF3 activation, IFN-β production and antiviral response [109].

1.6.3 OPN regulation

As previously mentioned, OPN expression is promoted by several pathways [110], mostly oncogenic, namely NFkB, PI3K/AKT/β-catenin, Hedgehog and estrogen receptor (ER) signaling cascade. Indeed, Ramchandani and Weber discovered a polymorphic site, in position −443 of the *SPP1* promoter, that showed differences between ER-positive and ER-negative breast cancers [111].

Among the several cis-regulatory elements identified in *SPP1* promoter, a Ras-activated enhancer (RAE) is bound by Ras-response factor (RRF), when Ras signaling pathway is stimulated [110]. Furthermore, T cell factor-4 (Tcf-4) binds the Tcf-4 binding site, retarding OPN transcription [110]. Additionally, the −94 to −24 region of the human SPP1 promoter is able to bind a variety of known transcription factors, including Sp1, Myc and Oct-1 [110].

On the other hand, to counteract OPN expression, there are many repressors that negatively regulate its transcription, for example Breast cancer metastasis suppressor 1 (BRMS1), the transcriptional repressor RUNX3, and wild type BRCA1, that acts by impounding OPN trans-activators [110].

1.6.4 OPN functions

Although sOPN and iOPN recognize and bind different partners, thus promoting distinct pathways, both isoforms participate in immune-related processes, and, in some cases, their functions are overlapping and synergistic.

OPN main immune-modulatory function is the enhancement of Th1 over Th2 immunity through two general mechanisms. Specifically, while the N-terminal region of OPN interacts with the αvβ3 integrin to induce pro-inflammatory IL-12, the C-terminal sequence of the protein binds to CD44, leading to the suppression of the anti-inflammatory cytokine IL-10 [112]. Furthermore, among CD4+ T cells, Spp1 mRNA is expressed in Th1, but not in Th2 subset [113], and this is in line with the notion that OPN gene expression in activated T cells is regulated by T-bet, a transcription factor important tor T cell commitment [114].

As concerns the role of OPN in B cells, in the 90's Cantor's group demonstrated that OPN is important for B cell activation and antibody production in MRL/lpr mice [115]. Additionally, the involvement of OPN in B cell development was also demonstrated by data showing that its deficiency prevented the expansion of lymphocytes in skin, spleen

and lymph nodes in a model of imiquimod-induced psoriasis [116].
Importantly, Benchang Guo et al. reported that OPN expression in B cells is regulated by both the classical BCR signaling (PI3K-, phospholipase C- and PKCβ-dependent) and the non-classical, IL4-triggered, BCR cascade (Lyn-dependent). Going deeply, while stimulating the canonical BCR signaling with anti-Ig did not increase the level of *Spp1*/OPN in murine B cells, [117], triggering both the canonical and non canonical BCR cascades with anti-Ig and IL4, respectively, allowed follicular B and marginal zone B cells to express and secrete OPN.

OPN activity, specifically mediated by its N-terminal fragment, has been described also in the regulation of the hematopoietic stem cell niche in which OPN expression is restricted to the endosteal region of the bone marrow and exterts a negative role on hematopoietic stem cell proliferation [118].
Interestingly, a study from Shinohara's group reported that, upon Candida infection or T cell-mediated colitis, sOPN and iOPN exert different role in skewing myeloid versus lymphoid population balance in the bone marrow [119]. Specifically, iOPN was able to promote apoptosis through the downregulation of survivin expression and the enhancement of pan-caspase activities in myeloid progenitors, while sOPN increased the population size of lymphoid cells.
Remarkably, phagocytic cells produce high levels of OPN mRNA but do not secrete OPN as much as activate T cells do, tending to store OPN in the cells [113].
Overall, based on the reported literature it seems that sOPN and iOPN participate mainly in adoptive and innate immunity, respectively.

1.6.5 OPN and autoimmune disorders

In line with its role in promoting inflammatory responses, the detrimental role of OPN in mediating a wide range of autoimmune diseases has long been described [120].
In patients affected by SLE, for example, OPN is a cytokine massively secreted in the blood and its abundance correlates with disease severity and poor outcome [121]. Indeed, high OPN levels are associated with the presence of autoantibodies against nucleic acids, elevated IFN-α levels in the serum and renal damage [122]. The relationship between OPN and SLE has also been confirmed at genetic level, since OPN polymorphisms are associated with specific clinical features of the disease, such as thrombocytopenia and hemolytic anemia, renal disease and opportunistic infections,

lymphadenopathy, high serum levels of IgE and IFN-α [123] [124]. Notably, also the lupus-prone MRL*lpr*/*lpr* mice, show an high secretion of OPN, that begins at the onset of autoimmunity and positively correlates with the symptom severity [125], which is also influenced by polymorphisms in OPN gene [126]. Also, Ciocchetti et al. proposed that OPN may contribute to the disease by inhibiting lymphocyte apoptosis, worsening the mutation-driven Fas defect [127]. Interestingly, Weber and Cantor highlighted a dual and opposite role of OPN during the progression of the disease in mice with the *lpr* mutation [128]. At early stages, OPN induces polyclonal B cell activation and isotype switching, leading to IgG, IgM and IgA production, thereby sustaining the pathology. On the contrary, during the late phases, OPN prevents further exacerbation of the disease by inhibiting the production of Th2 cytokines IL-10 and IL-4 [96].

In multiple sclerosis (MS) OPN is one of the most prominent cytokines expressed within lesions (especially during relapses), blood and cerebrospinal fluid of patients. In particular, the thrombin- and metalloproteinase-cleaved OPN fragments play a crucial role in mediating the recruitment of autoimmune T cells in MS lesions. In addition, genetic analyses have associated variations of the OPN gene with the disease as well [120]. In the mouse model of MS, the experimental autoimmune encephalomyelitis (EAE), where the pathology is mediated by myelin specific autoreactive T cells, administration of OPN to OPN-deficient mice worsened the disease by inducing relapse and neurological defects [96].

As a further illustration, rheumatoid arthritis (RA) is a chronic autoimmune disease characterized by an inflammatory attack of the joint space, site where several cytokines are highly expressed, including OPN, together with IL-1 and TNF-α [120]. Moreover, high levels of OPN have been reported in the peripheral blood of RA patients and have been associated with disease severity [120]. Importantly, OPN transcript is strongly expressed in CD4+ synovial T cells and correlates with co-expression of certain OPN receptors, including αv and β1 integrin chains and CD44. Although some studies did not find any association between OPN polymorphisms and susceptibility to RA, Ceccarelli et al. discovered a correlation between a specific SNP in the *SPP1* promoter and the susceptibility to the disease [129]. As demonstrated in the collagen-induced arthritis (CIA) model of RA, OPN recruits inflammatory cells to arthritic joints. Indeed, treatment of arthritic mice with an antibody against the SLAYGLR sequence, exposed after thrombin-mediated cleavage of OPN, decreased immune cell infiltration at the joint sites, proliferation of synovium and development of bone erosions [130].

1.6.6 OPN and cancers

If OPN plays beneficial roles in physiological processes like wound healing, bone homeostasis, and ECM functions, OPN is a cardinal mediator of tumor-associated inflammation and metastatic dissemination. Indeed, OPN has been widely implicated in the development and progression of several types of cancer and, in most cases, high expression levels of OPN or its specific isoforms are associated with poor prognosis [96] [131].

Indeed, several studies have demonstrated the correlation between elevated OPN secretion and advanced tumor stage in breast cancer, prostate cancer, squamous cell carcinoma, melanoma, osteosarcoma and gliobastoma [110,131]. Other than mediating the previously described signaling pathways that promote cell survival and proliferation, OPN exerts a crucial role in a wide range of processes referred as "hallmarks" of cancer.

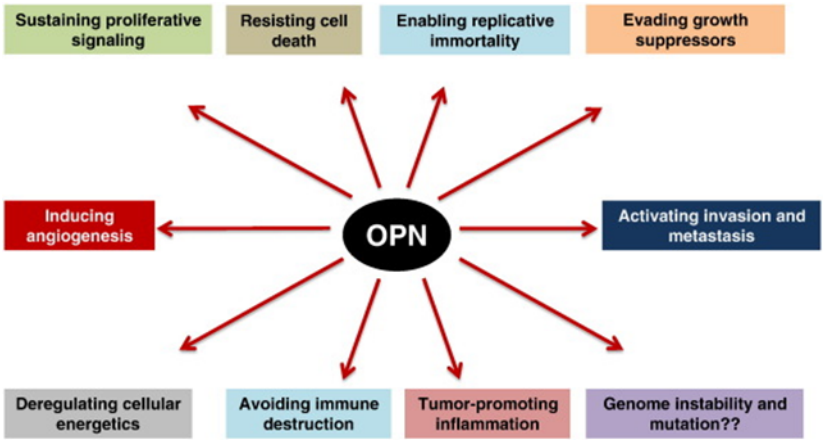

Figure 9. The association between OPN and the hallmarks of cancer [110].

As far as angiogenesis is concerned, one of the described mechanisms involving OPN relies on its high affinity for αvβ3, whose cascade is essential for endothelial cell survival. Also the association between OPN and cancer metastasis has been studied in several types of cancer, such as melanoma, colorectal and lung cancer [119, 131]. Notably, through an approach consisting in *Spp1* silencing in the 4T1 breast cancer cell line and the use of OPN-deficient mice, Sangaletti et al. found that tumor-intrinsic OPN protects breast cancer cells from apoptosis within the blood stream (anoikis), whereas myeloid cell-derived OPN, likely in its intracellular form, regulates their immunosuppressive activity in the local metastatic niche [132].

Epithelial-to-Mesenchymal Transition (EMT), the process in which epithelial cells revert back to their mesenchymal phenotype, is a further hallmark of cancer OPN has been associated with. There are three main types of EMT: type 1 refers to embryogenesis, type 2 is related to wound healing, and type 3 concerns cancer metastasis. OPN has been shown to play a crucial role in mediating type 2 and 3 EMT, the latter mainly in breast, hepatocellular carcinoma and colorectal cancer [131]. In particular, OPN can directly regulate the expression of EMT-related transcription factors including Twist, Snail and Slug. Furthermore, OPN is able also to indirectly activate Twist via hypoxia-inducible factor-1 alpha (HIF-1α), thus enhancing cell migration and invasion.

In addition, autophagy, the catabolic process occurring in stress conditions and in which cellular organelles are degraded by lysosomes, has been shown to promote chemo-resistance in some cancers. Remarkably, OPN was found to promote resistance to chemotherapeutic agents in pancreatic cancer, hepatocellular carcinoma and breast cancer by inducing NFkB, integrin αvβ3/MEK/ERK and PI3K/AKT pathways, respectively [131].

In line with all these findings, it is not surprising that the current research indicates that OPN inhibition would be a good therapeutic approach, particularly in a context of metastatic diseases [133]. Indeed, an increasing body of literature exploited the application of OPN inhibition in different cancers and experimental settings. In particular, small interfering RNA (siRNA) and short hairpin RNAs (shRNAs) against OPN showed high stability, resistance to immunogenicity and high efficacy in low dose [133]. Moreover, also the efficacy of molecules like aptamers and antibodies, both aimed at disrupting OPN binding to its receptor CD44 and integrins, was evaluated as a potential therapeutic strategy.

1.6.7 Human OPN splicing variants

In human, OPN precursor-mRNA (pre-mRNA) is subject to alternative splicing, which generates three splice variants, OPN-a (consists of all seven exons), OPN-b (which lacks exon 5) and OPN-c (which lacks exon 4). Since the expression of OPN splice variants in malignancies is cell-type and/or tissue specific, this may influence the potential role of OPN in distinct tumours and as cancer biomarker [134]. However, conflicting evidence exists regarding the expression and function of the different OPN

isoforms in different solid tumours. A variety of studies are in agreement with the notion that OPN-c is the variant mainly expressed in malignant tissues rather than the healthy ones. As an example, OPN-c was found to be selectively expressed in breast cancer tissue and to be inversely correlated with E-cadherin, an established tumour suppressor. Moreover, high levels of OPN-c staining in breast tumours are associated with tumour stage, recurrence and metastasis [134]. Additionally, it has been shown that OPN-c supports anchorage-independent growth via the expression of oxidoreductases [134].

On the other hand, it has been demonstrated that hepatocellular carcinoma tissues predominantly expressed OPN-a and OPN-b rather than OPN-c. In line with this work, OPN-a was found to be the most expressed isoform in lung cancer biopsies and cell lines [135]. Functionally, the authors described how OPN-a promotes angiogenesis by stimulating endothelial cells, likely by binding to the αvβ3 integrin and increasing VEGF expression and secretion.

1.6.8. OPN and hematological malignancies

While OPN functions have been deeply explored in the context of solid tumours, less is known about its contribution to lymphoid malignancies. Generally speaking, OPN was found to be highly expressed in hematological diseases, such as primary central nervous system lymphomas (PCNSL, a DLBCL confined to the CNS) and in bone marrow blasts of acute myeloid leukemia (AML) patients [136,137]. As concerns PCNSL, SPP1 gene was found to have a 10-fold increase in PCNSLs when compared to non-CNS DLBCLs [136]. Furthermore, OPN overexpression was also been reported in an aggressive subset of DLBCL characterized by a poor outcome [136]. From a pathogenic point of view, OPN was found to mediate invasion and dissemination of CNS lymphomas through the activation of metalloproteinases (MMP) via NFkB [136]. Notably, Rolf Mesters' study described how OPN is overexpressed in the bone marrow of AML patients compared with healthy individuals, and more importantly, that the protein is an independent prognostic marker in this disease [137]. In addition, OPN has also been involved in resistance to chemotherapy in acute lymphoblastic leukemia (ALL), since Boyerinas et al. demonstrated that stroma-derived protein, when localized to the endosteal region of the bone marrow, was able to adhere to ALL clones supporting their dormancy and insensitivity to cytotoxic agents [138].

Taken together, these findings indicate that OPN not only represents a potential biomarker for several lymphoproliferative diseases, but also exerts multifaceted roles in the pathogenesis of these tumours.

2. AIM OF THE STUDY

While OPN is widely described as a pro-inflammatory and pro-tumorigenic molecule, involved in the pathogenesis of autoimmune disorders and solid tumours, the role of this protein in B cell malignancies is poorly described.

The aims of my PhD project are:

-Deciphering the role of OPN in lymphoma development associated with an autoimmune condition (mice prone to develop a SLE-like syndrome) and investigating whether a specific isoform of the protein (soluble vs intracellular OPN) is relevant in this process.

-Investigating B cell-intrinsic and stromal-related dynamics at the basis of the autoimmunity-driven malignancy, also taking advantage from engineered cell lines and OPN+/+ and OPN-/- hosts.

-Translating the findings obtained with the spontaneous mouse model in the human setting, investigating the role of OPN in lymphoma biopsies.

3. MATERIALS AND METHODS

3.1 Animals

BALB/c mice were purchased from Charles River Laboratories. C57BL/6 *spp1*$^{-/-}$ mice (B6.129S6(Cg)-Spp1^{tm1Blh}/J were purchased from the Jackson laboratory and backcrossed on BALB/c background for 10 generations, obtaining BALB/c;Spp1^{tm1Blh} animals [132]. MRL/MpJ-Fas^{lpr}/J mice were originally purchased from the Jackson Laboratory and crossed with BALB/c mice for 10 generations to obtain BALB/c;Tnfrsf6lpr strain (referred as Fas$^{lpr/lpr}$). Fas$^{lpr/lpr}$ mice were crossed with BALB/c;Spp1^{tm1Blh}, obtaining OPN-/-Fas$^{lpr/lpr}$ animals (BALB/c;Spp1^{tm1Blh} x Tnfrsf6lpr). Only female mice were used for this study. Animals were maintained in pathogen-free conditions in our animal facility. Autoimmune mice (Fas$^{lpr/lpr}$ and OPN-/-Fas$^{lpr/lpr}$) were sacrificed for autoimmunity and lymphoma analyses between 4 and 6 months. Immunodeficient CNCr-*Foxn1*^{nu} mice (nu/nu) were maintained and crossed at the Fondazione IRCCS Istituto Nazionale dei Tumori (Milan, Italy). All animal experiments were approved by the Institutional Ethics Committee for Animal Use and by the Italian Ministry of Health (authorization number 1026/2016-PR and 419/2021-PR) and were performed following to the 3Rs' recommendations (Reduction, Refinement and Replacement).

3.2 Cell lines

The lymphoma cell lines OPL239 and OPL241 were established in our laboratory by *in vitro* seeding of cell suspension from the lymphomatous spleens of two 6-month-old OPN-/-Fas$^{lpr/lpr}$ mice. Cell lines were cultured in RPMI-1640 (Lonza, #12-115F), supplemented with 10% FBS (Euroclone, #ECS0180L), non-essential amminoacid (NEAA) mixture (Lonza, #13-114E), Hepes (Lonza, #17-737E), Na pyruvate (Lonza, #BE13-115E) and 51 μM β-mercaptoethanol (Sigma, #M7522).

3.3 Evaluation of autoimmunity in Fas$^{lpr/lpr}$ and OPN-/-Fas$^{lpr/lpr}$ mice

Swelling of neck, axillary and inguinal lymph nodes was evaluated using a caliper. Both the number and the volume (mm^3) were considered for the analysis. The percentage of autoimmune CD3+B220+ T cells was calculated by flow cytometry analysis on fresh

spleen and blood samples. Histopathological evaluation of spleen architecture was performed by a pathologist.

3.4 ELISA on mice sera

The serum was isolated from the blood through a thermal shock (incubation at 37 °C for 30 min and at 4 °C for 1 h) followed by a centrifugation at 13000 rpm for 1 min. Supernatants (sera) were stored at -20 °C. ELISA on sera was performed to test the amount of autoantibodies against circulating self ssDNA (Società Italiana Chimici, #5310) and dsDNA (Società Italiana Chimici, #5110), using pre-coated plates. To evaluate the serum level of OPN in OPN-sufficient mice, the DuoSet kit for mouse Osteopontin (R&D System, #DY441) was used.

3.5 Evaluation of lymphoma by histopathology

Autoimmune mice were sacrificed at 4-6 months of age and *hematoxylin* and *eosin* staining was performed on *formalin-fixed paraffin-embedded (FFPE)* spleen sections to evaluate the presence of lymphomatous cells**.** Histopathological analyses were performed according to the criteria for lymphoid neoplasm classification by the pathologist [139].

3.6 Flow cytometry

To identify and phenotypically characterize splenic B cells, mouse spleens were mechanically disaggregated using the bottom of a syringe, treated with ACK (Ammonium-Chloride-Potassium) solution to lyse red blood cells and cell suspensions were stained with the following monoclonal antibodies:

Marker	**Fluorochrome**	**Company**	**Clone**	**Catalogue n°**
CD19	FITC	BD	CL1D3	557398
B220	PE	BD	RA3-6B2	561868
IgM	PE-Cy7	eBioscience	Eb121-15f9	25-5890-82
CD3	APC	eBioscience	145-2c11	17-0031-82
TLR9	FITC	eBioscience	M9.D6	11-909382
CD86	PE	eBioscience	GL1	12-0862-82
Ki67	PE-Cy7	eBioscience	solA15	25-5698-82

To discriminate the different splenic B cell populations, mouse spleens disaggregated as described were stained with the following monoclonal antibodies:

Marker	Fluorochrome	Company	Clone	Catalogue n°
IgD	FITC	eBioscience	11-26c	11-5993-82
CD23	PE	eBioscience	B3B4	12-0232-82
CD21/35	PerCP-Cy5.5	BioLegend	7E9	123416
CD93	APC	eBioscience	AA4.1	17-5892-82
CD19	APC-eFluor780	eBioscience	Eb101D3	47-0193-82
CD3	BV510	BD	145-2c11	563024

Spleens from BALB/c, OPN -/-, $Fas^{lpr/lpr}$ and OPN-/-$Fas^{lpr/lpr,}$ as well as spleens from mice injected with DLBCL cell lines, were also analysed for the presence of the different immune cell populations, besides B cells, using antibodies against specific cell markers.

For myeloid cells, the following mixture was used:

Marker	Fluorochrome	Company	Clone	Catalogue n°
CD11c	FITC	eBioscience	N418	11-0114-85
CD11b	PE	TONBO	M170	50-0112-U100
CD3	PerCP-Cy5.5	TONBO	145-2c11	65-0031-U100
F4/80	PE-Cy7	BioLegend	BM8	123114
B220	APC	eBioscience	RA3-6B2	17-0452-82
LY-6C	BV421	BD	AL21	562727
GR-1	BV510	BD	RB6-8C5	563040

For lymphoid cells, the following antibodies were used:

Marker	Fluorochrome	Company	Clone	Catalogue n°
CD25	FITC	BioLegend	3C7	101908
CD8	PE	TONBO	2.43	50-1886-U025
FOXP3	PerCP-Cy5.5	eBioscience	FJK-165	45-5773-82
CD3	BV510	BD	145-2c11	563024
CD4	BV650	BD	RM4-4	740-446
CD3	FITC	eBioscience	145-2c11	11-0031-82
CD8	PE-Cy7	TONBO	2.43	60-1886-U100
Ki67	APC	BioLegend	16A8	652405
TIM-3	BV421	BD	5D12/TIM3	747026
PD1	BV711	BD	RPM1-30	748265

To assess the phenotype of DLBCL cell lines, cells were stained with the following antibodies:

Marker	Fluorochrome	Company	Clone	Catalogue n°
CD19	FITC	BD	CL1D3	557398
B220	PE	BD	RA3-6B2	561868
IgM	PE-Cy7	eBioscience	Eb121-15f9	25-5890-82
TLR9	FITC	eBioscience	M9.D6	11-909382
IgD	BV510	BD	11-26c.2A	563110
IgA	FITC	BD	c10-3	559354
CXCR4	PerCP-efluor710	eBioscience	2B11	46-9991-82

Samples were acquired on a LSRFortessa flow cytometer (BD) and analysed using FlowJo software.

3.7 Immunohistochemistry and immunofluorescence on murine and human tissues

Tissues were collected for fixation in 10% neutral buffered formalin overnight, washed in distilled water and paraffin-embedded. Four-micrometers-thick sections were deparaffinized, rehydrated and unmasked using Novocastra Epitope Retrieval Solutions, either pH6 (Leica Biosystem, #RE7113-CE), or pH9 (Leica Biosystem, #RE7119-CE) in thermostatic bath at 98°C for 30 minutes. Subsequently, the sections were brought to room temperature and washed in PBS. After that, slides underwent neutralization of the endogenous peroxidase with Novocastra Peroxidase Block (Leica Biosystems, #RE7101), and Fc bloking with Novocastra protein block (Leica Biosystems, #RE7102). Then, samples were incubated with primary antibodies. For multiple-marker immunostainings, sections were subjected to sequential rounds of single-marker staining and the binding of the primary antibodies was revealed by the use of specific secondary antibodies conjugated with different fluorophores or enzymes.
The following primary antibodies were adopted for IHC and IF:

Antibody	Company	Clone	Catalogue n°
Rat α-BCL6	Abcam	7D1	ab243150
Rabbit α-c-MYC	Abcam	Y69	ab32072
Rabbit α-CD4	CST*	D7D2Z	25229
Rabbit α-CD8α	CST	D4W2Z	98941
Rabbit α-F4/80	CST	D2S9R	70076

Rabbit α-Ki67	Abcam	Polyclonal	ab15580
Rabbit α-MPO	Abcam	Polyclonal	ab9535
Rabbit α-OPN	Abcam	EPR21138	ab218237
Rabbit α-PAX5	Abcam	EPR3730	ab109443
Rabbit α-ph-STAT3 (Tyr 705)	Millipore	EP2147Y	04-1059
Rabbit α-OPN (human)	Abcam	Epr3688	ab91655

CST*: Cell Signaling Technologies

After incubation with HRP-conjugated IgG (H&L) specific secondary antibodies (Life Technologies), signals were revealed with Novocastra DAB Chromogen (Leica Biosystems, #RE7105) in its Novocastra DAB Substrate Buffer (Leica Biosystems, #RE7106).

Double immunohistochemical staining was performed by applying SignalStain®Boost IHC Detection rabbit alkaline phosphatase-conjugated (Cell signaling technology, #18653) and Vulcan Fast Red chromogen kit (Bio-optica, #FR805M) as substrate-chromogens.

Anti-mouse and anti-rabbit Alexa Fluor 488- and 568-conjugated secondary antibodies were used for fluorescence detection.

At least 5 human samples per group were used. Slides were analyzed under a Zeiss Axioscope A1 microscope equipped with four fluorescence channels widefield IF. Microphotographs were collected using a Zeiss Axiocam 503 Color digital camera with the Zen 2.0 Software (Zeiss). Slide digitalization was performed using an Aperio CS2 digital scanner (Leica Biosystems) with the ImageScope software.

3.8 Gene Expression Profile on mouse CD19+ cells

We collected spleens from 5-month-old $Fas^{lpr/lpr}$ mice (without signs of lymphoma), 5-month-old OPN-/-$Fas^{lpr/lpr}$ mice (that showed initial lymphomatous foci) and the few 8 month-old $Fas^{lpr/lpr}$ and OPN-/-$Fas^{lpr/lpr}$ mice (both showing an overt lymphoma) that were able to survive that far. As controls, we collected also spleens from 5-month-old BALB/c and OPN -/- mice. CD19+ cells were purified through immunomagnetic beads anti-CD19 (Miltenyi, #130-121-301). 5 mice per group were used for this experiment.

RNA extraction was performed using Quick-RNA Microprep (Zymoresearch, #R1051) and its purity and yield were assessed using NanoDrop 2000c spectrophotometer (Thermofisher scientific). RNA samples were processed for microarray hybridization

through Agilent Technologies Scanner G2505C US11103886 by the Functional Genomics core facility at Fondazione IRCCS Istituto Nazionale dei Tumori, Milan. Raw data were imported in R software through read.maimages function from limma packages. Data were normalized through normalizeBetweenArrays function from limma package with method cyclicloess. Filtering and collapse were applied on probes, in particular the 95% percentile of the negative control probes was computed on each array. Probes that were at least 10% brighter than the negative controls on at least 5% of arrays were kept. Average expression of replicated probes were computed and then collapse with collapseRows function from WGCNA package (with method maxRowVariance) was performed. Class comparison was performed through limma package from Bioconductor for each pair of comparison, and p-value was corrected through Benjamini and Hockeberg method (BH). Pathway analysis was made through package pathfindR with REACTOME database with genes that were resulted significant (FDR < 0.05) from the previously described class comparison.

3.9 RNA SCOPE

RNA scope on fresh murine spleen sections was performed using RNAscope 2.5 HD Detection Reagent-BROWN (Advanced Cell Diagnostic) in accordance with the manufacturer's protocol. Mouse *Prdm1* (#441871) was used as probe.
Novocastra DAB Chromogen (Leica Biosystems, #RE7105) in its Novocastra DAB Substrate Buffer (Leica Biosystems, #RE7106) was used to reveal signals.

3.10 RT-qPCR

RNA extraction was performed using Quick-RNA Microprep (Zymoresearch, #R1051) and its purity and yield were assessed using NanoDrop 2000c spectrophotometer (Thermofisher Scientific). RNA was reverse transcribed using High Capacity cDNA Reverse Transcription Kit (Thermofisher, #4368814); the 20 µl reaction for RT-qPCR was prepeared using TaqMan Fast Universal PCR Master Mix no Amperase UNG (Thermofisher, #4352042) and run on a QuantStudio 3 instrument (Thermofisher). Primers and probes were synthesized by IDT or Applied Biosystems (AB).
The following probes were used:

Gene name	Company	ID probe
Gapdh	IDT	Mm.PT.39.a1
Bcl2	IDT	Mm.PT.58.7362966
Bcl6	IDT	Mm.PT.58.32669842
c-myc	IDT	Mm.PT.58.13590978
Irf4	IDT	Mm.PT.58.31041885
Spp1	IDT	Mm.PT.58.43709208
Gapdh	AB	Mm99999915_91
Il6	AB	Mm00446190_m1
Prdm1	AB	Mm00476128_m1
Tnf6f13b (Baff)	AB	Mm_00446347_m1
Tnf α	AB	Mm00443258_m1

Gene expression levels were normalized through the comparison with mouse *Gapdh* expression. The expression values are referred as $2^{-\Delta CT}$.

3.11 Evaluation of MYD88 signaling pathway in mouse CD19+ cells and DLBCL cell lines

CD19+ cells were isolated from mouse spleens using Microbeads anti-CD19+ (Miltenyi, #130-121-301) and the purity of cells was assessed by flow cytometry using an antibody against CD19 (CD19 FITC (BD, clone CL1D3, #557398). For western blot analysis, $2x10^6$ cells were seeded in 6-well plates and stimulated for 1h. For flow cytometry analysis and RT-qPCR $1x10^6$ cells were seeded in 12-well plates and stimulated for 3 days. The following TLR agonists were used: the TLR4 agonist LPS (Lipopolysaccharides from Escherichia coli O111:B4, Sigma, #L4130) (1 µg/ml), the TLR9 agonist CpG 1826 (TriLink Biotechnologies, #I66-G01A) (5 µg/ml), the TLR3 agonist Poly I:C (Polycytidylic-inosinic acid potassium salt, Sigma, #P1038) (5 µg/ml). After stimulation cells were collected and washed in PBS. Dry pellets were stored at -80 °C for western blot analysis, while fresh samples were stained with the different antibodies for flow cytometry analysis of activation (CD19 FITC, BD, clone CL1D3, #557398 and CD86 PE, eBioscience, clone GL1, #12-0862-82).

To evaluate TLR9-MYD88 cascade in OPL239/OPL241 DLBCL cell lines, $1,5\ x10^6$ cells were seeded in 6-well plates and stimulated with 5 µg/ml CpG (TriLink Biotechnologies, #I66-G01A) for 30 minutes (Western Blot), 3h and 6h for RT-PCR.

Then, cells were washed in PBS and dry pellet were stored at -80°C for Western Blot and RT-PCR analysis.

3.12 Western blot analysis

Cells were lysed in ice for 20 min using RIPA buffer, added with phosphatase (Phosphostop, Roche, #04906837001) and protease (Complete, #11836153001) inhibitor cocktails, and 1mM PMSF. Lysates were then centrifuged at 13000 rpm for 20 min and the supernatants containing proteins were stored at -80°C. Proteins were quantified through Pierce BCA Protein Assay Kit (Thermofisher, #23225) and optical density evaluated by Spark Multimode microplate reader. An equal amount of proteins (20 µg) was run on SDS-PAGE on NuPAGE 4-12% pre-casted minigels (Invitrogen, #NP0321BOX) and proteins were transferred to 0.45µm nitrocellulose membrane (Amersham, #10600002). Nonspecific binding sites were blocked in PBS containing 0.1 % Tween 20 (Sigma, #P2287-500ML) and 5 % BSA (Sigma, #A7906-100G).
Membranes were incubated overnight at 4 °C with the following antibodies:

Antibody	**Company**	**Clone**	**Catalogue n°**
Rabbit α-β-ACTIN	Sigma	A2066	090M4758
Rabbit α-BCL2	CST*	D17C4	34985
Rabbit α-c-MYC	CST	D84C12	56055
Rabbit α-IRAK1	CST	D51G7	45045
Rabbit α-IRAK4	CST	Polyclonal	43635
Rabbit α-IRF4/MUM1	Abcam	Polyclonal	ab104803
Rabbit α-MYD88	Abcam	Polyclonal	Ab2064
Goat α-OPN	Sigma	Polyclonal	07635-1MG
Rabbit α-ph-p65 (Ser536)	CST	93H1	3033
Rabbit α-p65	CST	D14E12	#82426
Rabbit α-ph-STAT3 (Y705)	CST	D3A7	#91456
Rabbit α-STAT3	CST	79D7	4904T

*CST: Cell Signaling Technologies

After incubation, membranes were washed three times, for 10 min each, in PBS containing 0.1 % Tween 20, and then incubated for 30 min at room temperature with the following secondary antibodies: Rabbit anti-goat (Invitrogen, #811620) and Donkey anti-rabbit (Invitrogen, #A16035).

After washing, blots were developed with Clarity Western ECL Substrate (Biorad, #1705061) and images were acquired using Chemidoc XRS system (Biorad). Quantification was made with ImageJ64.

3.13 Sorting of immune populations from mouse spleens

To assess *Spp1*, *Tnfsf13b* and *Il6* expression in the different immnune populations, spleens from 3/4-month-old BALB/c, OPN-/-, Fas$^{lpr/lpr}$ and OPN-/-Fas$^{lpr/lpr}$ mice (a pool of 3 animals per group) were mechanically disaggregated using the bottom of a syringe. Then, cell suspensions were divided in two samples, to be separately stained in order to obtain lymphoid and myeloid populations. Flow cytometry panel for lymphoid cells comprised the following antibodies:

Marker	**Fluorochrome**	**Company**	**Clone**	**Catalogue n°**
CD19	FITC	BD	CL1D3	557398
CD3	PE	TONBO	145-2c11	50-0031-u500
CD8	PerCP-Cy5.5	TONBO	53-6.7	65-0081-U100
CD4	APC	TONBO	RM4-5	20-0042-U100
B220	APC-Cy7	BD	RA3-6B2	552094

On the other hand, to separate myeloid cells, splenocytes were labeled with:

Marker	**Fluorochrome**	**Company**	**Clone**	**Catalogue n°**
F480	FITC	TONBO	BM8.1	35-4801-U500
CD169	PE	eBioscience	SER-4	12-5755-82
CD11c	PerCP-Cy5.5	BD	HL3	560584
GR-1	PE-Cy7	eBioscience	RB6-8C5	25-5931-81
CD11b	APC	eBioscience	M1/70	17-0112-83
B220	APC-Cy7	BD	RA3-6B2	552094

Sorted cells were collected in 10% FBS RPMI supplemented with β-mercaptoethanol and 2 mM EDTA, washed in PBS and then dry pellets were stored at -80°C. From dry pellets RNA was extracted and RT-PCR was performed.

3.14 Vector construction and lentiviral particles production

Lentiviral vectors containing the sequences encoding either for the full-length (Spp1-IRES Green) or the intracellular isoform (iOPN-IRES Green) of mouse OPN, were

obtained by cloning the Spp1 full-length sequence (from pUC57-Spp1 plasmid, from DBA Italia) or the iOPN sequence (kind gift from ML. Shinohara, Durham, North Carolina) into the lentiviral backbone pLVX-IRES-ZsGreen1. The empty pLVX-IRES-ZsGreen1 was used as control.

The production of lentiviral particles was performed using a third-generation packaging system involving the transfection of 293T producer cells. In particular, $5x10^6$ cells were seeded in 150mm plates using 10% FBS Iscove's IMDM (Lonza, #12-722F) and, the day after, a co-transfection was carried out using $CaCl_2$ of four plasmids: 16,25 µg of pMDLg/pRRE, 6,25 µg of pRSV-REV, 8,75 µg of envelope plasmid (pMD2-VSV-G) and 25 µg of the lentiviral vector with the gene of interest. After 24 h, the supernatant was removed and fresh medium was added. The next day supernatants containing viral particles were collected, centrifuged at 1500 rpm for 5 min to exclude residual cells and passed through a 0.45 mm filter.

3.15 Overexpression of sOPN and iOPN in DLBCL cell lines

$2x10^5$ cells were resuspended in the viral supernatants and seeded in 6-well plates. After 24 h the medium was changed and, two days later, the percentage of infected cells was assessed by flow cytometry evaluating the percentage of GFP+ cells. GFP+ cells were sorted to obtain a pure population of GFP-expressing cells. To confirm the expression of OPN at transcript level, $1x10^6$ cells were seeded in 6-well plates and RNA was extracted the day after, while to check the protein level of either sOPN or iOPN, $1,5x10^6$ cells were seeded in 6-well plates with or without the inhibitor of protein secretion BFA (Brefeldin A from Penicillium brefaldianum, Sigma, #B7651-5MG) at the concentration of 5µg/ml for 3 hours. Cells were collected for western blot analysis.

3.16 Immunofluorescence on cytospin preparations

To perform immunofluorescence on cytospin preparations $6x10^4$ cells were deposited on glass slides through centrifugation. The day after, cells were fixed with paraformaldehyde 4% in PBS for 10 minutes and, after a fast wash in PBS, permeabilized with Triton-X100 (SIGMA, #T8787-100ML) 0.1% in PBS for 10 minutes.

For OPN staining, after a washing step, cells were blocked with BSA (Sigma, #A7906-100G) 2% in PBS for 30 minutes, and incubated with antibody a-OPN (rabbit anti-mouse osteopontin, clone EPR21138, #218237) for 2 hours. Then, cells were washed and incubated with Alexa-Fluor 555 conjugated donkey anti-rabbit IgG (H+L) polyclonal antibody (Invitrogen; #A-31572) for 30 minutes.

For OPN/CD63 double staining, cells were blocked with BSA (Sigma, #A7906-100G) 2% in PBS added with a-CD16/32 1:100 (Thermofisher, #14-0161-86) antibody for 30 minutes. Then, cells were incubated with antibody a-OPN (rabbit anti-mouse osteopontin, clone EPR21138, Abcam, #218237) and a-CD63 (polyclonal goat anti-mouse, SICGEN, AB0047-200) for 2 hours. Then, cells were washed and incubated with Alexa-Fluor 555 donkey anti-rabbit IgG (H+L) antibody (Invitrogen; #A-31572) + Alexafluor 633 donkey anti-goat IgG (H+L) antibody (Invitrogen, #A21082) for 30 minutes.

Nuclei were highlighted with DAPI (Thermofisher, #D1306) for the last 10 minutes. Cover glasses were mounted using ProLong Gold antifade reagent (Invitrogen, #P36934). The day after, fluorescent images were acquired with Leica DM4 B optical microscope equipped with a DFC450 digital camera.

3.17 Cell viability assay

$4x10^3$ cells were seeded in 96-well plates. Cell proliferation Kit XTT (PanReac Applichem, #A8088) was used to evaluate the proliferation of DLBCL cells at 24, 48 and 72h. The optical density was evaluated by Spark Multimode microplate reader.

3.18 Injection of parental and transduced OPL239 lymphoma cells in BALB/c and OPN-/- mice

BALB/c and OPN-/- mice were sublethally irradiated using "RS 2000 RAD Source Technologies" instrument, with a dose of 5 Gy. 4 hours after irradiation, $5x10^5$ cells (for parental cell lines) or $1x10^5$ cells (for Spp1-IRES Green, iOPN-IRES Green and IRES Green variants) were resuspended in 200 µl of 0.9% NaCl with a 1 ml syringe and intravenously injected into the tail vein. About 10 days after the injection, at first signs of distress, mice were sacrificed and swelled organs (spleen and liver) were collected for histopathology, flow cytometry and RT-qPCR analyses.

3.19 GEP on human lymphomas

Raw CEL files data were downloaded through package GEOquery from public dataset GSE4475, containing gene expression profile from 221 DLBCL patient (58 ABC, 120 GC-DLBCL, 43 unclassified). Then, raw data were imported in R software through function readAffy from affy package and normalized with the RMA function. Quality control was performed, and than probe annotation was made with hgu133a annotation. Probes that did not match any gene symbol were removed. Multiple probes that were linked to the same gene symbol were collapsed through function collapseRow with method maxRowVariance from WGCNA package.

Differentially expressed genes between ABC and GCB patients were calculated through limma linear models and p.value was corrected with the Benjamini and Hockberg method.

3.20 Statistical analysis

Value differences between two groups were assessed by student t test. Differences among more than two groups was evaluated through ordinary one way ANOVA. When values were associated with two categorical variables, two way ANOVA was used to assess differences among two or more groups. Differences were considered statistically significant at p value (P)<0.05.

4. RESULTS

4.1 Autoimmunity severity of Fas$^{lpr/lpr}$ mice in absence of osteopontin

To assess whether in autoimmune-prone Fas$^{lpr/lpr}$ mice serum levels of OPN increase along disease progression, as already described for patients and mice affected by some inflammatory disorders [121,122], we evaluated OPN in mouse serum at different time points by ELISA. In line with the literature, we found that OPN is released along autoimmunity progression, from 2 months, when mice started showing initial signs of autoimmune disease, to 6 months, time of sacrifice, with a peak at 5 months of age (Fig. 10).

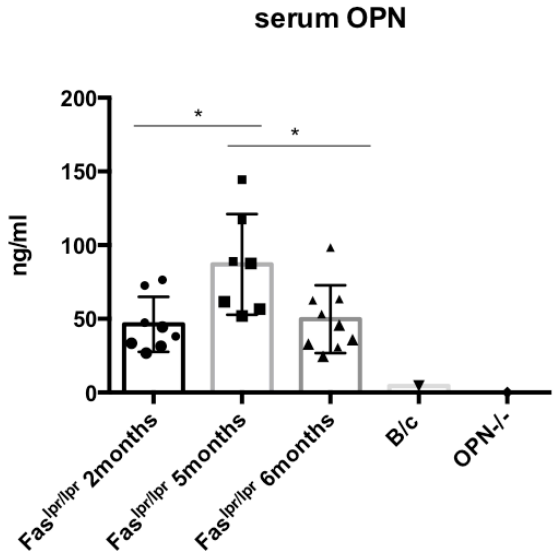

Figure 10. **OPN secretion in the serum of autoimmune mice.** ELISA measurement of OPN in sera from Fas$^{lpr/lpr}$ mice at 2, 5 and 6 months of age. OPN was already secreted at early stages, its level significantly increased at 5 months and decreased at late stages (*, P<0.05; Ordinary one way ANOVA). Sera from BALB/c and OPN-/- mice were tested as controls. Data are expressed as ng/ml and are a pool of 2 different experiments.

To investigate whether OPN deficiency affected the SLE-like syndrome of Fas$^{lpr/lpr}$ mice at different stages of the disease, we recorded lymph node swelling along time, from first appearance (around 2 months) until sacrifice (around 6 months). Despite a positive association between OPN and several autoimmune disorders, including SLE, has long been described [120], we found that Fas$^{lpr/lpr}$ and OPN-/-Fas$^{lpr/lpr}$ did not show any significant difference in the number (Fig. 11A, left) and volume (Fig. 11B, right) of swelled lymph nodes (neck, axillary and inguinal), although mice of both strains

displayed great variability in lymph node volume.

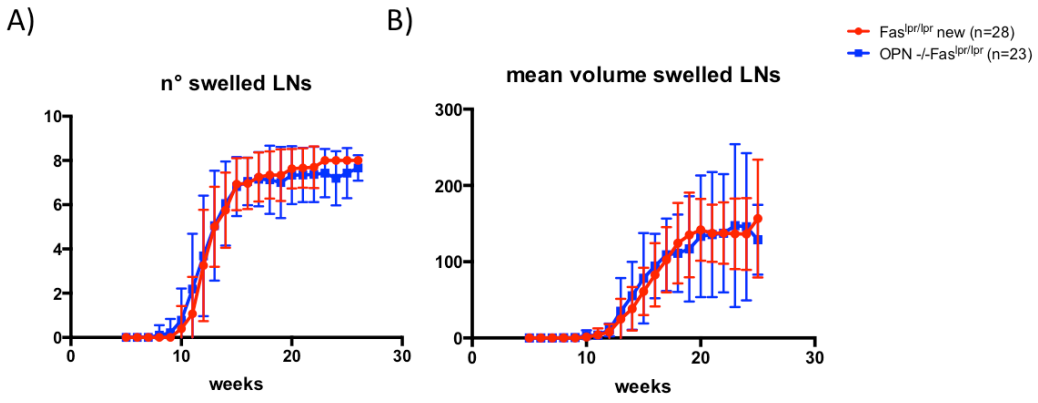

Figure 11. Lymph node swelling in autoimmune mice. Curves related to neck, axillary and inguinal lymph node swelling of autoimmune mice showing that both the number (A) and the mean volume (B) were similar between Fas$^{lpr/lpr}$ and OPN-/-Fas$^{lpr/lpr}$ mice.

Accordingly, the evaluation of auto-antibodies against self-antigens, which are a typical feature of autoimmune diseases [2, 51], confirmed a similar level of autoimmunity in the two strains. Indeed, the level of auto-antibodies against double strand (ds) and single strand (ss) DNA (Figure 12A and 3B) assessed by ELISA on mouse sera collected at different time points (2, 5 and 6 months) showed the expected increase along disease progression but no significant difference between Fas$^{lpr/lpr}$ and OPN-/-Fas$^{lpr/lpr}$ mice.

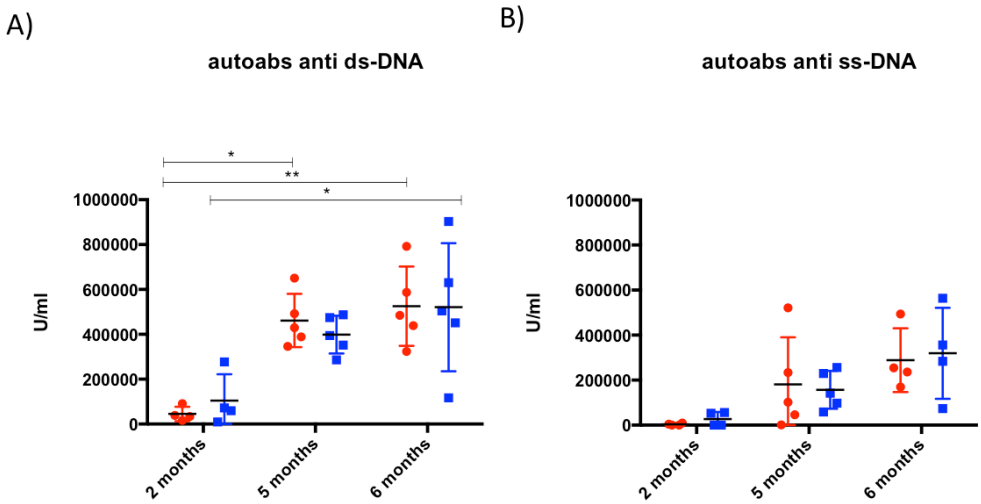

Figure 12. **Auto-antibodies production in autoimmune mice.** ELISA measurement of IgG anti-dsDNA (A) and anti- ssDNA (B) in sera from Fas$^{lpr/lpr}$ and OPN-/-Fas$^{lpr/lpr}$ mice at 2, 5 and 6 months of age. IgG

anti-dsDNA significantly increased during time (*, P<0.05, **, P<0.01; Two-way ANOVA), but no differences were found between the two strains. Data are expressed as U/mL.

The $Fas^{lpr/lpr}$ mutation leads to an expansion in the secondary lymphoid organs (SLOs) of the so-called "double negative" auto-reactive T cells (as they do not express neither CD4 nor CD8 while are positive for CD3 and B220) deriving from precursors unable to die through apoptosis in the thymus [140]. Thus, we also evaluated through flow cytometry the percentage of this population in the spleen of autoimmune mice at time of sacrifice, as another parameter of the autoimmune severity. Interestingly, despite no significant difference in lymph node swelling and auto-antibody serum levels, we found a higher expansion of CD3+B220+ cells in $Fas^{lpr/lpr}$ than OPN-/-$Fas^{lpr/lpr}$ mice (Fig. 13A, left). Notably, we found expansion of double negative cells also in the peripheral blood that mirrored the finding in the spleen, with increased number of CD3+B220+ cells in OPN-competent mice compared to OPN-deficient ones (Fig. 13B, right). In agreement with the data on double-negative cell expansion, the histopathological evaluation of mouse spleens revealed a marked expansion of the white pulp due to the massive infiltration of autoreactive lymphocytes in $Fas^{lpr/lpr}$ mice, that was less evident in OPN-deficient animals, that, viceversa, showed initial lymphomatous foci. (Fig. 13C).

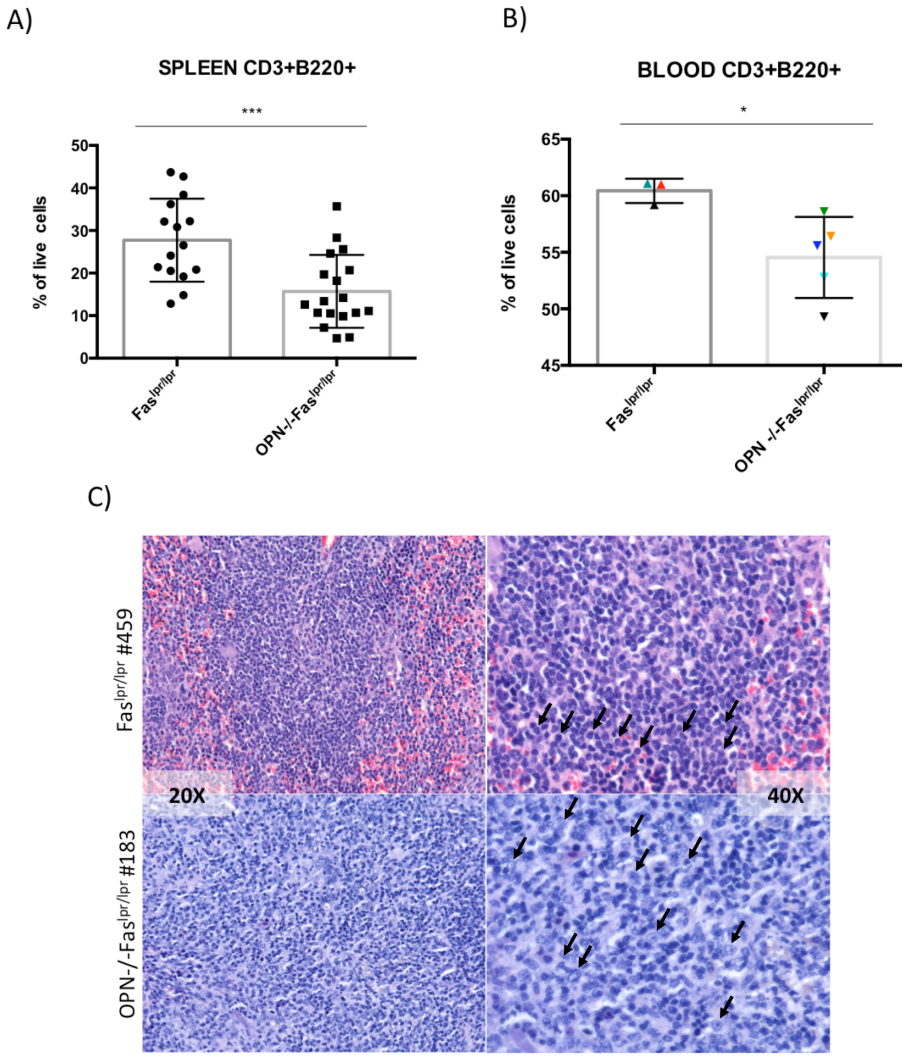

Figure 13. **Expansion of autoreactive T cells in autoimmune mice**. A) Flow cytometry analysis showing that the relative number of splenic autoimmune CD3+B220+ T cells was significantly lower in OPN-/-Fas$^{lpr/lpr}$ than Fas$^{lpr/lpr}$ mice at about 5-6 months of age (***, P<0.001; Student t test). The graph shows a pool of different experiments. B) Flow cytometry analysis showing that CD3+B220+ T cells significantly decreased in the peripheral blood of 5-month-old OPN-deficient autoimmune mice compared with age-matched OPN-competent ones (*, P<0.05; Student t test). The graph refers to one representative experiment. C) Histopathological analysis of spleen samples from Fas$^{lpr/lpr}$ and OPN-/-Fas$^{lpr/lpr}$ mice showing a marked expansion of the white pulp by reactive lymphoid cells (black arrows) in 5-month-old OPN-competent animals, less marked in aged-matched mice lacking OPN. OPN-/-Fas$^{lpr/lpr}$ spleens, in most cases, were characterized by initial lymphomatous foci, as the illustrated example (black arrows). Magnification 20x (left) and 40x (right).

Altogether these data suggest a less severe autoimmunity in the absence of OPN, highlighted by a reduced expansion of auto-reactive double-negative T cells, despite other autoimmune features, such as lymph node swelling and auto-antibody titers, do not seem affected by OPN deficiency.

4.2 OPN-/-Fas$^{lpr/lpr}$ mice develop lymphoma with higher incidence than Fas$^{lpr/lpr}$ mice.

In order to evaluate the impact of the absence of OPN in the autoimmunity-driven lymphomagenesis that characterises aged Fas$^{lpr/lpr}$ mice [52], we compared the incidence of splenic lymphomas in Fas$^{lpr/lpr}$ and OPN-/-Fas$^{lpr/lpr}$ mice at about 5-6 months of age. Unexpectedly, we found a much higher incidence of lymphoma in OPN-/-Fas$^{lpr/lpr}$ mice than Fas$^{lpr/lpr}$ animals [69% and 33% of cases, respectively (Fig. 14)]. As illustrated above, in figure 13C, histopathological analysis of the spleens of Fas$^{lpr/lpr}$ mice revealed a marked expansion of the white pulp by pleomorphic lymphoid cells with irregular nuclei and variable size from small to medium cells (autoreactive T cells), while the same analysis on OPN-/-Fas$^{lpr/lpr}$ spleens highlighted a subversion of the parenchymal architecture by a monomorphic proliferation of large elements, with abundant cytoplasm and central nuclei, with immunoblastic morphology. The features of these proliferating atypical elements suggest that these tumours are high-grade diffuse large B cell lymphomas, with morphology resembling the activated type (ABC-DLBCL).

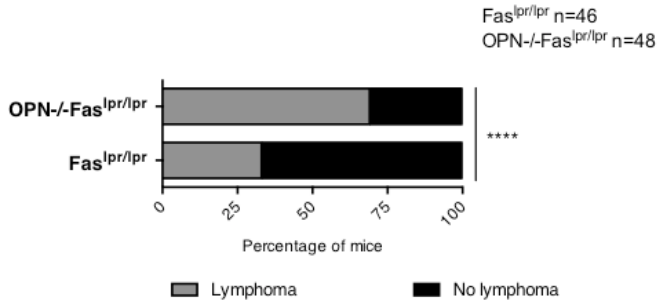

Figure 14. Incidence of splenic lymphoma in autoimmune mice. Graph showing that the incidence of splenic lymphoma is higher in OPN-/-Fas$^{lpr/lpr}$ (n=48) than Fas$^{lpr/lpr}$ (n=46) mice at about 5-6 months of age (69% and 33% and respectively). (****, $P < 0.0001$; Chi-square two-tailed test).

Flow cytometry analysis of splenic B cells with the classical B cell markers, CD19, B220 and IgM, showed in 5/6-month old OPN-/-Fas$^{lpr/lpr}$ mice a population of CD19+ cells that expressed variable levels of B220 and low to negative expression of surface IgM. These IgM negative CD19+ cells were very rarely detectable in Fas$^{lpr/lpr}$ spleens *(*Fig. 15).

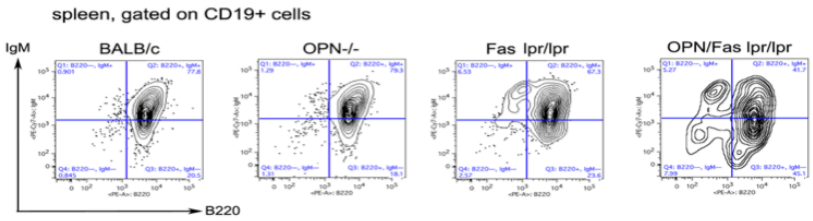

Figure 15. Flow cytometry characterization of autoimmune CD19+ B cells. Gates illustrating that CD19+ cells from OPN-/-Fas$^{lpr/lpr}$ mice were characterized by a low expression of surface IgM.

4.3 Lymphomas developing in OPN-/-Fas$^{lpr/lpr}$ mice show features of the activated type of diffuse large B cell lymphoma (ABC-DLBCL)

As the different subtypes of DLBCL, GC-DLBCL and ABC-DLBCL, classified according to the cell of origin, are characterized by a specific and distinct pattern of gene expression [64], we then verified key molecular features in B cell lymphomas spontaneously developing in OPN-/-Fas$^{lpr/lpr}$ mice to confirm the histopathological analysis suggestive of ABC-DLBCL subtype. To this aim we selected spleen samples from both Fas$^{lpr/lpr}$ and OPN-/-Fas$^{lpr/lpr}$ mice showing an overt lymphoma development for a correct comparison.

As illustrated in the immunofluorescence images of figure 16, while tumours developed in Fas$^{lpr/lpr}$ mice were positive for BCL6, a marker generally expressed by human GC-related DLBCLs, OPN-/-Fas$^{lpr/lpr}$ lymphomas did not show any positivity for this marker. Notably, lymphomas arose in OPN-deficient autoimmune mice were found to express a higher level of c-MYC (Fig. 16), an oncogene usually amplified in the so called “double expressor” lymphomas, according to the double expression of c-MYC and BCL2, than OPN-sufficient counterparts. These markers, together with IRF4, belong to the typical signature of human ABC-DLBCLs.

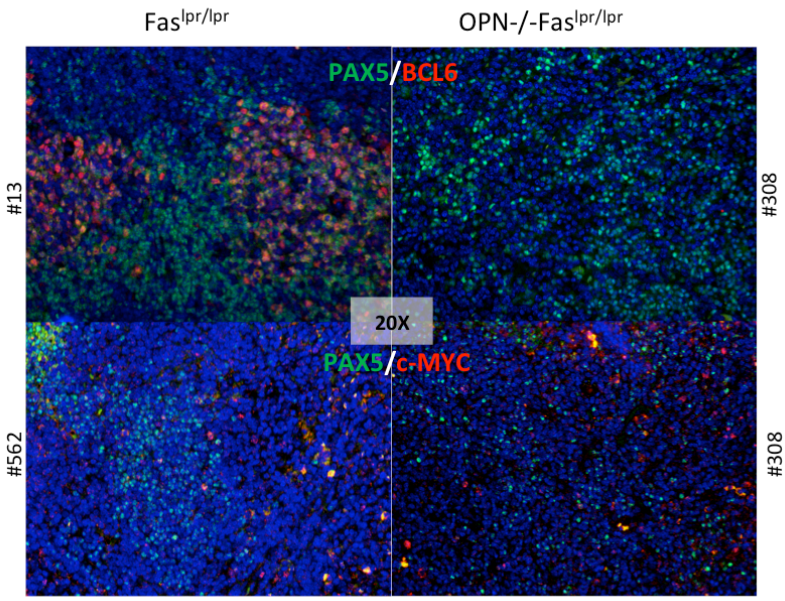

Figure 16. Evaluation of lymphoma phenotype by IF. Immunofluorescence staining on splenic tissues showing that BCL6 was expressed only by Fas$^{lpr/lpr}$ lymphomas (like human GC.DLBCLs), while OPN-deficient tumours express c-MYC (resembling human ABC-DLBCLs). PAX5 was used as a pan-B cell marker. Magnification 20x.

To further support our hypothesis of ABC-DLBCL lymphoma, we analysed these three markers by western blot on CD19+ B cells purified through immune-magnetic beads from the spleen of Fas$^{lpr/lpr}$ and OPN-/-Fas$^{lpr/lpr}$ mice and found them more expressed in samples from OPN-deficient autoimmune mice (Fig. 17A). Interestingly, B cells derived from OPN-deficient animals showed also a higher activation of STAT3 pathway (ph-STAT3), generally associated with B cell survival and proliferation (Fig. 17A). The increased activation of ph-STAT3 was also confirmed by both immunohistochemical and immunofluorescence staining on spleen sections from both autoimmune mice (Fig. 17B).

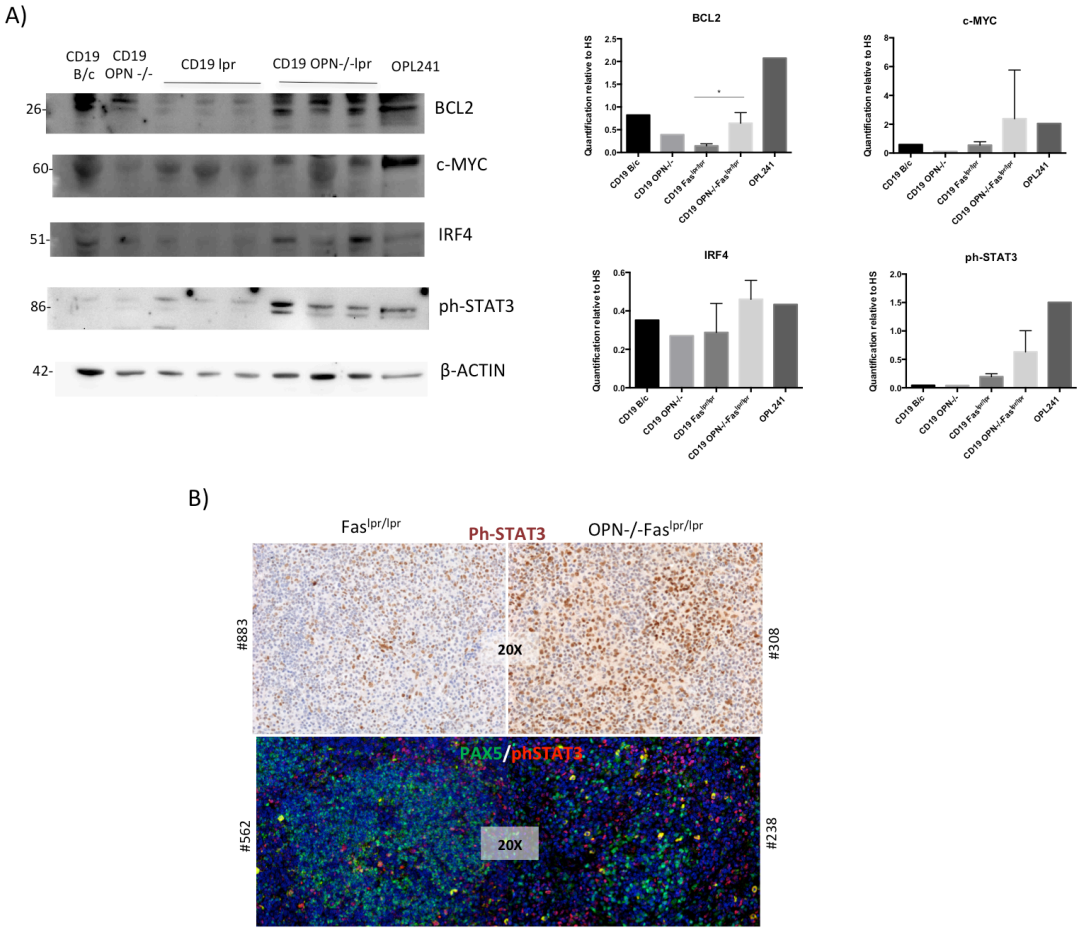

Figure 17. Evaluation of lymphoma phenotype by Western Blot, IHC and IF. A) Western blot on purified CD19+ B cells from OPN-competent and deficient autoimmune mice. CD19+ B cells lacking OPN showed a stronger expression of BCL2, c-MYC and IRF4, as well as ph-STAT3, compared to $Fas^{lpr/lpr}$ B cells. Lymphoma cell line, OPL241 has been used as positive control. B) Immunohistochemistry staining (upper panels) on FFPE spleens showing the stronger expression of ph-STAT3 in OPN-deficient lymphomas comparing with OPN-sufficient ones. (Magnification 20x). The immunofluorescence staining (lower panels) for PAX5 and ph-STAT3 illustrates the same up-regulations in OPN-/- tumours. Magnification 20x.

As ABC-DLBCLs are generally the most aggressive, we also compared the proliferative capacity of lymphomatous B cells from $Fas^{lpr/lpr}$ and OPN-/-$Fas^{lpr/lpr}$ mice. As demonstrated by immunofluorescence for the proliferation marker ki67 on lymphomatous spleens (Fig. 18A) and confirmed quantitatively by flow cytometry analysis performed on different cohorts of mice (Fig. 18B), there was a significantly higher number of Ki67+ CD19+ cells in OPN-/-$Fas^{lpr/lpr}$ spleens than in $Fas^{lpr/lpr}$ ones.

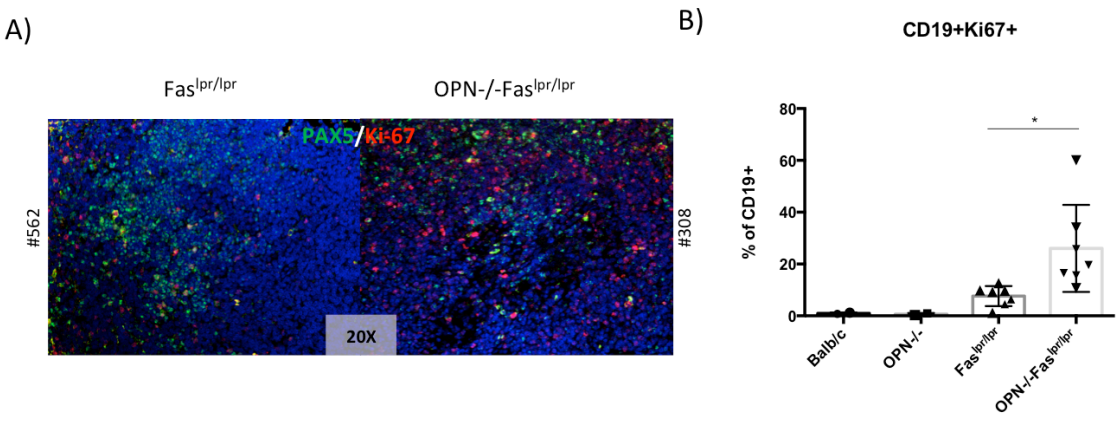

Figure 18. Ki67 expression in B cells from autoimmune mice. Immunofluorescence staining for PAX5 and Ki67 on FFPE spleens showing that OPN-deficient tumours were characterized by a strong expression of Ki67. Magnification 20x. B) Flow cytometry analysis showing a significantly higher number of CD19+Ki67+ cells in the spleen from OPN-/-Fas$^{lpr/lpr}$ than Fas$^{lpr/lpr}$ animals (*, P<0.05; Student t test). The graph shows a pool of two independent experiments.

Altogether, these data strongly indicate that the autoimmunity-driven lymphomas developing in mice in absence of OPN are high-grade DLBCL, likely of the activated and "double-expressor" type, with aggressive proliferative rate.

4.4 Gene expression profile on CD19+ B cells confirmed the phenotype of ABC-DLBCL of OPN-/-Fas$^{lpr/lpr}$ lymphomas

Aiming at investigating whether OPN deficiency affects B cell-intrinsic dynamics either in naive (BALB/c and OPN-/-) and/or autoimmune mice (Fas$^{lpr/lpr}$ and OPN-/-Fas$^{lpr/lpr}$), and which genes and pathways could drive lymphomagenesis in OPN-/-Fas$^{lpr/lpr}$ mice at early stages, we performed a gene expression profile (GEP) on CD19+ B cells, purified by magnetic beads from the spleen of animals at 5 and 8 months of age. Among 8-month old mice, we selected by flow cytometry and histopathological analysis only those with overt lymphomas for both Fas$^{lpr/lpr}$ and OPN-/-Fas$^{lpr/lpr}$ strains.

Comparison between the different groups are shown in the volcano plots in figure 19 below. Genes were considered significant with false discovery rate (FDR) ≤ 0.05 and fold-change ≤ -2 or ≥ 2. The greatest differences were found, as expected, when CD19+ cells from autoimmune and naive mice were compared, regardless of the presence of OPN. In samples from lymphoma-bearing Fas$^{lpr/lpr}$ and OPN-/-Fas$^{lpr/lpr}$ mice at 8 months of age, the absence of OPN modified the expression of very few genes. Interestingly, at early stages (5 months), most OPN-/-Fas$^{lpr/lpr}$ mice showed signs of lymphoma while

Fas$^{lpr/lpr}$ did not. To better identify the genes that could drive lymphoma development in OPN-deficient autoimmune mice, we selected in the 5-month time point OPN-/-Fas$^{lpr/lpr}$ mice with early sign of lymphoma and OPN-competent Fas$^{lpr/lpr}$ animals with no evidence of lymphomatous cells. The number of differentially expressed genes (DEG) at this time point, when lymphomagenesis likely occurs, were much higher than at 8 months of age, time with overt lymphomas.

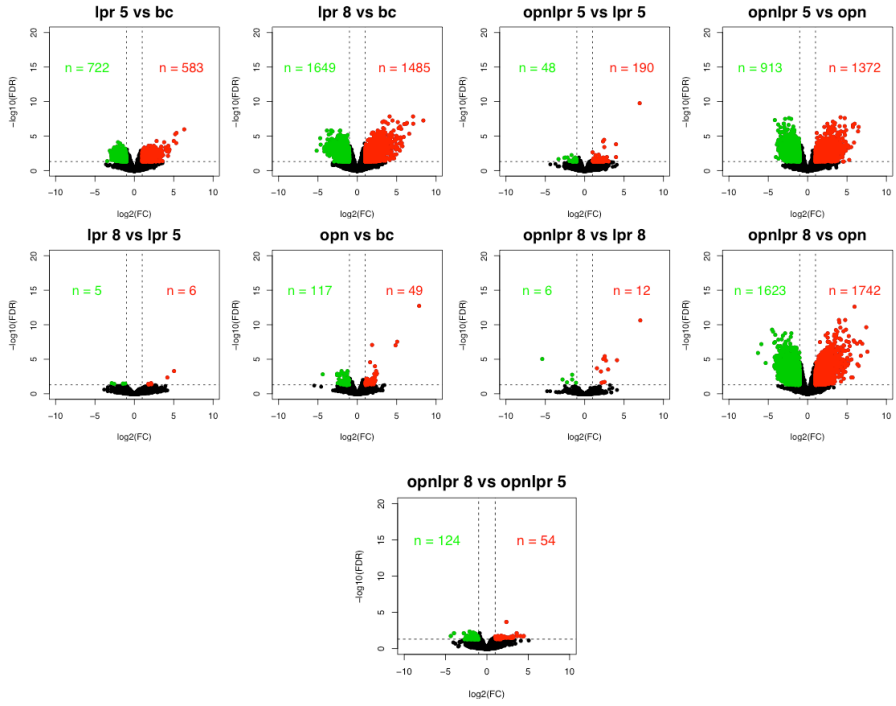

Figure 19. **Gene expression profile on CD19+ cells from naïve and autoimmune mice.** Volcano plots showing the differentially expressed genes (DEG) among the various groups of animals (B/c, OPN-/-, Fas$^{lpr/lpr}$ and OPN-/-Fas$^{lpr/lpr}$ mice at 5 and 8 months of age). Green dots represent down-modulated genes with a FDR ≤ 0.05 and fold-change ≤ -2 and red dots represent up-modulated genes with FDR ≤ 0.05 and fold-change ≥ 2. All comparisons were made using limma package.

Notably, the ABC-DLBCL like phenotype of lymphomatous B cells from OPN-/-Fas$^{lpr/lpr}$ mice was also confirmed by GEP, as we found up-regulated, in comparison with Fas$^{lpr/lpr}$ mice, some genes (*Prdm1*, *Prlr*, *Hsp90b1*) (Fig. 20) that have been found highly expressed and/or amplified in samples from human ABC-DLBCL patients [94, 95, 141]

OPN-/-Fas$^{lpr/lpr}$ 5m VS Fas$^{lpr/lpr}$ 5m

GeneName	FC	logFC	P.Value	FDR
St8sia1	8.09317	3.0167	0.00024	0.03902
Prdm1	**7.34129**	**2.87603**	**0.00009**	**0.03356**
Hamp2	7.20569	2.84914	0.00011	0.0339
Scn2b	7.14045	2.83601	0.00001	0.01102
Cpeb3	6.74906	2.75469	0.00037	0.04262
Chpf	5.90628	2.56225	0.00018	0.03541
Prlr	**5.61155**	**2.4884**	**0.00041**	**0.04517**
Psg16	5.5774	2.47959	0	0.00003
Creb3l2	5.29073	2.40347	0.00019	0.03541
Parm1	5.23531	2.38827	0.00001	0.01141
Klk4	5.1389	2.36146	0.00014	0.0349
Olfr570	5.0051	2.3234	0.00054	0.04959
Dgkg	4.99829	2.32144	0.00045	0.04695
Pak7	4.72796	2.24122	0.0005	0.04856
Abcc6	4.69999	2.23266	0.00011	0.03386
Rapgef3	4.67518	2.22502	0.00016	0.03535
Fam46c	4.64042	2.21426	0.00031	0.04216
Ap2a1	4.40257	2.13835	0.00026	0.03935
Lpar1	4.30443	2.10582	0.00017	0.03535
Osbpl3	4.20214	2.07112	0.00011	0.03386
Ddx43	4.05354	2.01918	0.00005	0.02788
B3galt5	4.043	2.01543	0.00018	0.03541
Adam24	3.98581	1.99487	0.00002	0.01682
Nxf3	3.93509	1.9764	0.00028	0.03996
Fads1	3.83377	1.93877	0.00002	0.01682
Olfr678	3.81185	1.93049	0.00015	0.03535
Miat	3.78104	1.91878	0	0.00983
Znrf3	3.76573	1.91293	0.00008	0.03326
Gpr149	3.7348	1.90103	0.00043	0.04617
Chsy3	3.66883	1.87532	0.00005	0.02865
Vcan	3.66673	1.87449	0.00009	0.03356
Cmtm5	3.65887	1.8714	0.00001	0.01257
Olfr362	3.62275	1.85708	0.00038	0.04321
Txndc5	3.61544	1.85417	0.00046	0.04695
Vmn1r174	3.57391	1.8375	0.00012	0.0349
Pramel6	3.54706	1.82662	0.00004	0.02445
Klra12	3.54699	1.82659	0.00017	0.03535
Tram2	3.54457	1.82561	0.00039	0.04413
Mki67	3.53732	1.82266	0.00008	0.03187
Ttc41	3.50981	1.81139	0.00014	0.0349
Olfr401	3.49948	1.80714	0.00014	0.0349
Olfr90	3.47395	1.79658	0	0.00464
Hsp90b1	**3.46117**	**1.79126**	**0.00007**	**0.03076**
Rrbp1	3.40413	1.76729	0.0001	0.03356
Car5b	3.4014	1.76613	0.00032	0.04216

Figure 20. Differentially expressed genes between CD19+ cells from 5-month old OPN-/-Fas$^{lpr/lpr}$ and Fas$^{lpr/lpr}$ mice. List of the top 45 significantly up-regulated genes calculated through limma models. Genes are listed in descending order of fold change.

Among the most up-regulated genes in the comparison of OPN-/-Fas$^{lpr/lpr}$ with Fas$^{lpr/lpr}$ mice at 5 months, we found *Prdm1* (7,3-fold increase) that encodes for BLIMP1 (B lymphocyte induced maturation protein-1), a transcriptional repressor, target of both NFkB and STAT3.

To verify the up-regulation of *Prdm1* in OPN-deficient tumours, we firstly confirmed its significant increase on the same RNA samples used for GEP analysis (Fig. 21A). Then, we evaluated its expression in CD19+ cells isolated with immunomagnetic beads from other animals of the four strains, at about 5 months of age, confirming a trend of increase in OPN-/-Fas$^{lpr/lpr}$ animals (Fig. 21B). To further validate this result, we used

RNA Scope technology to analyse its expression *in situ*, on spleen sections from 5/6-month old Fas$^{lpr/lpr}$ and OPN-/- Fas$^{lpr/lpr}$ mice. As illustrated in Fig. 21C, OPN-deficient tumours showed a higher positivity for *Prdm1* probe compared to OPN-competent ones and to the other groups.

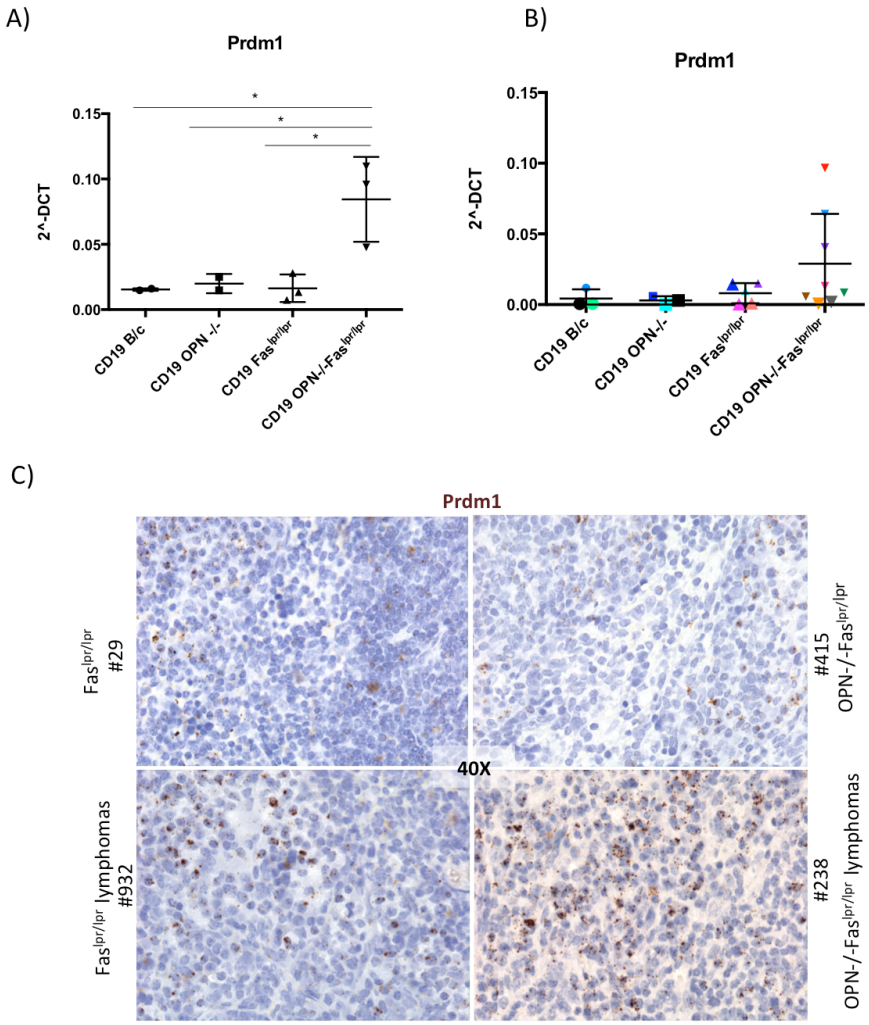

Figure 21. Expression of *Prdm1* in B cells. A) Technical validation (RT-PCR) on the same RNA samples used for GEP analysis showing a significant up-regulation of *Prdm1* in CD19+ cells from OPN-Fas$^{lpr/lpr}$ mice compared with all other groups (*, P<0.05, Ordinary one way ANOVA). B) RT-PCR on CD19+ cells from a different cohort of mice showing a trend in the *Prdm1* increase in OPN-deficient autoimmune mice. C) RNA-scope for *Prdm1* showing its strong expression in FFPE spleens from tumor-bearing OPN-/- mice. Magnification 40x.

In order to evaluate whether B cells from Fas$^{lpr/lpr}$ and OPN-/-Fas$^{lpr/lpr}$ mice could activate different signaling cascades, we performed an enrichment score analysis through the package pathfindR on Reactome Pathway with DEG between the two strains at 5 months of age, finding that OPN-Fas$^{lpr/lpr}$ B cells up-regulated pathways

important for B cell development and often hyper-activated in several malignancies of the B cells, including DLBCL, such as NOTCH pathways [69] (Fig. 22A). Interestingly, when performing a longitudinal analysis comparing OPN-/-Fas$^{lpr/lpr}$ B cells at 8 months and 5 months, NFkB and TNF-a signaling pathways, associated with TLR cascades and important for B cell survival and inflammation, were significantly up-regulated at the late disease stage (Fig. 22B).

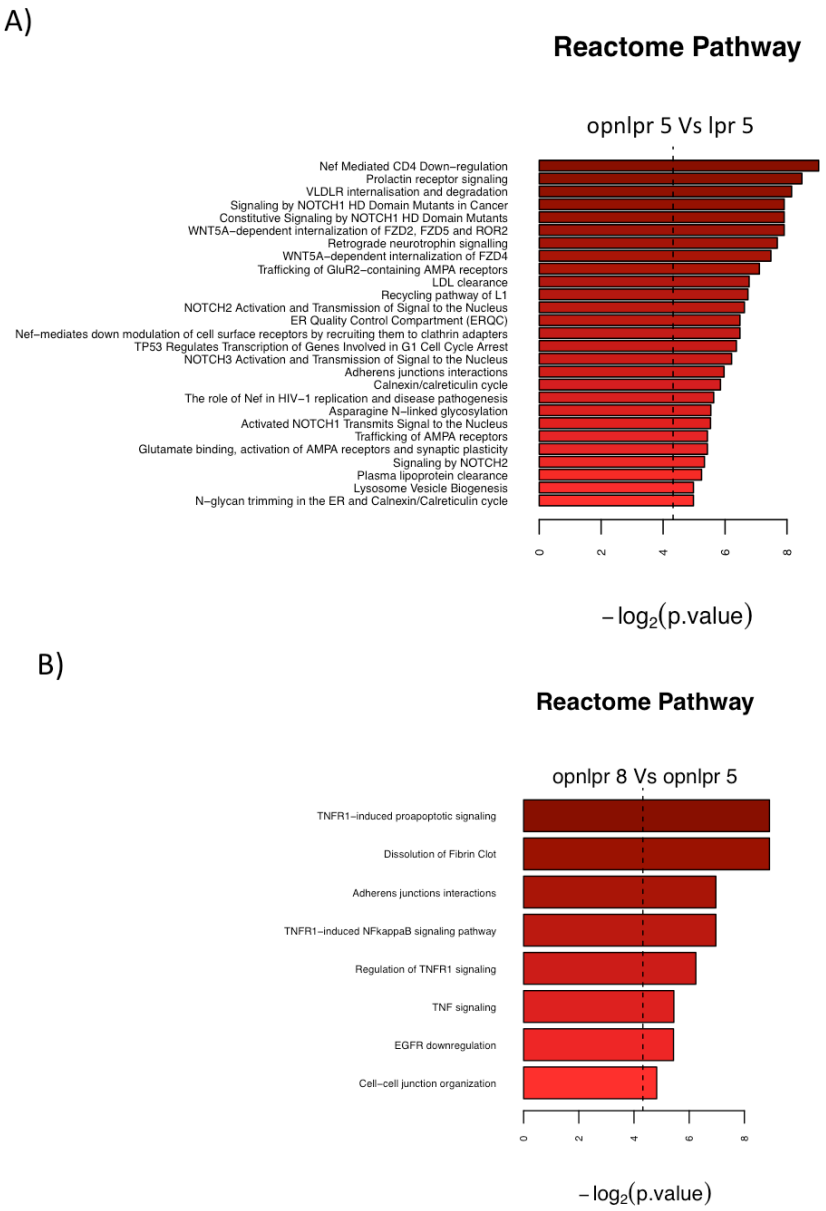

Figure 22. Pathway analysis. PathfindR analysis on Reactome pathway illustrating the modulated signaling pathways in the comparison between OPN-/-Fas$^{lpr/lpr}$ and Fas$^{lpr/lpr}$ B cells mice at 5 months of age (A), and OPN-/-Fas$^{lpr/lpr}$ mice CD19+ B cells along the disease (8 months versus 5 months) (B) (FDR < 0.05).

Overall, these data indicate that the most relevant transcriptional changes in B cells from OPN-deficient autoimmune mice occur at early stages of the disease, when the absence of OPN seems to induce *Prdm1* and other genes and pathways described to be important for sustaining lymphoid malignancies, including DLBCL.

4.5 Splenic B cells undergoing malignant transformation in OPN-/-Fas$^{lpr/lpr}$ mice likely belong to a mature CD19+CD93- subset, but are neither follicular nor marginal zone B cells.

In order to investigate whether B cell development within primary and secondary lymphoid organs is impaired in absence of OPN, bone marrow and spleen of both naïve and autoimmune Fas$^{lpr/lpr}$ and OPN-/-Fas$^{lpr/lpr}$ mice were analysed by flow cytometry using Hardy's multiparametric panel able to distinguish the different B cell populations [142]. The gating strategy of both bone marrow and spleen is shown in figure 23A and B.

A)

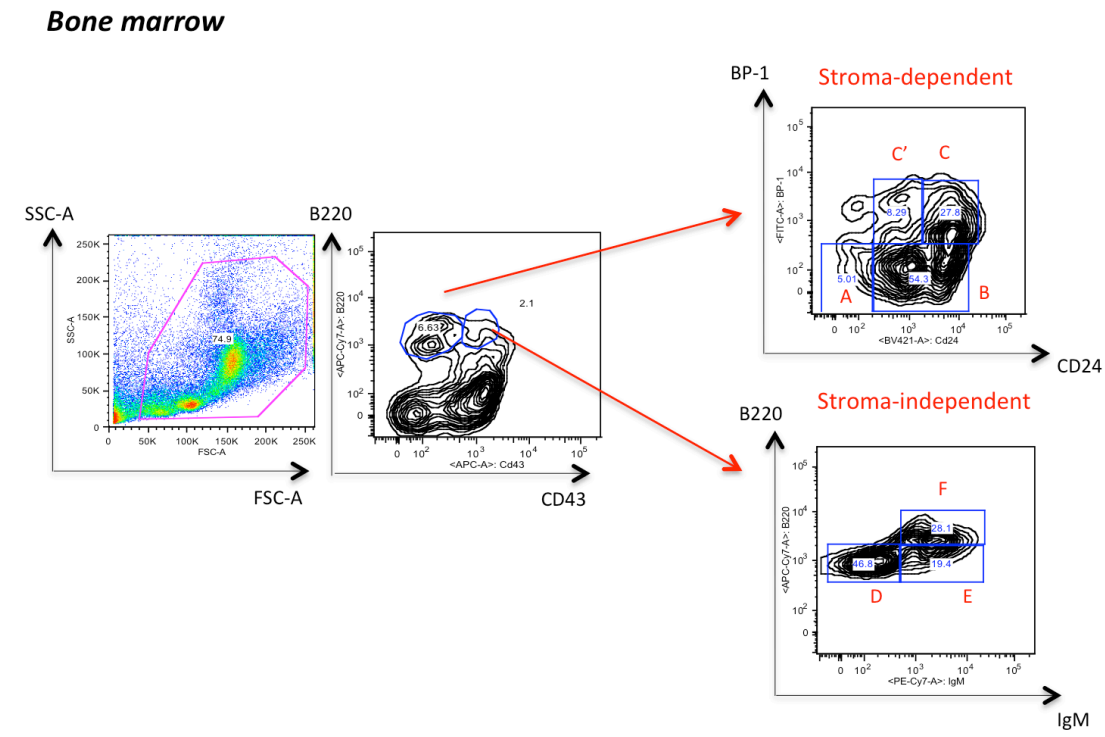

B)

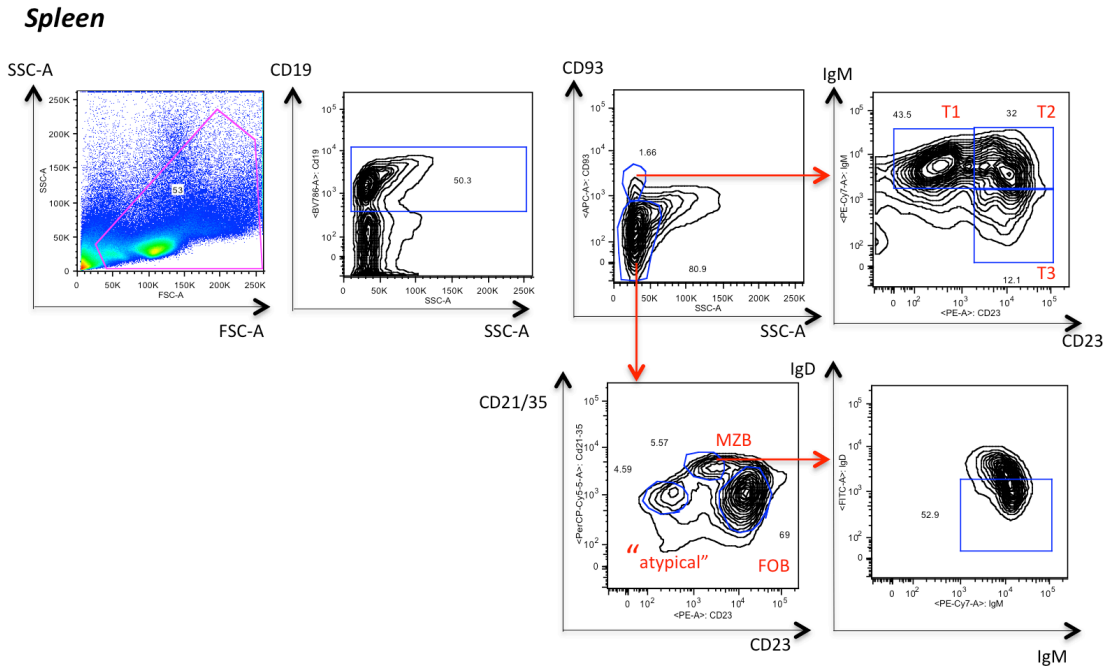

Figure 23. Hardy's gating strategy applied to bone marrow and spleen from a BALB/c mouse. A) Example of gating strategy for discriminating B220+CD43- stroma-dependent (A, B, C, C') and B220+CD43+ stroma-independent (D, E, F) B cell populations in the bone marrow from a BALB/c mouse. B) Example of gating strategy to discern the different CD93+ immature (transitional 1, 2, 3) and CD93- mature (follicular B, marginal zone B and CD21/35-CD23-) B cell subsets in the spleen from a BALB/c mouse.

As expected, the percentages of the different B cell subsets in naïve and autoimmune mice were different, both in the bone marrow and in the spleen, but no major difference were detected between OPN-competent and -deficient animals within the naïve or the autoimmune group (Fig. 24 A and B). However, in the spleen, the site of transformation of DLBCL, we interestingly noticed that, inside the mature CD19+CD93- population, which comprises the classical follicular B (FOB) (CD23+) and marginal zone (MZB) (CD21/35+) B cells, OPN-/-Fas$^{lpr/lpr}$ mice showed a significant reduction of FOB in favor of an atypical CD23-CD21/35- population that was strongly increased in OPN-deficient autoimmune animals (Figure 24B and C). In light of this observation, we speculated that this atypical CD23-CD21/35- population could represent the subset undergoing transformation in OPN-/-Fas$^{lpr/lpr}$ mice.

A)

BM

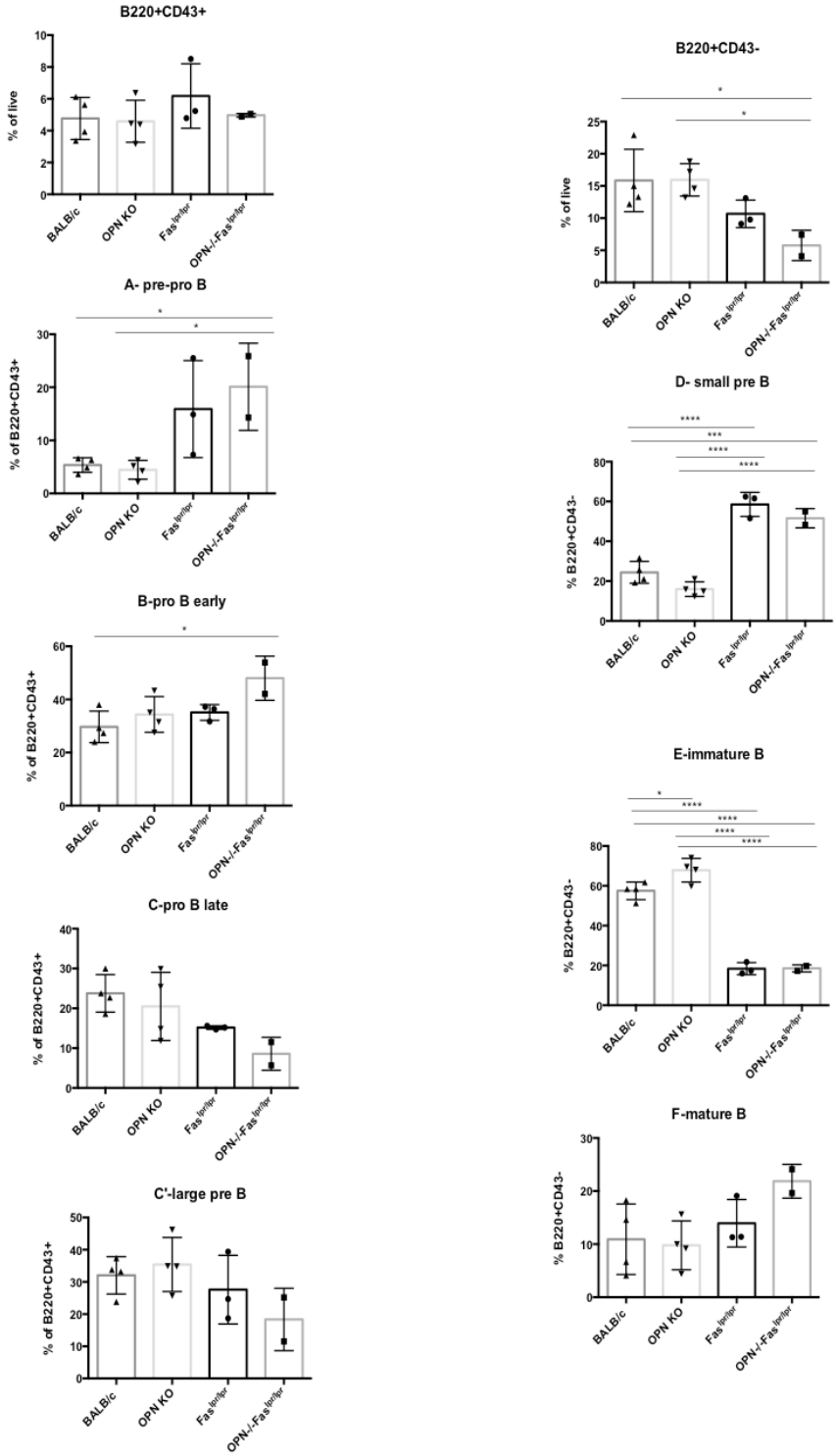
B220+CD43+
% of live
BALB/c
OPN KO
Fas lpr/lpr
OPN-/-Fas lpr/lpr
A- pre-pro B
% of B220+CD43+
B-pro B early
C-pro B late
C'-large pre B
B220+CD43-
D- small pre B
% B220+CD43-
E-immature B
F-mature B

B)

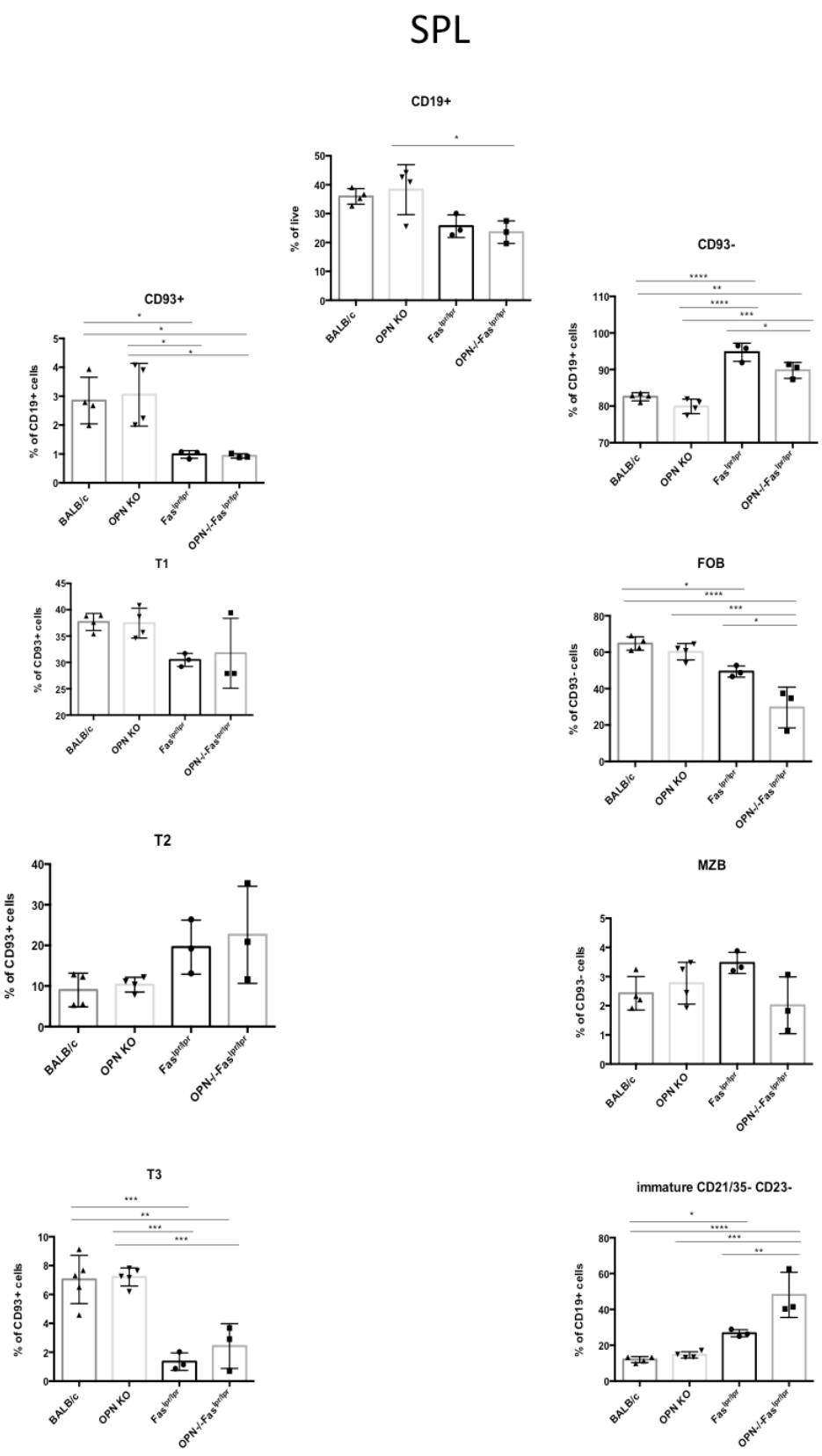
SPL
CD19+
% of live
CD93+
% of CD19+ cells
CD93-
% of CD19+ cells
T1
% of CD93+ cells
FOB
% of CD93- cells
T2
% of CD93+ cells
MZB
% of CD93- cells
T3
% of CD93+ cells
immature CD21/35- CD23-
% of CD19+ cells
BALB/c
OPN KO
Fas lpr/lpr
OPN-/-Fas lpr/lpr

C)

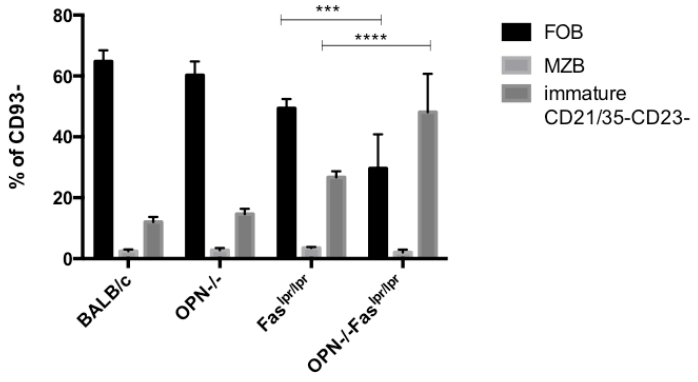

Figure 24. **Quantification of the different B cell populations in bone marrow and spleen from naïve and autoimmune mice.** A) Graphs showing the percentage of different B cell populations in the bone marrow (A) and spleen (B, C) from 3 B/c, 3 OPN-/-, 3 Fas$^{lpr/lpr}$ and 3 OPN-/-Fas$^{lpr/lpr}$ mice, assessed by flow cytometry. A) In the bone marrow, only differences between naïve and autoimmune mice were observed, but none between OPN-competent and -deficient animals inside each group. B) In the spleen, besides differences between naïve and autoimmune mice, CD23+ follicular B cells (FOB) were significantly reduced in OPN-/-Fas$^{lpr/lpr}$ compared with Fas$^{lpr/lpr}$ mice (*, P<0.05; Ordinary one way ANOVA), while the CD23-CD21/35- fraction augmented in the same animals (**, P<0.01; Ordinary one way ANOVA). C) Fraction of splenic CD23+ FOB, CD21/35+ marginal zone (MZB) cells, and CD23-CD21/35- cells from the spleens of all groups of mice. OPN-/-Fas$^{lpr/lpr}$ showed a reduction of FOB cells (***, P<0.001; Two-way ANOVA) that was associated with the expansion of an atypical CD23-CD21/35- population. (****, P<0.0001; Two-way ANOVA). Data are referred to one representative experiment out of 3.

These data suggest that B cells undergoing transformation in OPN-/-Fas$^{lpr/lpr}$ mice are a mature, but atypical CD21/35-CD23- population, which does not belong to neither FOB nor MZB cell subsets.

4.6 Expression of OPN within the splenic microenvironment of BALB/c and Fas$^{lpr/lpr}$ mice

In order to investigate which cells are the main producers of OPN in the SLOs of both naïve and autoimmune mice, we firstly evaluated the mRNA level of *Spp1* in the different immune cell populations sorted from the spleen of 3-month-old BALB/c and Fas$^{lpr/lpr}$ mice (Fig. 25A). Specifically, we analysed the following cell types: CD4+ and CD8+ T lymphocytes, B lymphocytes (CD19+), granulocytes (CD11b+ Gr-1^{hi}), classical (CD11c+B220-) and plasmacitoid (CD11c+ B220+) dendritic cells, marginal

macrophages (F480+CD169+) and autoimmune T cells (CD3+B220+), the latter only in the case of Fas$^{lp/lpr}$ mice. Interestingly, as shown in figure 25A, immune cells expressing *Spp1* were different between naïve and autoimmune mice, suggesting that, in such inflammatory scenario, cellular and molecular dynamics in SLOs could undergo modifications. Notably, whereas in BALB/c mice granulocytes were the population expressing the highest level of *Spp1,* in the spleen of Fas$^{lpr/lpr}$ mice *Spp1* was mostly expressed by CD4+ T and CD3+B220+ cells, and, at a lower level, also by Gr1^{hi} cells.

Since, the mRNA level of *Spp1* does not discriminate between the soluble and the intracellular isoforms of OPN, we evaluated its protein expression by performing IHC on spleen sections from naïve and autoimmune Fas$^{lpr/lpr}$ mice. In order to understand whether B cell-intrinsic dynamics were responsible for the increased B lymphomagenesis in OPN-deficient animals, we firstly investigated the expression of OPN in splenic B cell zones of autoimmune mice. Notably, IHC for OPN showed a moderate expression of OPN by B cells in the spleen follicles of Fas$^{lpr/lpr}$ mice that did not develop DLBCL, that was greatly increased in lymphomatous B cells from mice with lymphoma (fig. 25B). Noteworthy, the localization of OPN showed a specific and particular pattern, either with a cytoplasmatic distribution or with dots surrounding the nuclear region, suggesting that the OPN form mainly expressed by lymphomatous cells is the intracellular one. Remarkably, also double immunofluorescence staining performed on CD19+ cells purified from Fas$^{lpr/lpr}$ mice indicates that OPN and the endosomal marker CD63 showed a very similar expression pattern, suggesting that, in autoimmune B cells, OPN has an intracellular localization, and, more precisely, localises in the endosomal compartment.

A)

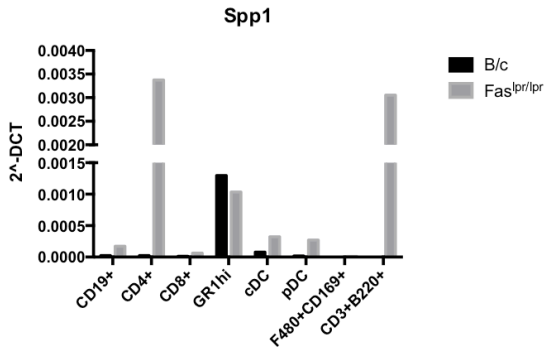

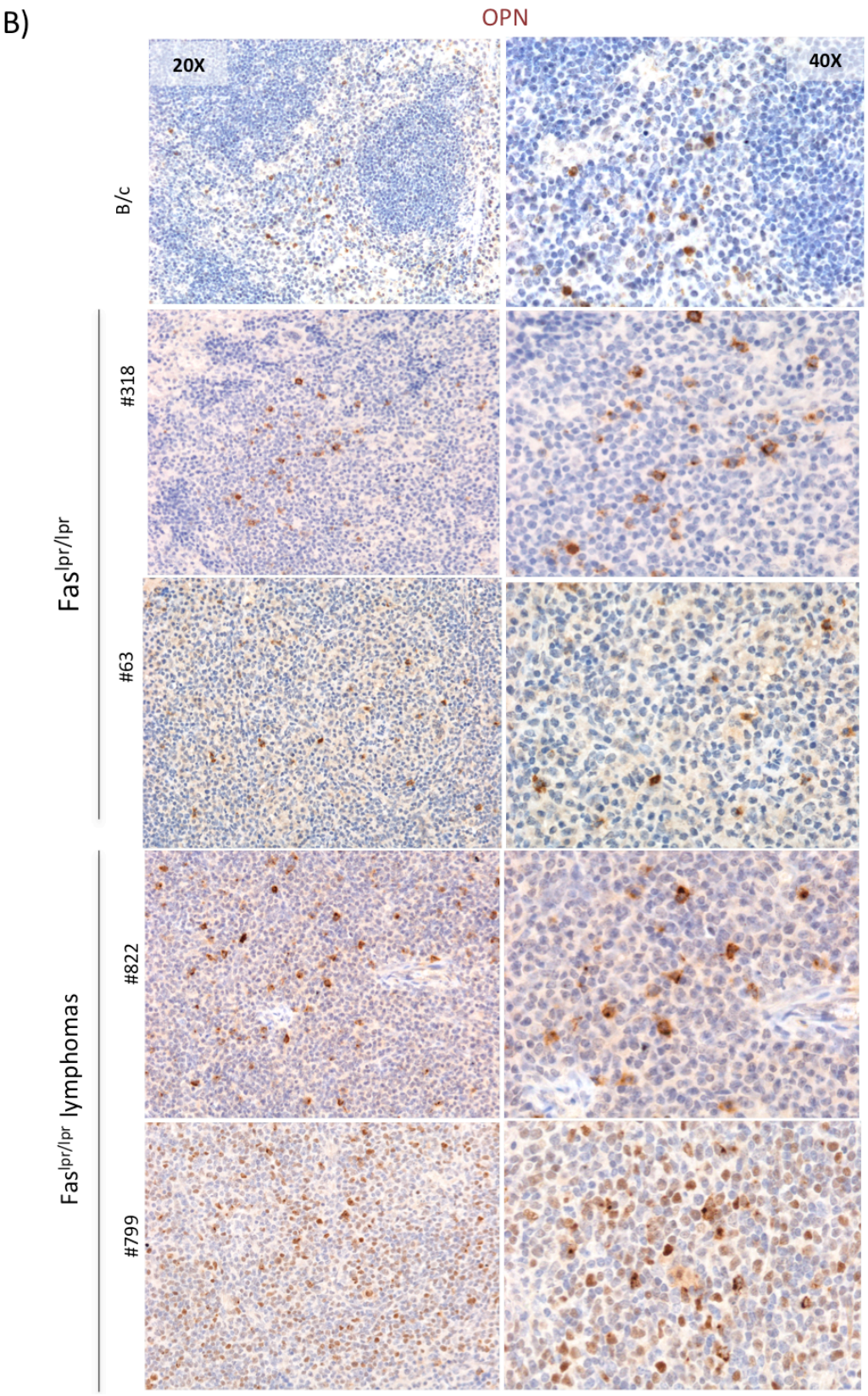
B)
OPN
20X
40X
B/c
#318
#63
#822
#799
Fas lpr/lpr
Fas lpr/lpr lymphomas

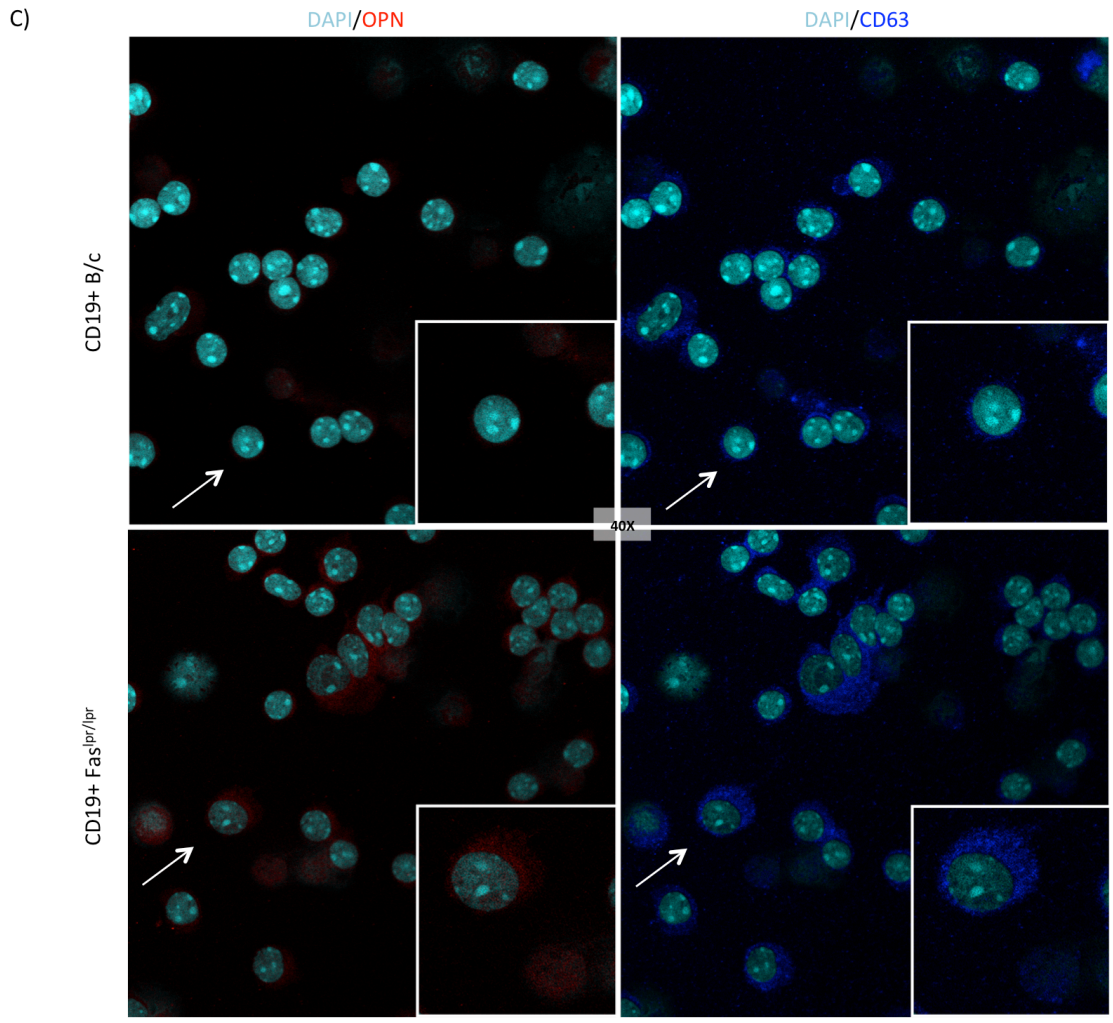

Figure 25. **Expression of OPN in splenic B cells.** A) RT-PCR on *Spp1* performed on different immune cell populations sorted from B/c and Fas$^{lpr/lpr}$ spleens (pool of 4 mice per group). Gr1^{hi} cells were the main producer of OPN in B/c mice, while CD4+, CD3+B220+ and, at a minor extent, Gr1^{hi} cells, expressed *Spp1* in autoimmune animals. Values are referred as 2^-DCT. B) Expression of OPN in splenic B cell zones. IHC on OPN performed on splenic FFPE tissues from B/c and autoimmune mice showing that OPN is expressed by lymphoid cells in the splenic follicles of Fas$^{lpr/lpr}$ mice, and its level increases within the lymphomatous zones in tumour-bearing mice. The localisation of OPN is intracellular, with dots localising nearby the nuclear membrane. Magnification 20x (left) and 40x (right). C) Double IF for OPN (red) and the endosomal marker CD63 (blu), showing that OPN is localised in the endosomal compartment of purified CD19+ cells from Fas$^{lpr/lpr}$ mice. B/c CD19+ cells did not show detectable signal for OPN. Magnification 40x.

IHC for OPN performed on splenic tissues showed that, apart from B cells, the protein is expressed also by other cell types, specifically macrophages and dendritic cells found to be localised in autoimmunity-caused granulomas, and by granulocytes, enriched in the peri-vascular zone of the splenic red pulp (Fig. 26). Notably, as expected by the

literature, also myeloid cells were characterized by the expression of intracellular OPN, with a staining very similar to that one observed in B cells.

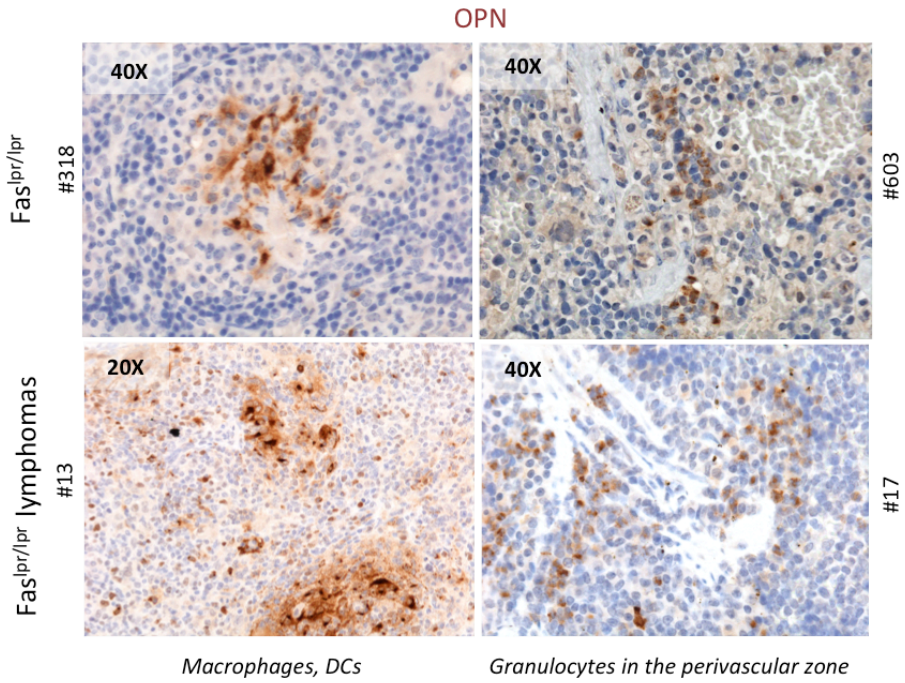

Figure 26. Expression of OPN by cells of the splenic microenvironment. IHC for OPN performed on FFPE sections from the spleen of Fas$^{lpr/lpr}$ mice indicates that OPN is expressed by some cells of the microenvironment, namely macrophages, DCs and granulocytes of the perivascular zone of the red pulp. Magnification 40x and 20x.

4.7 The activation of TLR9-MYD88 signaling pathway is enhanced in B cells from OPN-/-Fas$^{lpr/lpr}$ mice

To identify OPN-related pathways that could be implicated in driving B cell proliferation and transformation in autoimmune mice, we focused our attention on TLR9-MYD88 signaling pathway, since TLR9 binds double strand DNA, chronically circulating in the blood of autoimmune mice, and MYD88 has been described to co-localise with, and to be regulated by, iOPN [101,108,109]. Additionally, *MYD88* gene mutation has been identified as one of the most prevalent driver mutations in the ABC-DLBCL [84].

With the purpose of investigating whether MYD88 activity is influenced by the absence of OPN, we isolated through immunomagnetic beads CD19+ cells from the spleen of 4-month-old OPN-competent and -deficient animals, and stimulated them with CpG 1826, a TLR9 agonist. Interestingly, while naive B cells did not show any significant

difference upon stimulation (Fig. 27A), flow cytometry analysis indicated that CD19+ B cells from OPN-/-Fas$^{lpr/lpr}$ mice are more activated, based on the increased expression of CD86, compared to OPN-competent autoimmune B cells, after TLR9 triggering (Fig. 27B).

In agreement with the hypothesis of a more activated phenotype upon TLR9 stimulation, the protein level of molecules belonging to MYD88 signaling, such as IRAK1, and IRAK4, and MYD88 itself, are up-regulated in B cells deficient for OPN, both in steady state conditions and after stimulation with CpG 1826 (Fig. 27C), suggesting that the presence of OPN is able to restrain MYD88 signaling pathway.

Furthermore, OPN-sufficient and -deficient autoimmune CD19+ cells did not show any difference in the MYD88-related protein machinery when stimulated with TLR4 (MYD88-dependent) and TLR3 (MYD88-independent) agonists LPS and Poly I:C, respectively (Fig. 27C). These results suggest that the negative role exerted by B-cell intrinsic OPN mostly involves the TLR9 cascade, at least in this specific setting.

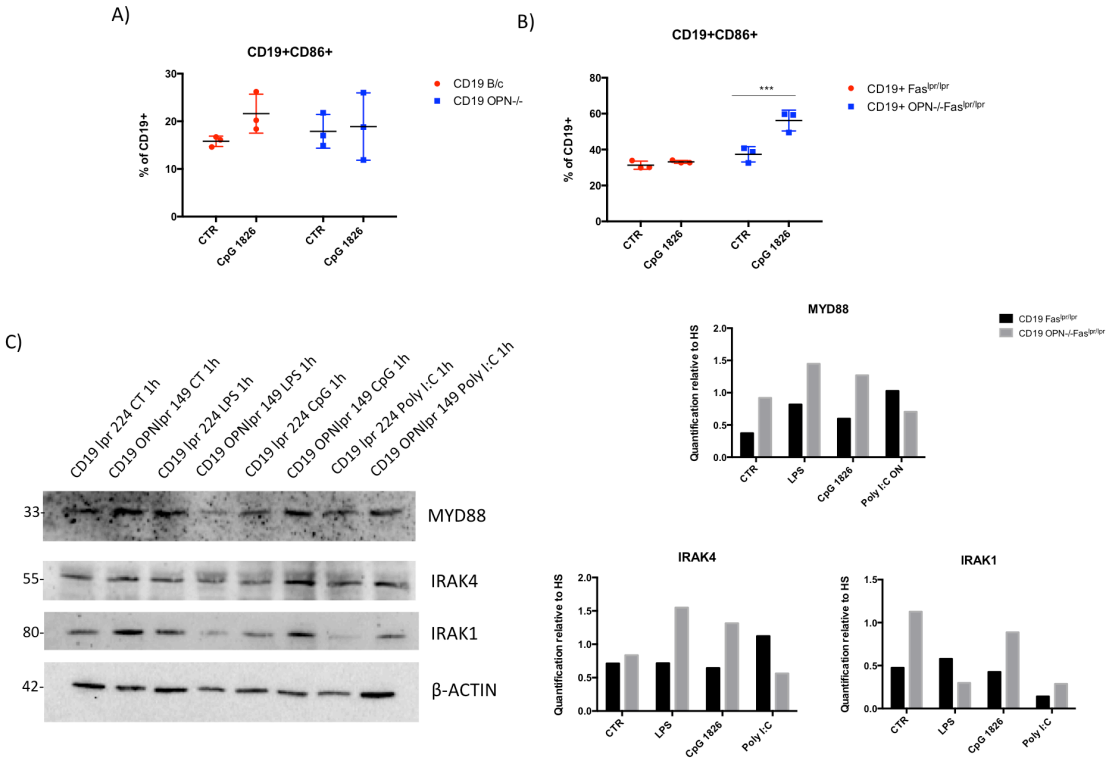

Figure 27. Evaluation of MYD88 signaling pathway in B cells from autoimmune mice. Flow cytometry analysis showing that, while no differences were found between OPN-deficient and -competent naïve mice (A), OPN-/-Fas$^{lpr/lpr}$ B cells had a significant increased activation, based on the expression of CD86, compared to Fas$^{lpr/lpr}$ CD19+ cells (B) after 3-day stimulation with CpG 1826. (***, P<0.001, Two-way ANOVA). C) Representative western blot performed on CD19+ B cells purified from OPN-competent and -deficient autoimmune mice revealing that the level of IRAK1, IRAK4 and MYD88 are enriched in OPN-/-Fas$^{lpr/lpr}$ mice at steady state condition and/or after TLR9-triggering with CpG 1826.

The same increase was not found between groups after TLR4- and TLR3- triggering with LPS and Poly I:C, respectively.

At this point, we wondered if the MYD88-dependent cascade was more activated in absence of OPN because of an increased amount of TLR9. For this reason, we evaluated its expression on CD19+ B cells through flow cytometry, finding a striking up-regulation of the receptor in 5/6-month-old OPN-/-Fas$^{lpr/lpr}$ mice in comparison with age-matched OPN-competent animals, both in terms of percentage of TLR9+ cells (Fig. 28A) and mean fluorescence intensity (MFI) of the protein (Fig. 28B).

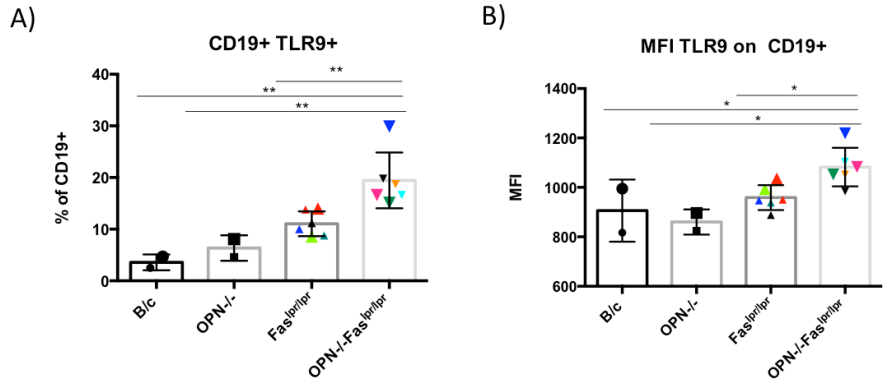

Figure 28. TLR9 expression in B cells from naïve and autoimmune mice. Flow cytometry analysis showing the expression of TLR9 gated on splenic CD19+ cells from B/c, OPN-/-, Fas$^{lpr/lpr}$ and OPN-/-Fas$^{lpr/lpr}$ mice. OPN-/-Fas$^{lpr/lpr}$ mice showed a significantly higher level of CD19+TLR9+ cells (**, P<0.01; Ordinary one way ANOVA) and TLR9 protein level (MFI) on CD19+ cells (*, P<0.05; Ordinary one way ANOVA) comparing to Fas$^{lpr/lpr}$ mice. Data in the graphs are referred to a pool of two independent experiments.

Together, these findings indicate that the TLR9-MYD88 signaling is enhanced in B cells from OPN-/-Fas$^{lpr/lpr}$ mice. To such increase, it may contribute not only a regulatory role exerted directly by iOPN, located in the endosomal compartment where TLR9 resides and signals, but also the higher expression of TLR9 in OPN-deficient B cells from autoimmune animals.

4.8 Lymphoma cell lines established from OPN-/-Fas$^{lpr/lpr}$ mice maintain the features of ABC-DLBCL

In order to more easily study the molecular mechanisms behind the observed phenotype, we tried to establish cell lines from the spleens of mice developing lymphomas, either

Fas$^{lpr/lpr}$ or OPN-/-Fas$^{lpr/lpr}$ mice. To this aim, once we had indication by flow cytometry of a lymphomatous phenotype (CD19+B220low/+IgM-), we seeded in *in vitro* culture splenic cells (as bulk or purified CD19+ cells). After several attempts, we managed to obtain only two cell lines, named OPL239 and OPL241, from the spleen of two 6-month-old OPN-/-Fas$^{lpr/lpr}$ mice. According to histopathological evaluation and immunofluorescence staining of their spleen (showed in Fig. 29), while OPL239 was derived from an early-stage DLBCL that still preserved the nodular architecture, OPL241 originated from a more advanced DLBCL, already spread in the spleen.

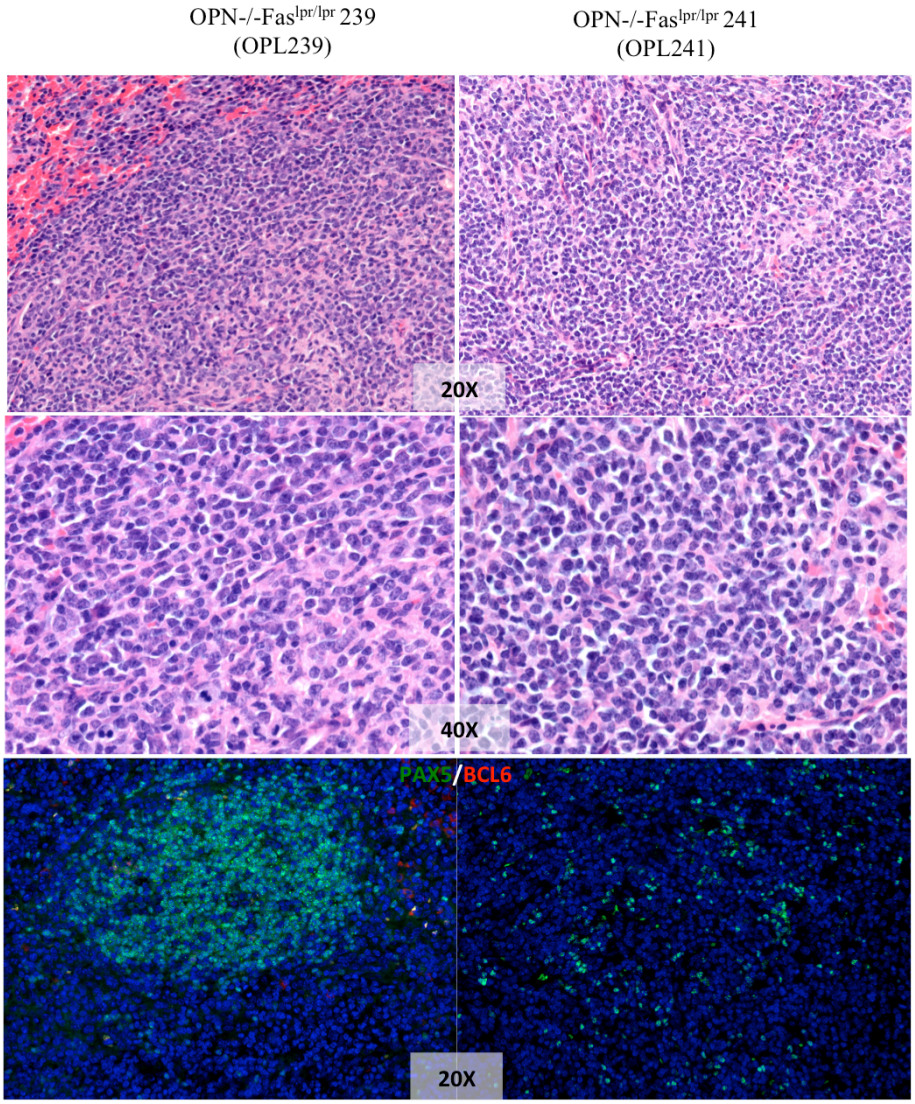

Figure 29. Phenotype of OPL239 and OPL241 cell lines through E/E and IF. Hematoxylin/eosin and immunofluorescence staining for PAX5/BCL6 performed on OPN-/-Fas$^{lpr/lpr}$ mouse spleens #239 and #241, from which OPL239 and OPL241 cell lines derive. According to the morphology and to PAX5 pattern, the former lymphomas is an early stage DLBCL still preserving a nodular architecture, while the latter is a widely spread DLBCL. Magnification 20x and 40x.

Both cell lines maintained *in vitro* the phenotype observed in the spontaneous lymphomas developing *in vivo*, with complete loss of surface IgM and positivity for B220 (Fig. 30). B cell lymphomas are usually B cell receptor (BCR)-dependent, although lymphomatous B cells that survive without BCR do exist [143]. In light of this evidence and of our finding of negativity for surface IgM, we wondered whether these lymphoma cell lines express on their membrane other surface immunoglobulins. By flow cytometry analysis, we observed that both cell lines maintained the expression of IgA, but not of IgD (Fig. 30), suggesting that they may still preserve the signaling of BCR.

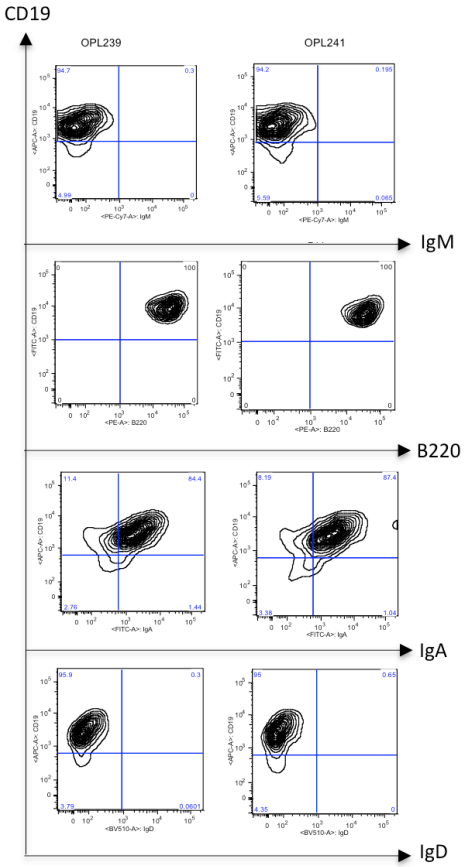

Figure 30. Flow cytometry characterization of OPL239 and OPL241 cell lines. Gates show that both cell lines express B220, are negative for surface IgM and IgD but are positive for IgA.

Furthermore, in line with the data observed in the spontaneous lymphomas, RT-qPCR showed that both cell lines expressed low levels of *Bcl6* and high levels of *Irf4/Mum1, Bcl2* and *c-myc* (Fig. 31A). The protein expression of IRF4, BCL2 and c-MYC was

confirmed by western blot (Fig. 31B).

We also compared the two cell lines for the activation of STAT3 and NFkB signaling pathways through Western blot. OPL241 line showed a stronger expression of phospho- and total p65, ph-STAT3 and of BCL2, in agreement with the histological evaluation of the original lymphomas (Fig. 31B)

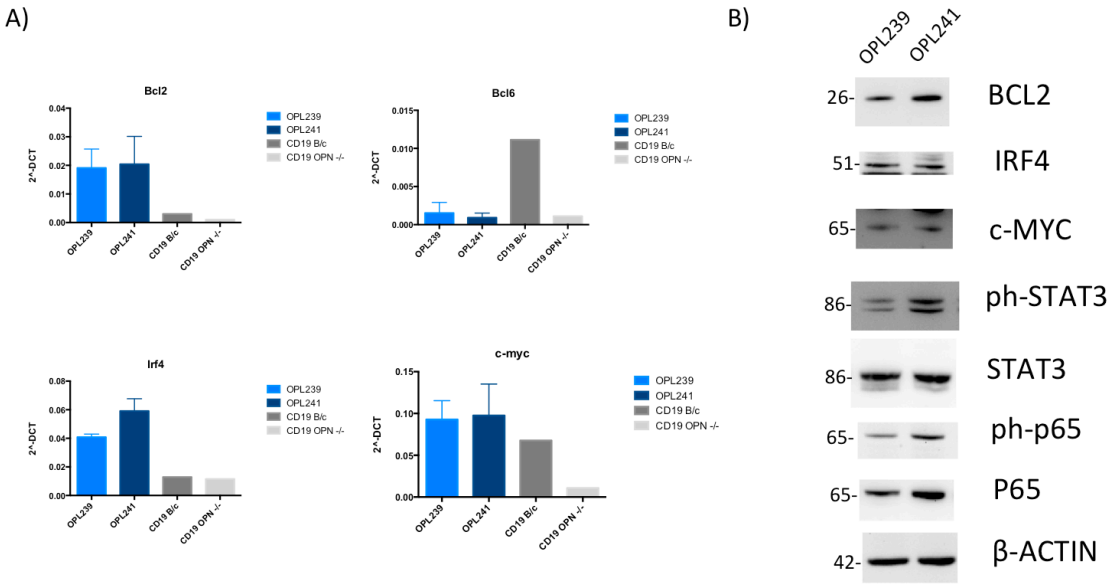

Figure 31. Phenotype of OPL239 and OPL241 cell lines through RT-PCR and Western Blot. A. RT-PCR showing that OPL239 and OPL241 cell lines did not express *Bcl6*, while were positive for *Bcl2*, *Irf4* and *c-myc*. CD19+ from B/c and OPN-/-mice were used as controls. Values related to transcripts are referred as 2^-DCT. B) Western blot on OPL239 and OPL241 lysates illustrating the protein level of BCL2, c-MYC, IRF4 and the basal level/activation of STAT3 and NFkB (p65) pathways. OPL241 was characterized by a greater expression of BCL2, ph-STAT3 and ph/total-P65 compared with OPL239.

Additionally, both OPN-deficient cell lines express also CXCR4 (Fig. 32) another feature that makes OPN-deficient lymphomas resembling the human ABC-DLBCLs.

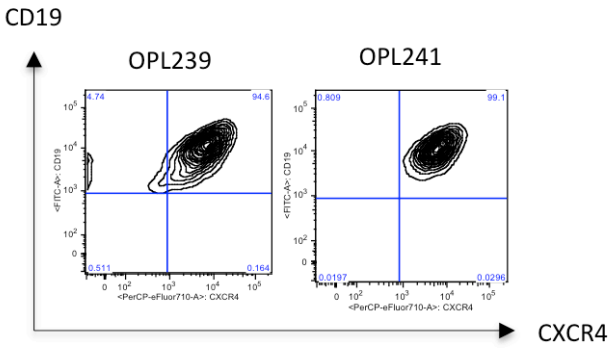

Figure 32. Expression of CXCR4 by OPL239 and OPL241 cell lines. Flow cytometry analysis showing that OPL239 and OPL241 cell lines expressed high level of CXCR4 (like human ABC-DLBCLs).

In line with the finding that the B cell population expanding and likely transforming in OPN-/-Fas$^{lpr/lpr}$ mice is the mature CD23-CD21/35- one, we evaluated the expression of these markers in OPL239 and OPL241 lines. Indeed, we found that, besides being negative for CD93, they were negative for CD21/35 and expressed very low level of CD23 (Fig. 33).

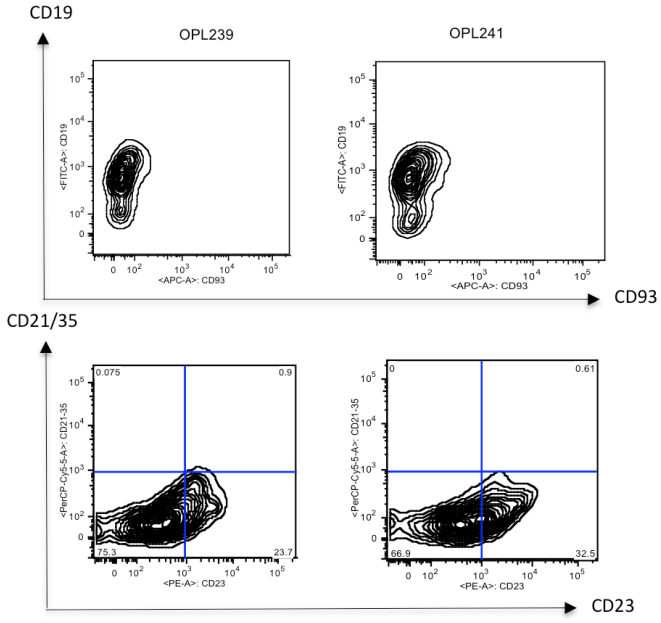

Figure 33. Hardy's multiparametric panel applied to OPL239 and OPL241 cells. Flow cytometry-derived gates showing that OPL239 and OPL241 DLBCL cell lines were negative for CD93 and CD21/35, and expressed very low level of CD23.

4.9 In vivo injection of DLBCL cell lines in OPN-/- hosts increases their ABC-like features.

To assess the *in vivo* tumorigenicity of the two lymphoma cell lines, we firstly intravenously injected them into immune-compromised mice (*nu/nu* nude mice and sub-lethally irradiated (5Gy) BALB/c mice), or immunocompetent (non-irradiated BALB/c mice), in the latter case at different doses (from $2{,}5x10^5$ up to $1x10^6$ cells). We found that both OPL239 and OPL241, identified as CD19+B220+/-IgM- cells, were able to grow in spleen and liver only in nude (Fig. 25A) and irradiated mice (Fig. 34B) but not in immunocompetent animals.

A)

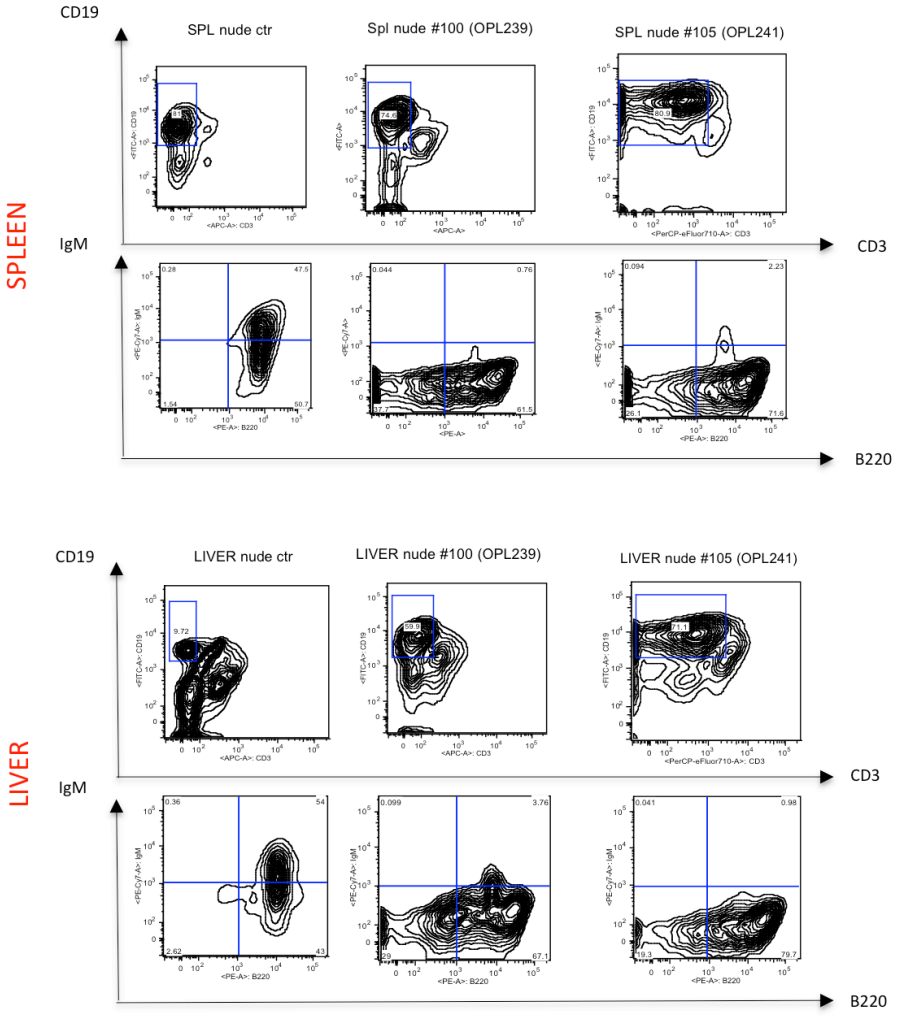

B)

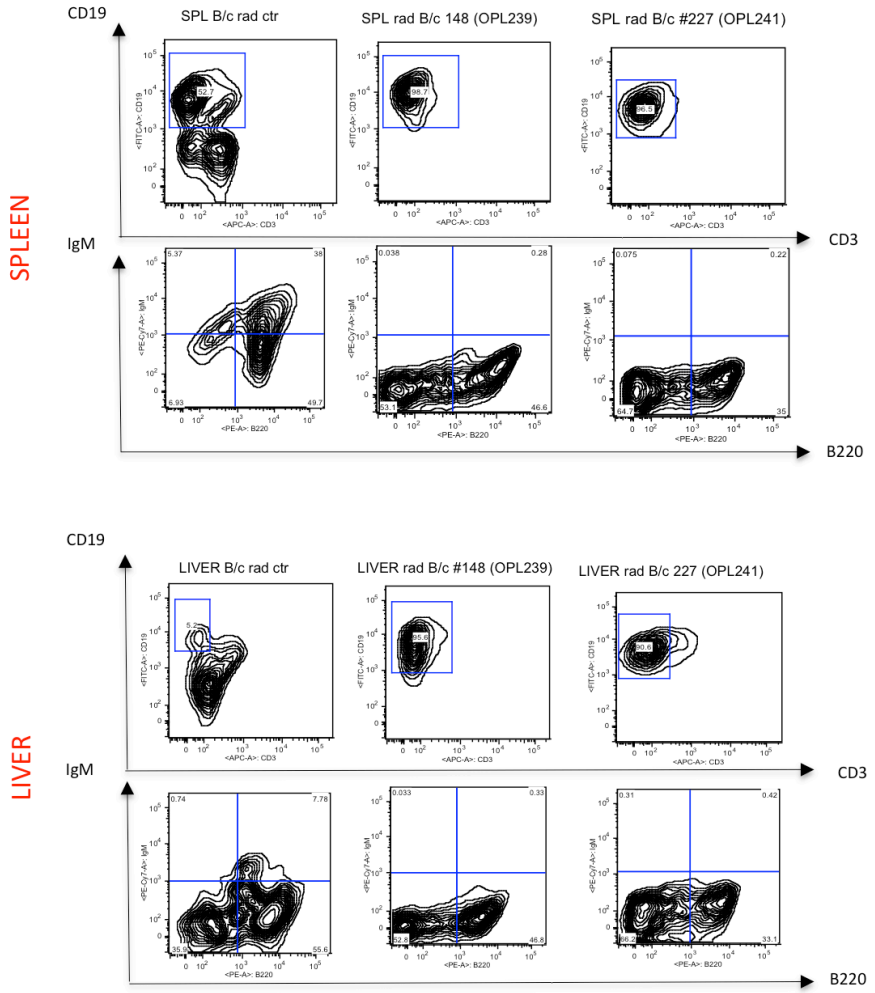

Figure 34. Injection of OPL239 and OPL241 in nude and irradiated B/c mice. Flow cytometry-derived plots showing the phenotype (CD19+IgM-B220+/-) of OPL239 and OPL241 grown in spleen (top) and liver (bottom) of nude (A) and sub-lethally-irradiated B/c mice (B). Spleens from nude and irradiated B/c mice were used as controls.

Additionally, in order to evaluate a possible role of the splenic microenvironment, either OPN-competent or -deficient, in their aggressiveness and phenotype, we injected OPL239 and OPL241 lines in sub-lethally irradiated BALB/c and OPN-/-hosts to study eventual difference in tumor growth and gene expression.

Considering that lymphomatous B cells have invaded the whole spleen of the animals from both strains (Fig. 35A), and comprised the totality of B cells present in the organ, we could not detect any difference in tumor take. However, we have been able to isolate tumor cells and analyse their expression of relevant genes by RT-PCR. Interestingly, both OPL239 and OPL241 tumors showed a significantly higher level of the MYD88-

target gene *Prdm1* when grown in OPN-/- animals, in comparison with lymphomas derived from OPN-competent mice (Fig 35B and C). In addition, we also observed a trend in the increase of the NF-kB target gene *Il6* and of the ABC/DE-DLBCL markers *Bcl2*, *Irf4* and *c-myc* in tumors from both cell lines when isolated from OPN-deficient hosts (Fig. 35B and C).

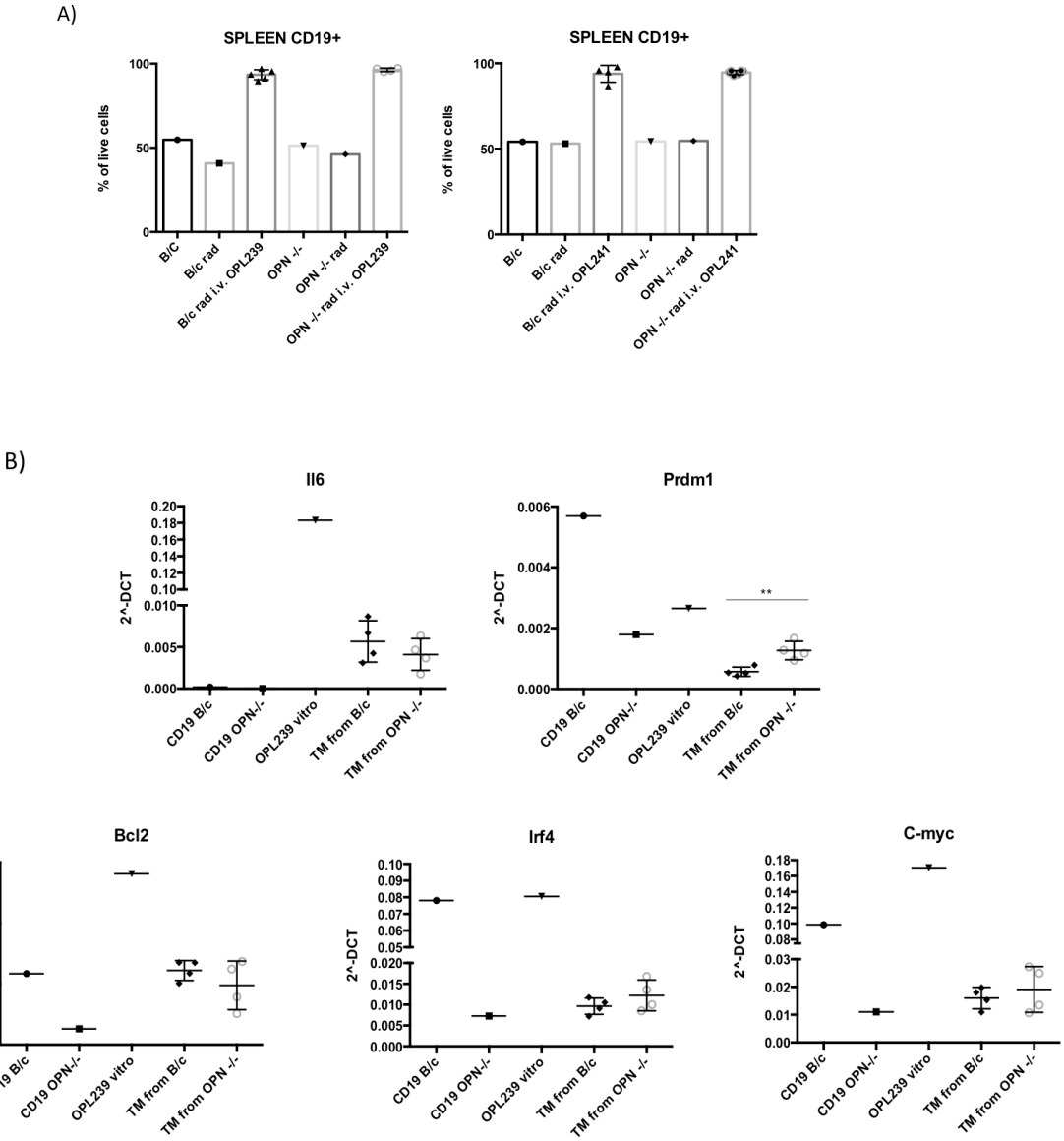

C)

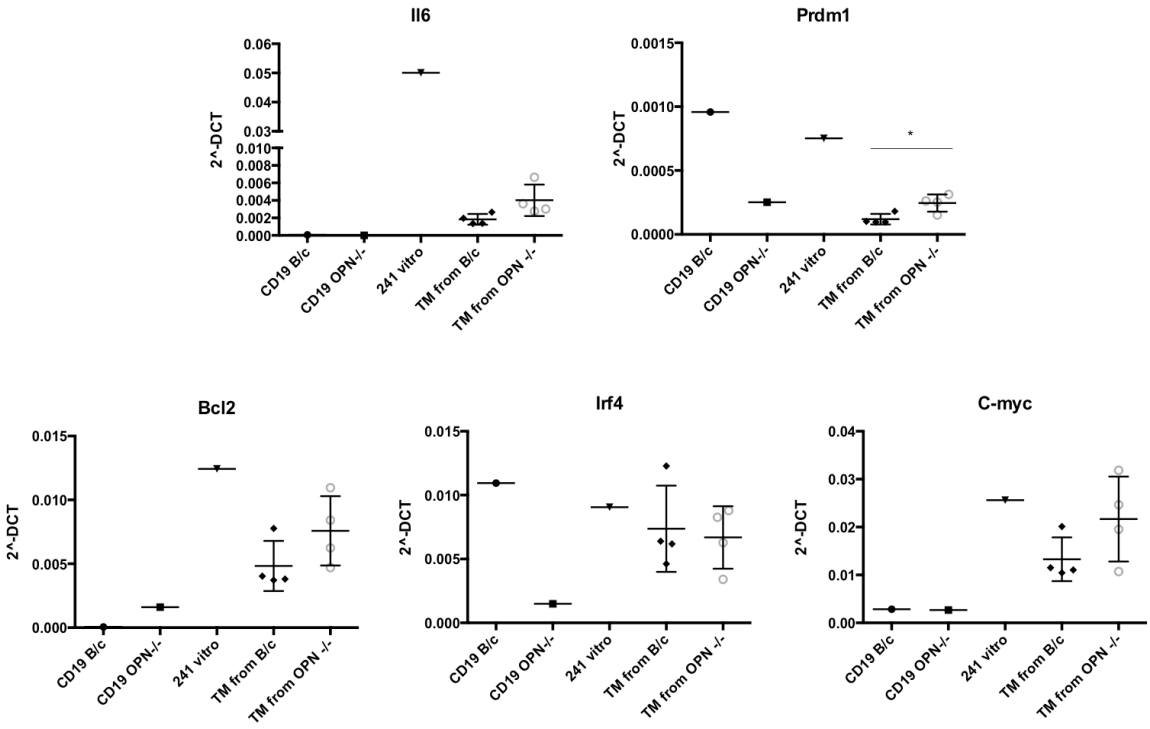

Figure 35. Injection of OPL239 and OPL241 in B/c and OPN-/- hosts. A) Flow cytometry analysis of the spleen of 4 B/c and 4 OPN-/- mice intravenously injected with OPL239 (left) and OPL241 (right), showing that tumour cells infiltrated the whole organ. One B/c and one irradiated B/c were used as controls. RT-PCR performed on OPL239 (B) and OPL241 (C) cells re-isolated from the spleen of 4 B/c and 4 OPN-/- after 10 days from i.v. injection. *Prdm1* was significantly upregulated in OPL239 (**, P<0.01; Student t test) and OPL241 (*, P<0.05, Student t test) if re-isolated from OPN-/- hosts. *Bcl2, Irf4, c-myc* and *Il6* showed no differences or a trend of increase in the same conditions. CD19+ cells from B/c, OPN-/- and the cell lines cultured *in vitro* were used as controls.

These findings may suggest that an OPN-deficient stroma is more supportive than a competent one in sustaining the dynamics of B lymphomagenesis, in agreement with the results observed in the spontaneous mouse model (see paragraphs 13).

4.10 Intracellular OPN prevents CpG-mediated STAT3 and/or NFkB activation in OPL239 and OPL241

Aimed at understanding which isoform of OPN is relevant in protecting from autoimmunity-driven lymphomagenesis, we decided to overexpress in the two lymphoma cell lines, which were derived from OPN-deficient autoimmune mice, either the full-length, secreted OPN (sOPN) or its intracellular isoform (iOPN), using

lentiviral vectors expressing, beside OPN sequence, also the GFP sequence as reporter. We infected cells with vectors expressing only IRES Green (empty/control vector), Spp1-IRES Green and iOPN-IRES Green, and, after sorting them based on GFP positivity, we checked the transcript level of *Spp1* through RT-PCR (Fig. 36A) and protein level of OPN, with or without the presence of Brefeldin A (BFA) to block protein secretion, through Western blot (Fig. 36B). Of note, the over-expression of the full-length secreted form was lower compared to that of the intracellular OPN, in both cell lines.

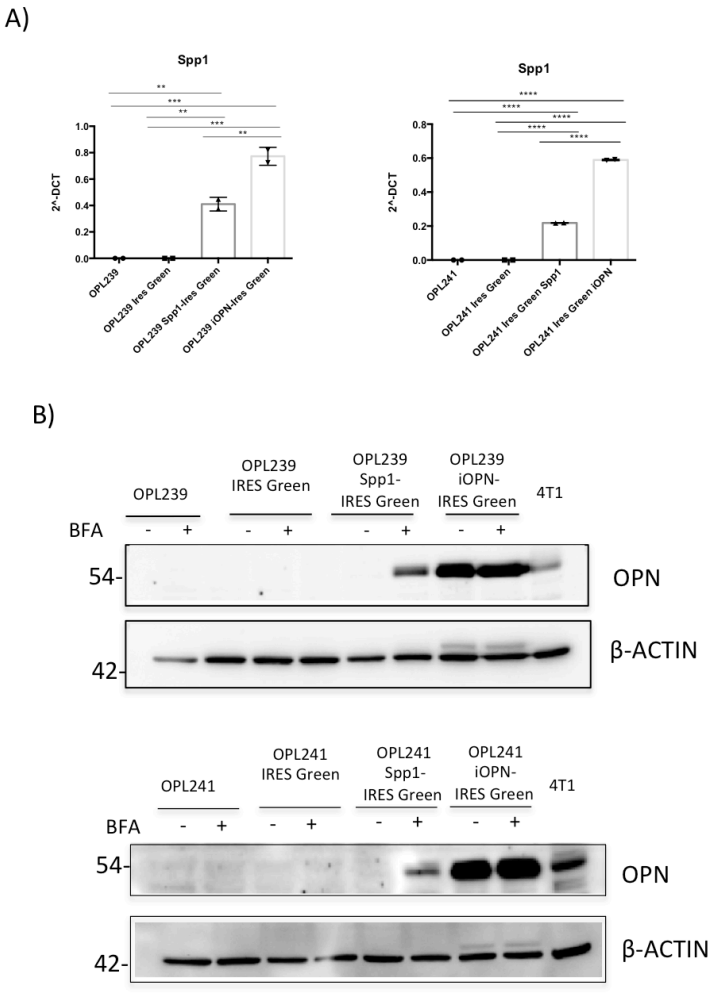

Figure 36. **Overespression of sOPN and iOPN in OPL239 and OPL241.** RT-PCR (A) and Western blot (B) on parental and IRES-Green based cells illustrating the *Spp1* mRNA level and OPN protein expression (in presence or not of BFA, that blocks protein secretion), respectively. Both techniques indicated that both *Spp1*- and iOPN overexpressing lines expressed OPN, although the infection was less efficient in the former type of cells. 4T1 mammary cell line was used as positive control.

Additionally, in order to visualize the localization of the ectopic OPN in the overexpressing variants, we performed immunofluorescence staining on cytospin

preparations (Fig. 37). We found that *Spp1*-overexpressing OPL241 cells are characterized by a small amount of OPN in steady state conditions, as it is secreted, while in presence of BFA the protein level increases and shows a cytoplasmatic/Golgi distribution, as expected. Interestingly, intracellular OPN, whose expression does not change upon BFA treatment, shows a peri-nuclear distribution.

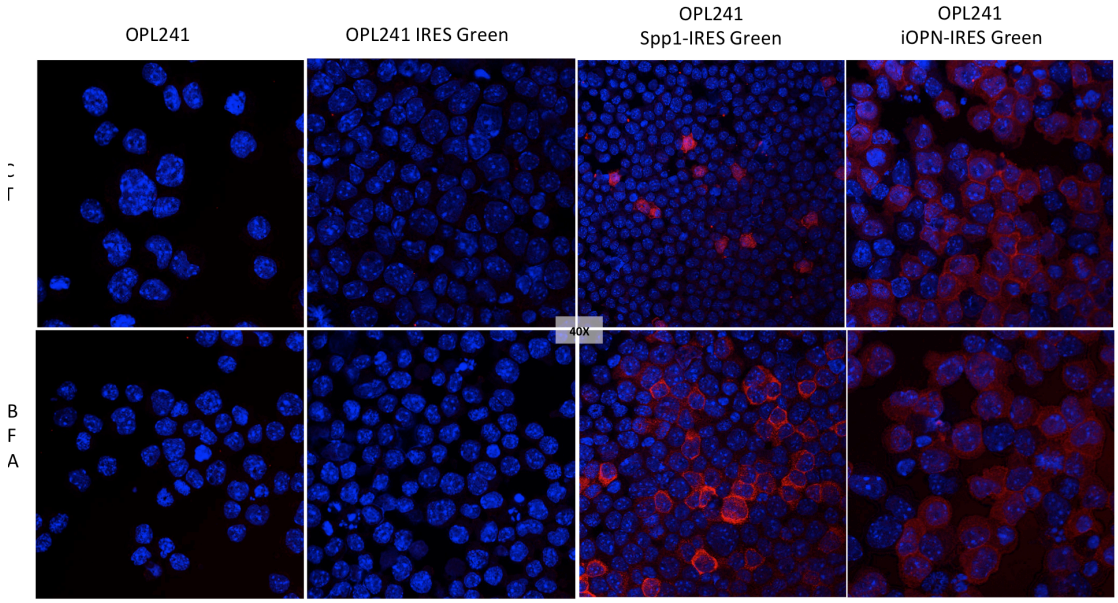

Figure 37. Representative IF for OPN on OPL241 parental and IRES Green-based variants. *Spp1*-overexpressing cells showed a discrete amount of OPN, increased upon BFA treatment, that preserved a cytoplasmatic/Golgi distribution. In iOPN-overexpressing cells, OPN showed a peri-nuclear distribution and did not increase upon BFA treatment. Magnification 40x.

To mimic the physiological scenario present in autoimmune mice in which ds-DNA constantly circulates in the blood and to trigger TLR9, we decided to stimulate parental and genetically-modified cells with the TLR9 agonist CpG 1826 and check the activation of pathways important for B cell survival and proliferation. Firstly, as shown in figure 38A, we confirmed the expression of TLR9 through flow cytometry in both parental cell lines. Remarkably, as concerns OPL239 variants (Fig. 38B), we found that the activation of STAT3 (ph-STAT3) is almost abolished in iOPN-overexpressing cells, despite similar amount of total protein, suggesting that the presence of iOPN is able to inhibit TLR9-MYD88-STAT3, whereas secreted OPN does not affect this pathways. Differently, NFkB pathway does not seem significantly modulated by 30-minute CpG stimulation in all cell variants, although the overall level of both total and phospho-p65 protein is slightly decreased in iOPN-overexpressing cells, indicating that a 30 minutes

stimulation may not be the right time point to detect NF-kB activation in this specific setting.

In the same experiment we also collected RNA at 3h and 6h after CpG stimulation, to check the induction of genes target of the TLR9 cascade, such as *Il6* and *Tnfa* (Fig. 38C). Interestingly, at 3h time point we found that OPL239 over-expressing *Spp1* significantly up-regulated both genes upon TRL9-triggering, whereas in the presence of iOPN, the level of the same transcripts did not change after administration, in line with Western Blot result. At 6h, all genes returned at their basal level as non-stimulated cells, suggesting a fast kinetics of CpG stimulation in OPL239 cell line variants.

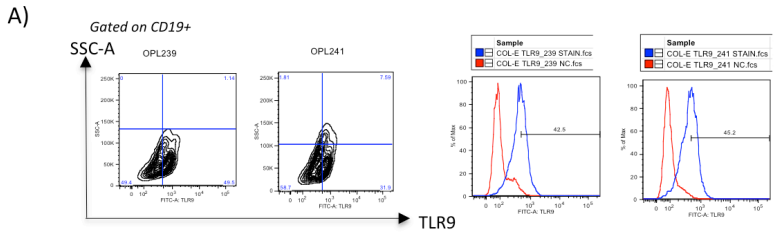

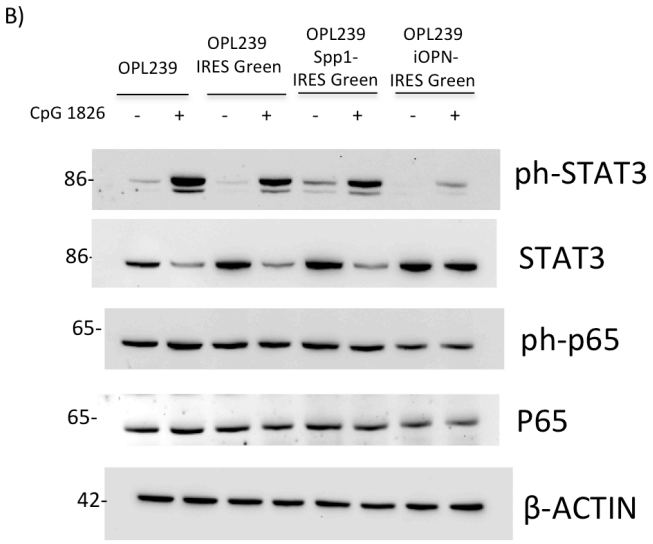

C)

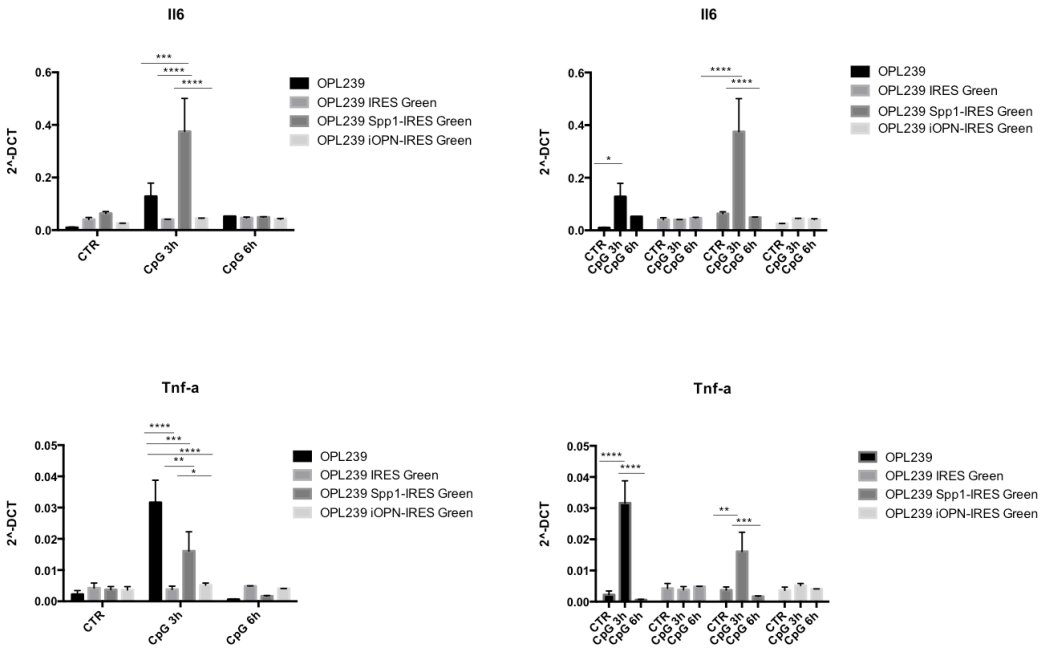

Figure 38. **Evaluation of TLR9-MYD88 pathway in OPL239 cell lines.** A) Flow cytometry plots and histograms showing that OPL239 and OPL241 cell lines express TLR9. B) Western blot analysis performed on OPL239 parental cells and IRES Green-based variants, stimulated or not with TLR9 agonist CpG 1826 for 30 min. Only in OPL239 iOPN-IRES Green the CpG-mediated activation of STAT3 is dampened. iOPN-expressing cells showed a minor level of ph- and total p65 regardless the stimulus. C) Evaluation through RT-PCR of *Il6* and *Tnfa* in OPL239 parental and IRES-Green-based cells, after 3h- and 6h-stimulation with CpG 1826. Comparing all variants in the condition of 3h-stimulation, OPL239 Spp1-IRES Green showed a significantly higher level of *Il6* compared with parental cells (***, P<0.001; Two-way ANOVA), cells with the empty vector (****, P<0.0001; Two-way ANOVA) and iOPN-overexpressing cells (****, P<0.0001; Two-way ANOVA). In the setting of 3h-stimulation, OPL239 Spp1-IRES Green showed a significantly increased level of *Tnfa* compared with iOPN-overexpressing cells (*, P<0.05; Two-way ANOVA) and cells with the empty vector (**, P<0.01; Two-way ANOVA), but decreased compared to parental cells (***, P<0.001, Two-way ANOVA).

The same experiment was performed with OPL241 and its variants, finding, unexpectedly, a different behavior. Basically, OPL241 and its variants seem less sensitive to TLR9 stimulation than OPL239, as none of them show significant activation of both STAT3 and p65 pathways, with only a slight induction of ph-STAT3 in the parental OPL241 line (Fig. 39A). The most relevant observation was the complete absence of total and, consequently, of phospho-p65 in OPL241 iOPN-IRES Green after TLR9-stimulation (Fig. 39A), indicating that likely iOPN blocks this

pathway also at transcriptional level. Furthermore, the phosphorylation of STAT3 was reduced in iOPN-overexpressing cells regardless the stimulus (Fig. 39A).

OPL241 cell variants showed differences also in the transcriptional level of *Il6* and *Tnfa* in comparison to OPL239 cells. Particularly, *Il6* was up-regulated at 3h time point in OPL241 over-expressing *Spp1* at the same level of control cells, while iOPN-overexpressing cells did not show any increased expression (Fig. 39B). Only the parental OPL241 line up-regulated *Tnfα* expression upon TLR9 triggering, whereas its levels were not modified in any of the genetically-modified variants (Figure 39B).

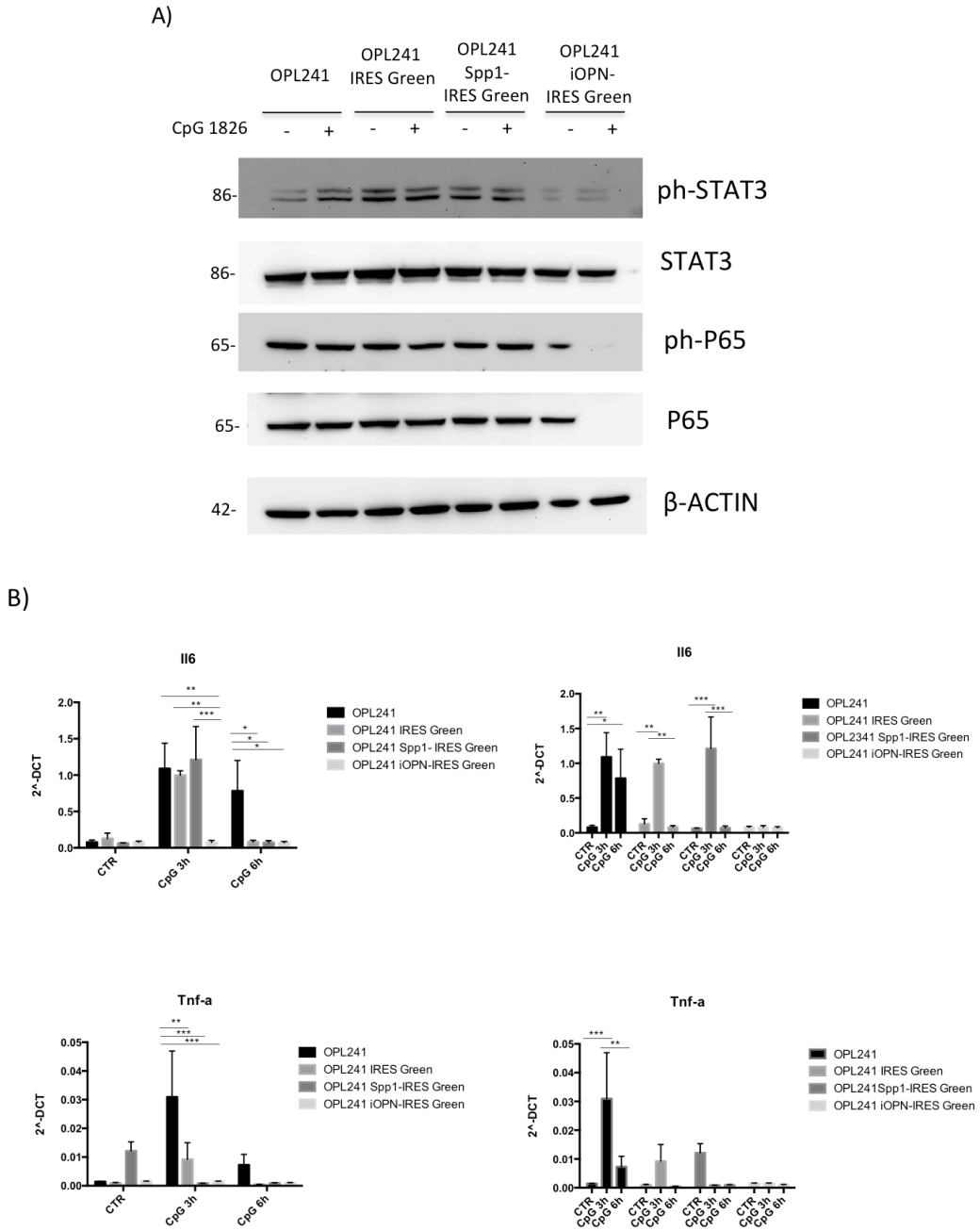

Figure 39. Evaluation of TLR9-MYD88 pathway in OPL241 cell lines. A) Western blot analysis performed on OPL241 parental and IRES-Green-based cells, stimulated or not with TLR9 agonist CpG 1826 for 30 min. OPL241 iOPN-IRES Green totally abrogated the expression of both ph-NFkB and total NFkB, while no effect on STAT3 could be detected upon stimulus. B) RT-PCR on *Il6* and *Tnfa* after 3 and 6 hours of CpG 1826 stimulation. *Il6* was significantly decreased after 3h-stimulation in OPL241 iOPN-IRES Green comparing with parental cells (**, P<0.01, Two-way ANOVA), OPL241 IRES Green (**, P<0.01, Two-way ANOVA), and OPL241 Spp1-IRES Green (***, P<0.001, Two-way ANOVA). At the same time point, OPL241 showed a significant higher level of *Tnfa* compared with cells with the empty vector (**, P<0.01; Two-way ANOVA), *Spp1*- (***, P<0.001; Two-way ANOVA) and iOPN-overexpressing cells (***, P<0.001; Two-way ANOVA).

A possible explanation for the different behaviour of the two cell lines upon genetic modification with OPN-expressing vectors could be a baseline different activation of the MYD88 pathway in OPL241 in comparison to OPL239, as STAT3 and p65 pathways were more activated even at steady state conditions in OPL241 cells, as already described in Figure 40B. This hypothesis is in line with the histological evaluation of the spleens from which OPL239 and OPL241 have been derived, as OPL239 is an early-stage lymphoma, likely more dependent on the microenvironment than OPL241, which derives from a more advanced and aggressive DLBCL.
These results overall indicate that the intracellular isoform of OPN could represent a brake in MYD88-triggered STAT3 and NFkB pathways in autoimmunity-driven B cell lymphomas, likely explaining why in OPN-deficient mice the transformation of B cells occurs more frequently, and likely faster, than in OPN-competent animals.

4.11 In vivo effect of OPN over-expression in lymphoma cells

At this point, we wondered whether the over-expression of either sOPN or iOPN in lymphoma cells could affect their behaviour *in vivo,* in terms of tumor growth and immune infiltrate. We therefore intravenously injected OPL239 IRES Green, Spp1-IRES Green and iOPN-IRES Green cells in sub-lethally irradiated BALB/c mice.
Notably, as shown in figure 40A, OPL239 Spp1-IRES Green cells showed a striking increase in tumor take, assessed as CD19+GFP+ population, both in spleen and liver, in comparison to control and iOPN-overexpressing cells, confirming the well-established pro-tumorigenic role of secreted OPN also in this hematological setting. Remarkably, iOPN-IRES Green cells showed a reduced tumor take compared with OPL239 IRES Green control cells in the spleen. In the liver, which is affected by lymphoma al lower

levels than spleen, *Spp1* over-expression in tumor cells confirmed the increased growth, whereas the tumor take of control cells was too low to detect any difference with iOPN-expressing cells.

These results indicate that iOPN not only does not exert the pro-tumorigenic and pro-inflammatory activities as sOPN does, but also that it may be able to restrain DLBCL growth.

In line with these findings, we found that OPL239 Spp1-IRES Green tumors promoted a significant enrichment in CD4+Foxp3+ T regulatory (Tregs) cells in the spleen, compared with OPL239 IRES Green and OPL239 iOPN-IRES Green cells, that were also highly proliferating, based on Ki67 expression (Fig. 40B). As concerns the myeloid compartment (C), OPL239 Spp1-IRES Green showed a marked reduction of the total CD11b+ cells compared with OPL239 IRES Green and OPL239 iOPN-IRES Green cells, presumably due to the significantly diminished percentage of F480+ cells (macrophages). No differences were observed in the granulocyte subset.

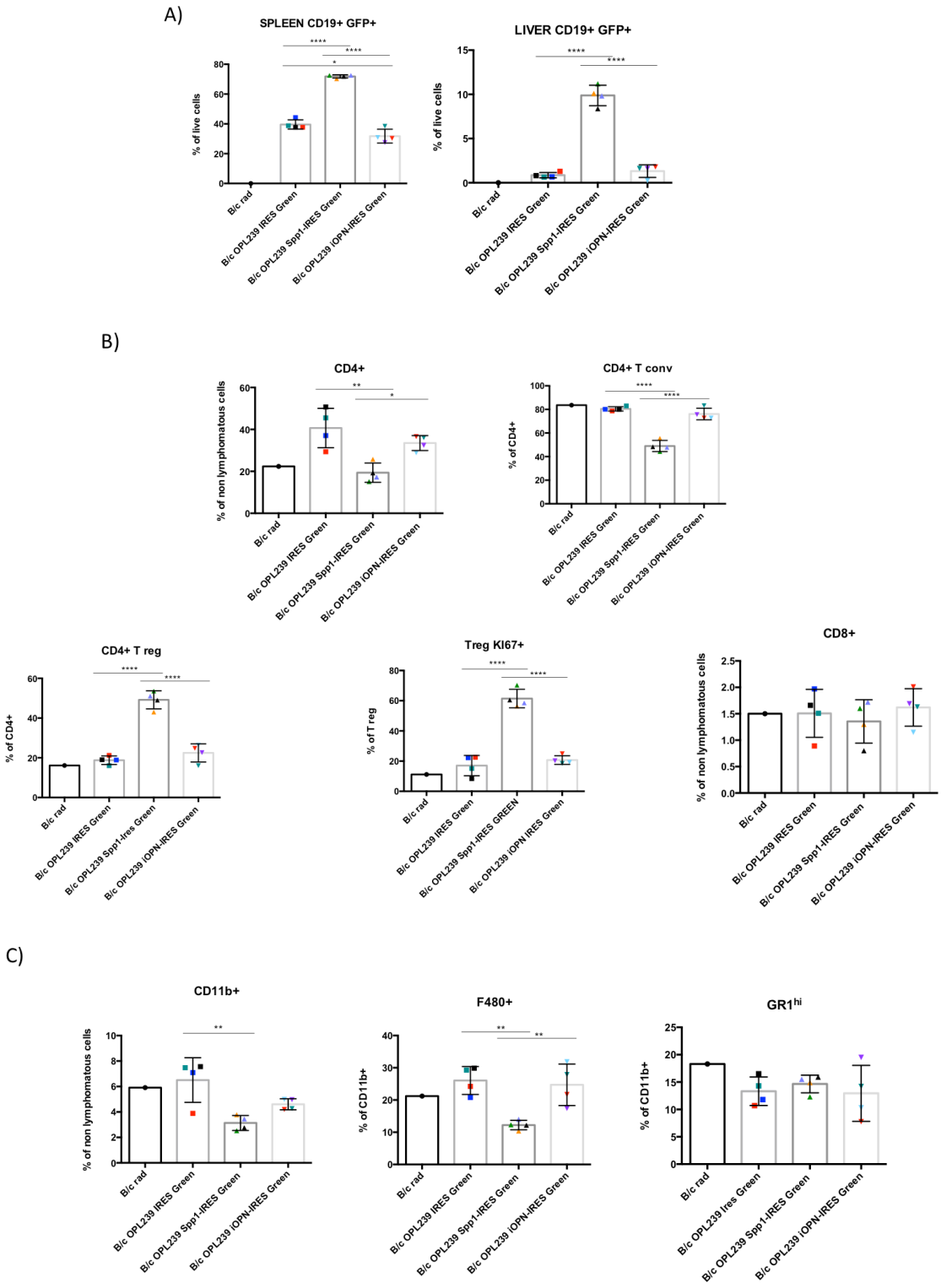

Figure 40. Injection of OPL239 variants in BALB/c mice. A) Flow cytometry analysis showing that, in the spleen, OPL239 overexpressing *Spp1* had a significantly higher tumour expansion than OPL239 IRES Green (****; P<0.0001; Ordinary One-way ANOVA) and OPL239 iOPN-IRES Green (****, P<0.0001; Ordinary one way ANOVA). iOPN-overexpressing cells showed a significant lower tumor growth compared with the control cells (*, P<0.05; Ordinary one way ANOVA). In the liver, *Spp1*-overexpressing cells showed a strikingly higher tumor growth compared with cells with the empty vector

(****, P<0.0001; Ordinary one way ANOVA) and cells overexpressing iOPN (****, P<0.0001; Ordinary one way ANOVA). B) Flow cytometry analysis showing that *Spp1*-overexpressing cells recruited a significantly higher number of Treg cells compared with OPL239 IRES Green (****, P<0.0001; Ordinary one way ANOVA) and iOPN-IRES Green (****, P<0.0001; Ordinary one way ANOVA). Treg cells were also more proliferating (Ki67+) in the same comparisons (****, P<0001; Ordinary one way ANOVA). C) Flow cytometry-derived graphs illustrating that *Spp1* overexpressing cells showed a significantly reduced percentage of CD11b+ cells compared with empty vector (**, P<0.001; Ordinary one way ANOVA), and a trend of reduction compared to iOPN overexpressing line. OPL239 Spp1-IRES Green significantly reduced F480+ macrophages in comparison to the other two variants. (**, P<0.01; Ordinary one way ANOVA). An irradiated B/c mouse was used as control.

To assess whether the different *in vivo* growth was due to a different proliferation rate *in vitro*, we analysed their proliferation by XTT assay (Fig. 41), finding no significant difference between the different variants.

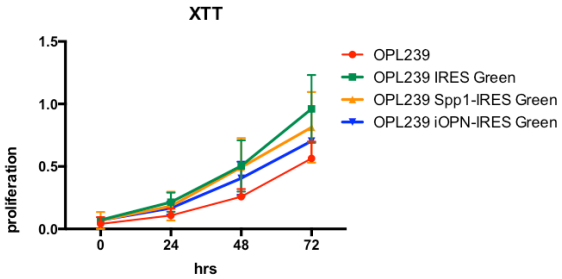

Figure 41. Proliferation capacity of OPL239 variants *in vitro*. XTT-related graph illustrating the proliferation capacity of OPL239 variants along time (0 h, 24 h, 48 h, 72 h). No significant differences were found among cell lines. The graph shows a pool of two independent experiments.

Altogether, these results confirm that the over-expression of secreted OPN by lymphoma cells induces an aggressive phenotype, associated to a tolerant microenvironment, allowing tumour cells to proliferate and colonize organs and indicate that, on the contrary, iOPN does not exert such effects but rather, it may restrain inflammation and possibly tumor growth.

4.12 OPN-/-Fas$^{lpr/lpr}$ mice show alterations in the splenic immune populations during the lymphomagenesis process

Although DLBCL seems to be one of the lymphoma subtypes less dependent on the tumor microenvironment [144], we wanted to assess whether the absence of OPN affected other immune cells of the SLO microenvironment in association with either autoimmune features or the expansion of neoplastic clones. At this purpose, we

performed a flow cytometry analysis on the spleen of 5/6-month-old mice to evaluate the percentage of B cells (CD19+), autoimmune cells (CD3+B220+), CD4+ and CD8+ T cells, myeloid cells (CD11b+), and, among the latter, granulocytes ($Gr1^{hi}$), monocytes ($Ly6c^{hi}$), classical dendritic cells (cDCs ;CD11c+B220-) and plasmacytoid dendritic cells (pDCs; CD11c+B220+). As illustrated in figure 42, an expected massive infiltration of CD3+B220+ autoreactive T cells was observed in $Fas^{lpr/lpr}$ mice, higher than that in OPN-deficient autoimmune animals. Notably, $Fas^{lpr/lpr}$ mice showed also a higher percentage of pDC (CD11c+B220+ cells), in line with the exacerbate autoimmunity of this strain and with the role of this population in autoimmunity. CD19+ cells showed a reduction in their relative number in OPN-deficient autoimmune mice compared with OPN-competent ones, but were characterized by a higher proliferation rate (CD19+Ki67), as already described in figure 18. No differences in the other lymphoid populations were observed among OPN-competent and -deficient strains.

A significant difference between $Fas^{lpr/lpr}$ and OPN-/-$Fas^{lpr/lpr}$ animals was observed in the myeloid compartment (CD11b+) that was expanded in the latter strain, mainly due to an increase in the granulocytic ($Gr1^{hi}$) and monocytic ($Ly6c^{hi}$) subsets (Fig. 42).

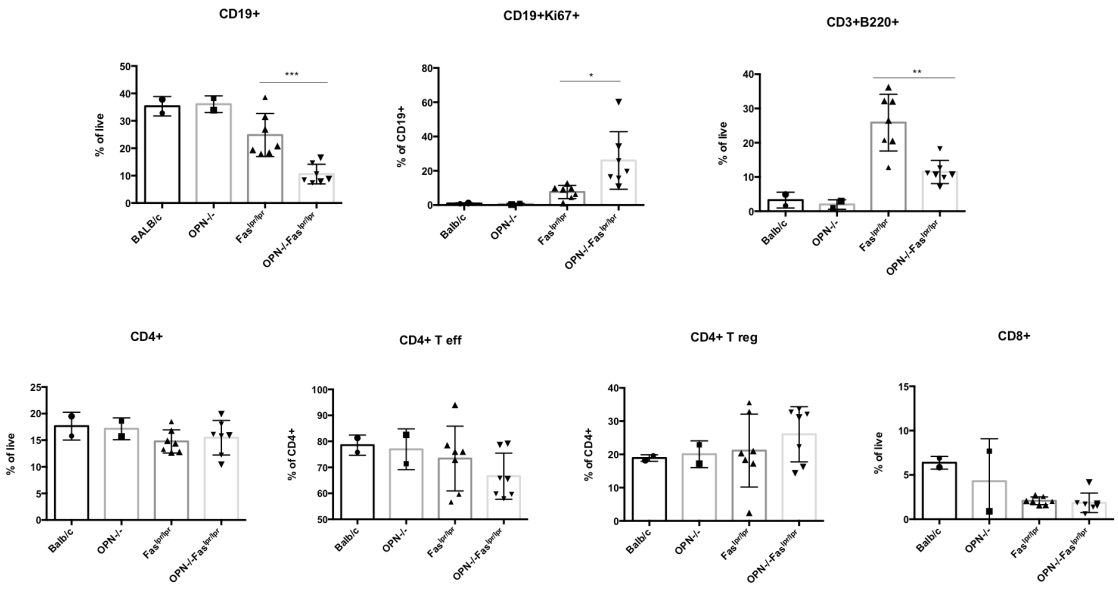

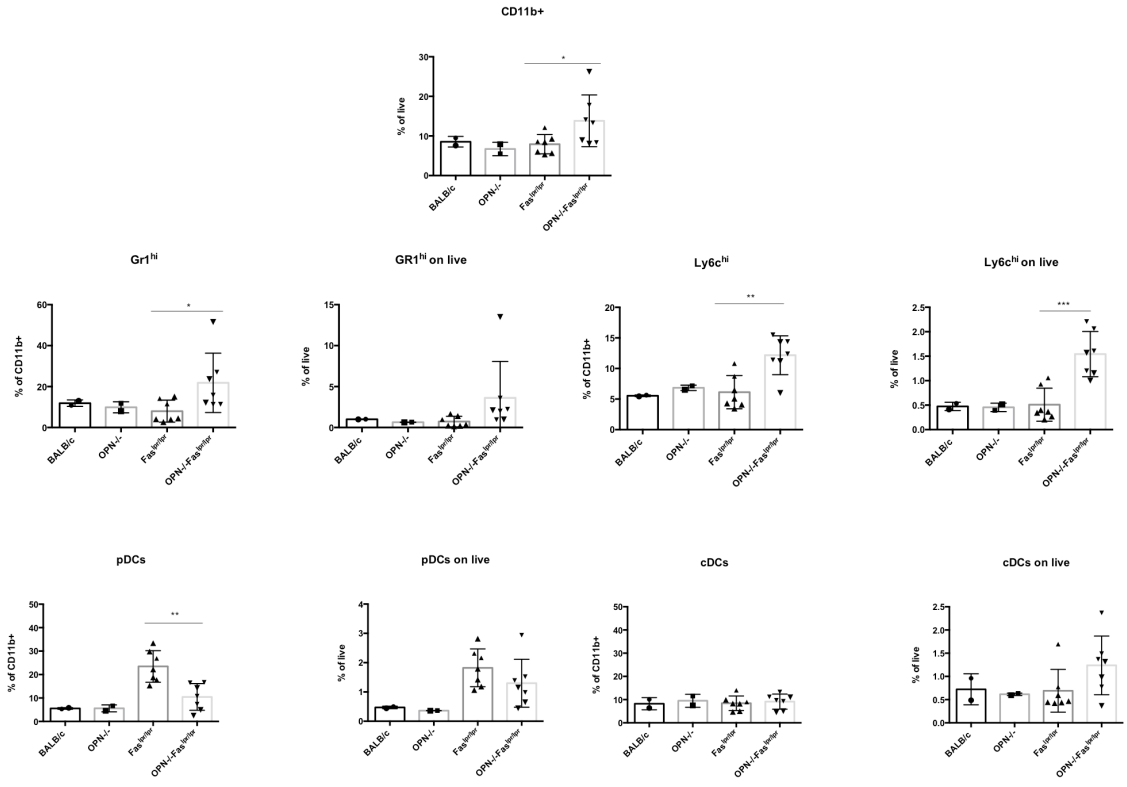

Figure 42. Flow cytometry characterization of the splenic immune populations from naïve and autoimmune mice. Flow cytometry analysis showing the different lymphoid and myeloid populations in the spleen of B/c, OPN-/-, Fas$^{lpr/lpr}$ and OPN-/-Fas$^{lpr/lpr}$ mice at time of sacrifice (5-6 months of age). Relative number of CD19+ cells was reduced in OPN-deficient autoimmune mice compared with OPN-sufficient counterparts (***, P<0.001; Student t test), but their proliferation rate (CD19+Ki67+) was much higher in the same comparison (*, P<0.05; Stuent t test). CD3+B220+ autoimmune T cells diminished in the same group (**, P<0.01; Student t test). CD11b+ myeloid cells were enriched in OPN-/-Fas$^{lpr/lpr}$ compared with Fas$^{lpr/lpr}$ mice (*, P<0.05; Student t test), due to an increase of Gr1^{hi} cells (*, P<0.05, Student t test) and Ly6c^{hi} cells (**, P<0.01, Student t test). Autoimmunity-associated pDCs were enriched in Fas$^{lpr/lpr}$ compared to OPN-/-Fas$^{lpr/lpr}$ spleens (**, P<0.01; Student t test. The graphs show a pool of two independent experiments.

To confirm the flow cytometry analysis and to assess whether the absence of OPN also affected the spatial localization of the different immune cell subsets in the spleen in relation to the neoplastic clones, we performed IHC on spleen sections from both Fas$^{lpr/lpr}$ and OPN-/-Fas$^{lpr/lpr}$ mice for MPO (granulocytes), F4/80 (macrophages), CD4+ and CD8+ T cells (Fig. 43A). Despite MPO+ and F480+ myeloid cells are moderately present in the splenic parenchyma of both autoimmune mice without any relevant changes in tumorigenic spleens, their localization is at the edge of the lymphomatous zones (c-MYC+). T lymphocytes, both CD4+ and CD8+, are in close contact to the neoplastic clones. In particular, CD4+ T cells are abundant in the spleen of both Fas$^{lpr/lpr}$

and OPN-/-Fas$^{lpr/lpr}$ mice. In presence of lymphomas, while in Fas$^{lpr/lpr}$ mice, CD4+ T cells are reduced, in OPN-/-Fas$^{lpr/lpr}$ lymphomas at early stages they are still abundant and in contact with c-MYC+ tumor cells, whereas in late stages OPN-deficient lymphomas they are almost completely lost. The most significant finding is related to CD8+ cells, which are discretely present in the splenic autoimmune parenchyma of both strains and strongly increased in presence of lymphomas in Fas$^{lpr/lpr}$ mice, and even more, in OPN-/-Fas$^{lpr/lpr}$ lymphomatous spleens. Another interesting feature of CD8+ T cells is that, only in the case of early OPN-deficient tumours, they showed the typical morphology of activated stellate T cells and heavily infiltrate the lymphomatous zones. These observations indicate that OPN-deficient tumours induce the recruitment of adaptive T cells that, however, seem to have a dysfunctional phenotype, as suggested by the expression of TIM3 and PD1, detected by flow cytometry analysis, on CD8+ T cells infiltrating OPN-/-Fas$^{lpr/lpr}$ spleens (Fig. 43B).

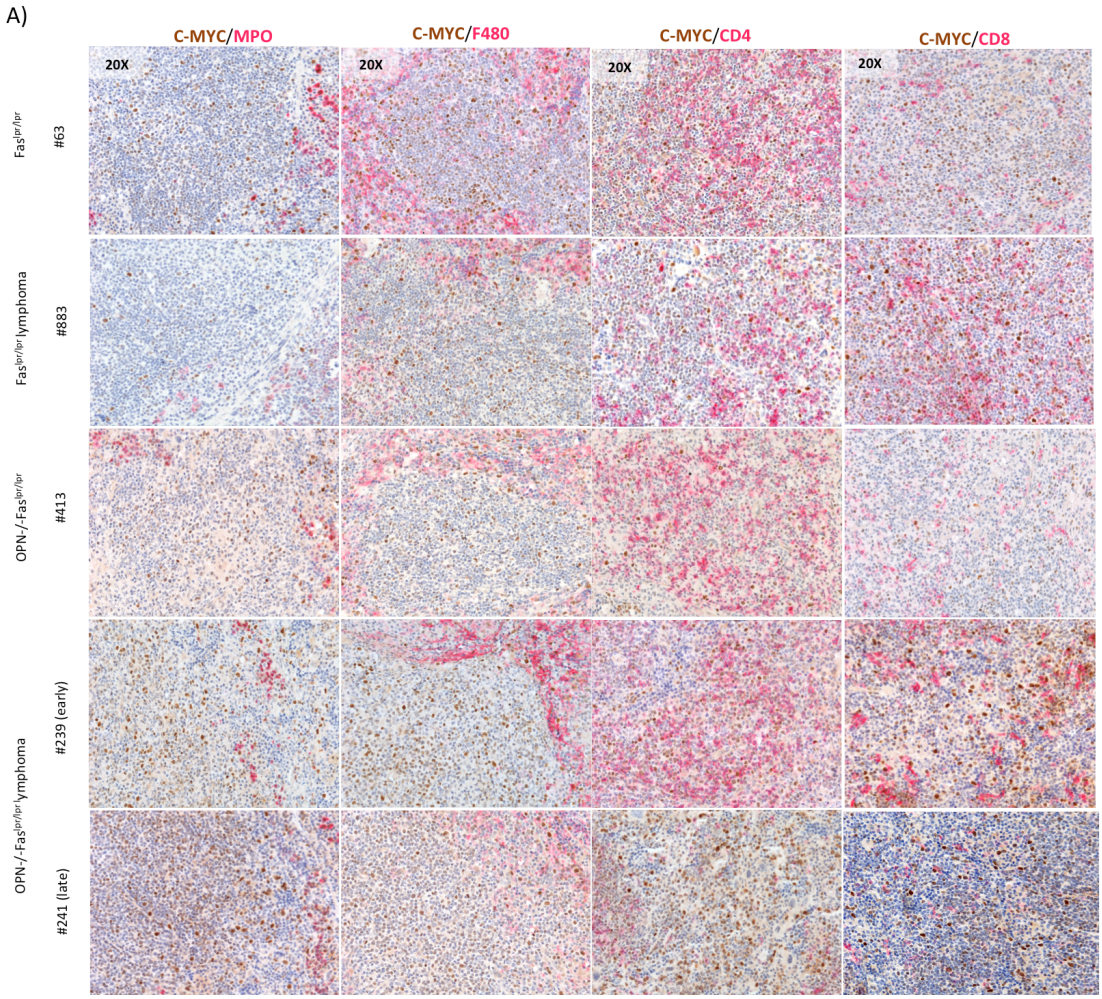

B)

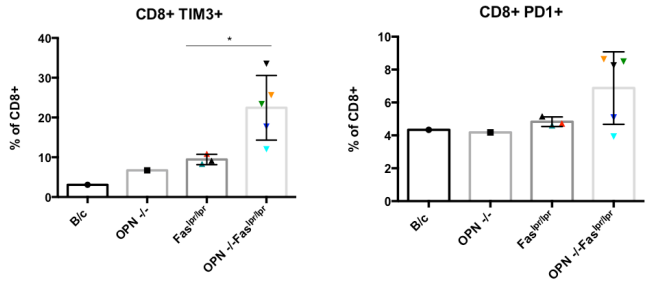

Figure 43. Evaluation of splenic immune population *in situ.* A) Double IHC on FFPE spleens for c-MYC/MPO (tumour cells/granulocytes), c-myc/F480 (tumour cells/macrophages), c-MYC/CD4 and c-MYC/CD8. Figures show that F480+ and MPO+ cells are present nearby the early stage lymphomas but are excluded from the representative lymphomatous zone of the late-stages tumours. CD4+ and CD8+, with an activated morphology in case of OPN-deficient mice, infiltrate lymphomatous areas. Magnification 20x. X. B) Flow cytometry graph showing that the percentage of CD8+TIM3+, likely exhausted cells, are significantly enriched (*, $P<0.05$, Student t test), while CD8+PD1+ showed a trend of increase, in OPN-/-Fas$^{lpr/lpr}$ mice.

Altogether, these data describe how lymphoid cells, more than the myeloid counterparts, abundantly infiltrate autoimmune and lymphomatous parenchyma, and that CD8+ infiltrating OPN-/- tumours are recruited but likely disfunctional. On the other hand, myeloid cells (granulocytes and macrophages,) are localised is at the edge of the lymphomatous areas.

4.13 Stromal dynamics within the splenic microenvironment of OPN-/-Fas$^{lpr/lpr}$ mice cooperate in the process of B cell transformation

Aiming at investigating whether also stromal dynamics regulated by OPN, other than B cell-intrinsic processes, contribute to the earlier and more aggressive lymphomagenesis of OPN-/-Fas$^{lpr/lpr}$ mice, we wondered whether immune populations of the OPN-deficient splenic microenvironment may better sustain B cell proliferation through the expression of factors that are important for their survival and/or activation. For this purpose, we evaluated the expression of *Tnfsf13B*, encoding for B cell activating factor (BAFF), in the different cell populations sorted from the spleen of BALB/c, OPN -/-, Fas$^{lpr/lpr}$ and OPN-/-Fas$^{lpr/lpr}$ mice at 3-4 months of age. In particular, we sorted CD19+ B

cells, CD4+, CD8+ T cells and, in the case of autoimmune mice, also autoreactive CD3+B220+ cells. Among the myeloid populations, gated on CD11b, we sorted granulocytic Gr-1^{hi} cells, classical (CD11c+B220-) and plasmacytoid (CD11c+B220+) dendritic cells, and marginal macrophages (F480+CD169+). BAFF, member of TNF-family, is crucial for B cell survival-related functions (such as protein synthesis and metabolism necessary to extend the half-life of immature, transitional, and mature B cells. [145]. Interestingly, we observed that the main producers of BAFF in the spleen of both naïve and autoimmune mice were Gr-1^{hi} cells, showing expression levels significantly higher than all other immune cell populations (Fig. 44, upper panel). In general, its expression is higher in cells from autoimmune mice, which is consistent with a more inflamed and activated microenvironment than in naive mice. If we compare the expression of BAFF in Gr-1^{hi} from the four different strains, granulocytic cells from OPN-/- mice showed a significant increase in the transcript level of *Tnfsf13B* in comparison to Gr1^{hi} cells from BALB/c mice, and a similar trend, although not statistically significant, is maintained also in autoimmune mice (Fig. 44). Considering that Gr1^{hi} cells are significantly enriched in the spleen of OPN-/-Fas$^{lpr/lpr}$ mice compared with Fas$^{lpr/lpr}$ mice, as shown in figure 42 and that this cell subset is the main producers of BAFF, the net result is an higher production of this factor in the spleen of OPN-/-Fas$^{lpr/lpr}$ mice.

Notably, also F480+CD169+ marginal macrophages showed differences in the mRNA level of BAFF that was higher in OPN-/- macrophages, either from naïve or autoimmune mice (Fig. 44), despite the expression in this population was much lower than in granulocytic cells.

As concerns CD4+ and CD8+ T cells, cDCs and pDCs, no significant differences in *Tnfsf13B* expression were observed between Fas$^{lpr/lpr}$ and OPN-/-Fas$^{lpr/lpr}$ mice.

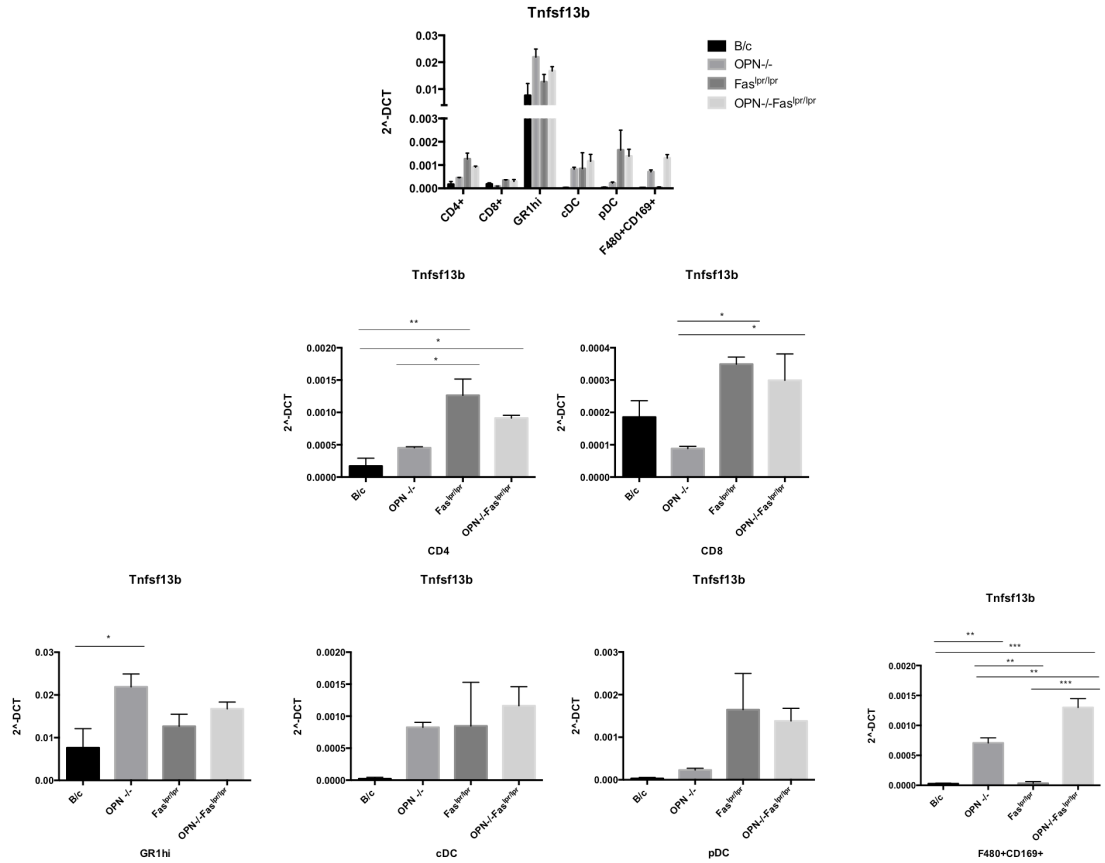

Figure 44. **mRNA level of *Tnfsf13b* (BAFF) evaluated through RT-PCR on sorted splenic immune populations from B/c, OPN-/-, Fas$^{lpr/lpr}$ and OPN-/-Fas$^{lpr/lpr}$ mice**. Gr1^{hi} cells expressed the highest level of *Tnfsf13b* (upper panel). Gr1^{hi} cells from OPN-/- spleens showed a significantly higher level of BAFF in comparison to B/c mice (*, P<0.05, Ordinary one way ANOVA), but only a trend was observed when comparing autoimmune animals. OPN-/- marginal zone macrophages (F480+CD169+) expressed a higher level of BAFF both in naïve (**, P<0.01,Ordinary one way ANOVA) and in autoimmune context (***, P<0.001; Ordinary one way ANOVA). Values are referred as 2^-DCT. A pool of 3 mice per group was used

(Statistical significance is shown only in the graphs specific for each cell type for a matter of space).

Additionally, since IL-6 is another molecule critical for B cell survival and it is a target gene of MYD88 signaling cascade, we evaluated its mRNA level in the same cell subsets from the four strains. Overall, almost all immune cells from OPN-deficient autoimmune mice, namely CD8+ T cells, Gr1^{hi}, and cDCs showed a significant higher expression of *Il6* in comparison with those from OPN-competent animals (Fig. 45). Among the different cell subsets, classical dendritic cells were the main producers of *Il6* (Fig. 45, upper panel). We observed a trend of increase in *Il6* expression by CD4+ and pDCs from OPN-/-Fas$^{lpr/lpr}$ mice.

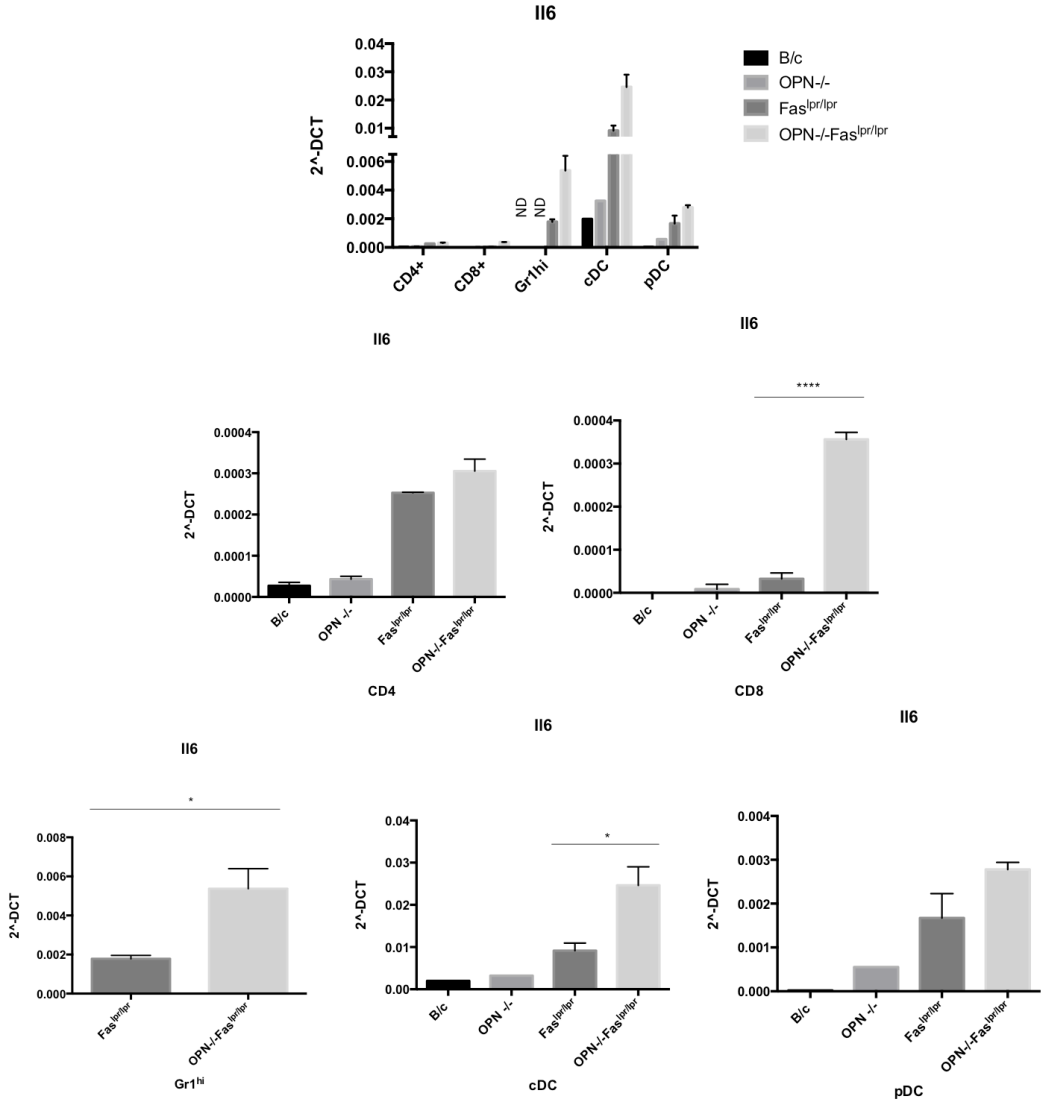

Figure 45. mRNA level of *Il6* evaluated through RT-PCR on sorted splenic immune populations from B/c, OPN-/-, Fas$^{lpr/lpr}$ and OPN-/-Fas$^{lpr/lpr}$ mice. Autoimmune classical DCs were the main producers of *Il6* in comparison to the other cell subsets (graph above). OPN-/-Fas$^{lpr/lpr}$ CD8+ cells (****, P<0.0001; Student t test), Gr1^{hi} cells (*, P<0.05; Student t test) and cDCs (*, P<0.05; Student t test) expressed a significantly higher level of *Il6* in comparison to Fas$^{lpr/lpr}$ counterparts. CD4+ T cells and pDCs showed a similar trend. Values are referred as 2^-DCT. A pool of 3 mice per group was used. (data from Gr1^{hi} cells from B/c and OPN-/- are not showed because RNA from the latter was not enough to perform RT-PCR (ND: Not done).
(Statistical significance is shown only in the graphs specific for each cell type for a matter of space).

Together, these results suggest that the also the stromal microenvironment may play a role in sustaining the lymphomatous phenotype observed in OPN-/-Fas$^{lpr/lpr}$ mice, and that OPN may restrain the production of B cell-sustaining factors in specific immune cell subsets within the splenic microenvironment.

4.14 OPN is down-regulated in human ABC-DLBCL in comparison with GC-DLBCL patient samples

To assess the translation relevance of our findings and the potential role of OPN in human DLBCLs, we firstly analyzed its expression by IHC on biopsies derived from patients affected by different haematological diseases (5 per group), specifically follicular hyperplasia, GC- and ABC-DLBCL, follicular and mantle cell lymphomas (Fig. 46). Despite this was only a qualitative evaluation, we could appreciate how the highest expression of OPN was detected in biopsies of follicular- and germinal center-related diseases, whereas it was poorly expressed in ABC-DLBCL compared to GC-DLBCL samples, in line with our spontaneous mouse model, that develops ABC-like DLBCLs if genetically deficient for OPN. However, this staining does not clearly distinguish the cellular localization of the protein, nor it is definitely established the presence of a specific intracellular form of OPN in the human setting.

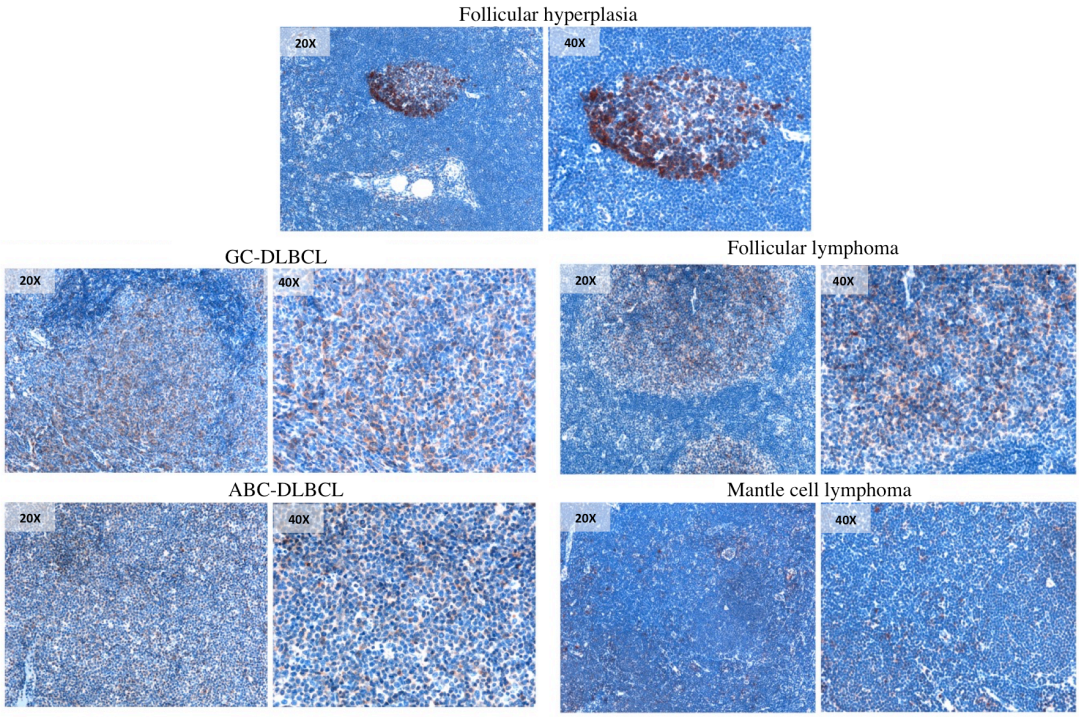

Figure 46. **IHC for OPN performed on human lymphoma biopsies.** OPN is more expressed in follicular lymphoma and GC-DLBCL than mantle cell lymphoma and ABC-DLBCL. Magnification 20x (left) and 40x (right).

Additionally, we performed some *in silico* analysis on a publicly available dataset, GSE4475, which compares gene expression profile from 221 DLBCL patients (58 ABC-, 120 GC-DLBCL and the remaining 43 samples unclassifiable). As shown in the

Volcano plot of figure 47A, comparing ABC- versus GC-DLBCL, 1411 genes were down-regulated and 1718 were up-regulated in the ABC-DLBCL group. Notably, *SPP1* was among the genes that were down-regulated in ABC-DLBCL (fold change: 1,75) (Fig. 47B), confirming the IHC data.

Remarkably, *PRDM1* (fold change: 1,12) and *STAT3* (fold change: 2,53) expression were significantly higher in patients affected by ABC- than GC-DLBCL disease (Fig. 47 B), in line with the data from our mouse models.

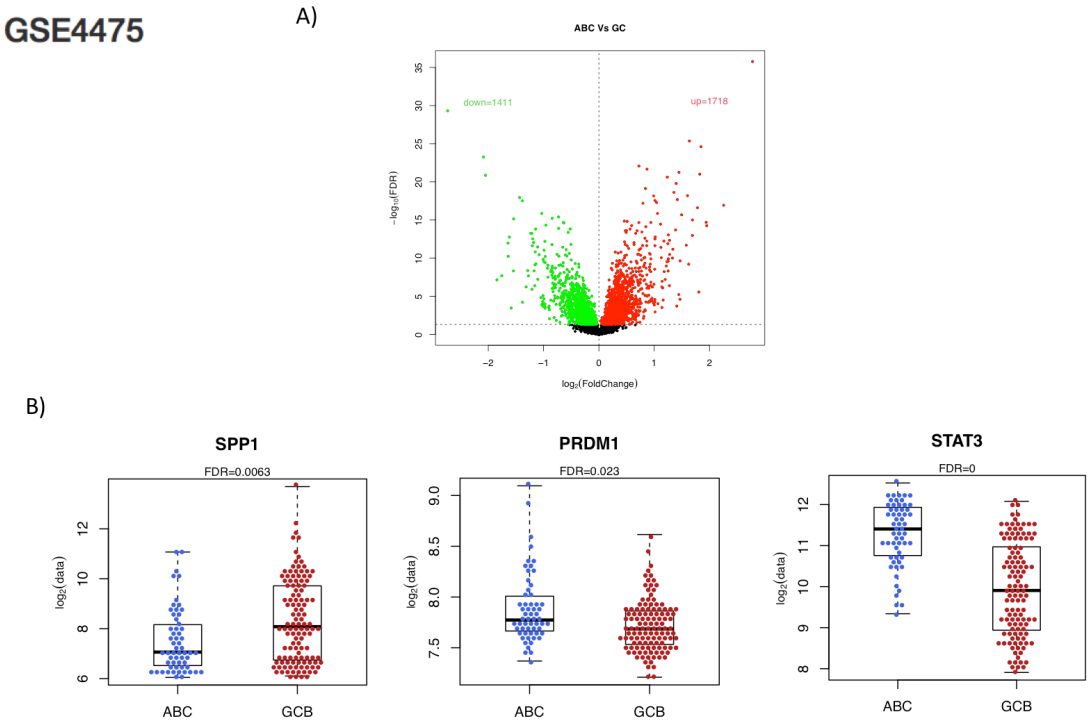

Figure 47. Analysis of human dataset GSE4475. A. Volcano plot of differentially expressed genes calculated using limma linear models comparing ABC samples Vs GCB samples. P-value was corrected with the Benjamini and Hockberg method. Green dots represent down-regulated genes with FDR < 0.05 and a negative log2 fold change, while red dots are up-regulated genes with a positive log2 fold change. B) Boxplots showing that *SPP1* is downregulated, while *PRDM1* and *STAT3* up-regulated, in ABC VS GCB DLBCL samples. Dots in boxplot represent the expression of the selected genes in each sample.

These results indicate that OPN-/-Fas$^{lpr/lpr}$ lymphomas recapitulate the scenario of human ABC-DLBCL patients, with similar phenotype and gene expression of specific markers, and suggest that, also in human setting, OPN may exert a protective role, as patients affected by GC-DLBCL, which expresses higher levels of the protein, have better prognosis than those with ABC-DLBCL.

5. DISCUSSION

This study demonstrates that osteopontin (OPN) protects autoimmunity-prone mice ($Fas^{lpr/lpr}$) from the development of B lymphomas. Indeed, $Fas^{lpr/lpr}$ mice on OPN-deficient background (OPN-/-$Fas^{lpr/lpr}$) showed a 2-fold increase in developing splenic diffuse large B cell lymphoma (DLBCL), of prevalent high-grade ABC-DLBCL subtype, than OPN-sufficient counterpart developing the less aggressive GC subtype. ABC-DLBCL was characterized based on the expression of BCL2 and IRF4 along with the absence of BCL6. Additionally, these cells express high level of the oncogene c-MYC, thus suggesting that OPN-deficient tumors may belong to the very aggressive "double expressor" lymphoma subset, characterized by the concomitant expression of both c-MYC and BCL2 [73]. These features were conserved in the two lymphoma cell lines we have established from OPN-/-$Fas^{lpr/lpr}$ mice, the "early stage" OPL239, and the "late stage" OPL241, both of the ABC-DLBCL subtype. On the other hand, the few lymphomas developed in $Fas^{lpr/lpr}$ animals showed a strong positivity for BCL6, a classical marker of human GC-DLBCLs, and negligible expression of the ABC-related proteins. Notably, a striking difference between lymphomas occurring in OPN-competent and -deficient mice was the higher activation of STAT3 pathway in absence of OPN, suggesting that OPN-/-$Fas^{lpr/lpr}$ tumours may rely on this signaling pathway for their proliferation/survival.

OPN-deficient autoimmune mice showed a significant increase in a splenic CD93- mature population, a CD23-CD21/35- fraction that comprises neither follicular (CD23+) nor marginal zone (CD21/35+) B cells. This result suggests that OPN may act as a brake in the expansion of these "atypical" cells and that the accumulating CD23-CD21/35- fraction in OPN-/-$Fas^{lpr/lpr}$ mice may represent the B cells undergoing malignant transformation toward ABC-DLBCs. In agreement with this hypothesis, also OPL239 and OPL241 cell lines are negative for these markers.

The hypothesized underline mechanism is that B cell-intrinsic OPN is able to prevent the exacerbation of autoimmunity-driven B cell transformation, through the impairment of MYD88 signaling pathway. In absence of OPN, a striking up-regulation of Toll-like receptor 9 (TLR9) occurring on splenic CD19+ B cells, could likely increase the binding of the circulating autoimmune double strand DNA, and its pathway activation.

Indeed, an increase in MYD88-protein machinery (i.e. IRAK1, IRAK4 and MYD88) was observed both in steady state conditions and after stimulation with CpG 1826, a TLR9 agonist. Accordingly, OPN-deficient autoimmune B cells are more activated, (higher CD86 expression) than OPN-sufficient counterparts. These findings seem to contradict the well-established role of OPN in promoting processes leading to inflammation and cancer [110,120]. Such discrepancy may be explained by the fact that OPN isoform generally associated with the hallmarks of cancer is the secreted (sOPN) [97,131, 132] rather than the intracellular one (iOPN). Indeed, the more recently identified iOPN exerts some anti-inflammatory activities [101,119,146], that fit well with our findings. The co-localization and interaction between iOPN and the scaffold protein MYD88 has been documented in a few reports [101,108], although with different outcomes. One report shows that iOPN promotes MYD88-mediated IFNα production in plasmacytoid dendritic cells [108], while the other one demonstrates that the lack of OPN in macrophages results in a more activated NFkB pathway and that replacing iOPN in these cells antagonize this cascade. [101] Despite not investigate for iOPN-MYD88 co-localization, another paper shows that iOPN negatively controls TLR4-mediated inflammation by regulating GSK3β and 4EBP1 phosphorilation [146]. The results I have presented are in agreement with the two latter works in supporting an anti-inflammatory role of iOPN. Indeed, the presence of iOPN in B lymphocytes in the spleen of autoimmune mice was documented by IHC showing an intracellular staining of the protein, characterized by evident dots surrounding the peri-nuclear region.

Furthermore, the lymphomatous areas arising in $Fas^{lpr/lpr}$ mice showed a further increase in the OPN expression, that preserved an intracellular localization. Immunofluorescence on cytospin preparations also showed that OPN and the endosomal marker CD63 display the same pattern of expression in B cells from $Fas^{lpr/lpr}$ mice, demonstrating that iOPN exerts is role in the endosomal compartment, where TLR9 resides. These results are the first showing the presence and the anti-inflammatory role of iOPN in autoimmune B lymphocytes.

In a translational perspective, the findings of more active TLR9-MYD88 signaling in OPN-/-$Fas^{lpr/lpr}$ mice are in line with the well-established hyper-activation of MYD88 pathways detected in human DLBCLs, which, however, is mainly due to activating mutations in MYD88 gene [84].

Further evidence for the anti-inflammatory role of iOPN was obtained by

overexpressing either the secreted or the intracellular isoform of OPN into OPL239 and OPL241 DLBCL cell lines and comparing the activation of key pathways such as STAT3 and NF-kB. Results showed that the forced expression of iOPN inhibited their activation, either at steady state or upon CpG 1826 stimulation. Accordingly, when intravenously injected in sub-lethally irradiated BALB/c mice, OPL239 cells over-expressing the iOPN form showed a significantly slower growing tumor in the spleen than *Spp1*-overexpressing and control transduced (IRES Green) cells.

Together, these evidences strongly suggest that B-cell intrinsic iOPN constrasts lymphomagenesis in $Fas^{lpr/lpr}$ mice, exerting a negative feed-back loop on STAT3 and NFkB signaling cascades, a process otherwise promoted in its absence (OPN-/- mice). Neverthless, 33% of $Fas^{lpr/lpr}$ mice still develop B cell lymphomas, in an OPN-competent setting, suggesting that, in mice characterized by the highest inflammation associated with autoimmune conditions, the endogenous iOPN is not sufficient to restrain B cell transformation. The increased expression of iOPN detected in B cells from lymphomatous areas of $Fas^{lpr/lpr}$ mice, in comparison to naïve mice, may represent an unsuccessful attempt to restrain STAT3 and NFkB signaling activation.

During B cell differentiation in secondary lymphoid organs, a distinct pattern of genes is transcribed or repressed in a controlled manner. BLIMP1 is a master regulator of plasma cell differentiation, and it is repressed during the initial germinal center reaction, while upregulated in the post-activated state of B cell maturation [88]. In line with these notions and with the phenotype of DLBCL developed in OPN-/-$Fas^{lpr/lpr}$ mice, GEP of splenic B cells from autoimmune mice showed a 7,3-fold increase of *Prdm1*, encoding for BLIMP1, in B cells derived from OPN-/-$Fas^{lpr/lpr}$ mice, compared with those from $Fas^{lpr/lpr}$ mice at 5 months of age, a time point in which most OPN-/-$Fas^{lpr/lpr}$ mice show already signs of lymphomas, whereas OPN-competent $Fas^{lpr/lpr}$ mice do not. However, as far as hematological malignancies are concerned, BLIMP1 is usually genetically inactivated or transcriptionally repressed in DLBCL [92], being activated as a tumor suppressor. However, my data are not in disagreement with the reported literature, as both PRDM1α and PRDM1β transcriptional variants are generally expressed only in non-GCB subtype of DLBCL and, additionally, PRDM1β correlated with short survival in non-GCB patients treated with CHOP [95]. Interestingly, BLIMP1 belongs to the MYDD88-NFkB axis, as LPS-stimulated B cells from MYD88-/- mice show decreased expression levels of PRDM1 [89], and STAT3 signaling [91]. Overall, the up-regulation

of *Prdm1* expression in OPN-deficient lymphomas, detected in the GEP and confirmed *in situ* by RNA Scope technique, is in line with the aggressive ABC phenotype characterizing lymphomas developing in OPN-/-Fas$^{lpr/lpr}$ mice.

Other than B cell-intrinsic, the dynamics promoting the aggressive lymphomagenesis described in OPN-deficient autoimmune mice likely involve the stromal compartment. Indeed, OPN is expressed also by other immune cells of the splenic microenvironment of Fas$^{lpr/lpr}$ mice, as shown at transcript and protein levels in both lymphoid (mainly CD4+ T cells and autoimmune CD3+B220+ cells) and myeloid cells (mainly granulocytes). Generally speaking, lymphoid cells are known to produce the secreted protein that acts as a pro-inflammatory cytokine by binding surface receptors and promoting inflammatory signaling cascades, whereas the intracellular form has been shown to be produced by cells of the myeloid lineage [103,119,132]. My data are in line with the reported literature, as autoimmune CD3+B220+ are "pro-inflammation" by definition, and are present in the Fas$^{lpr/lpr}$ spleen and also in the peripheral blood, where they likely release a consistent amount of OPN. In agreement, increasing levels of OPN have been detected by ELISA in the serum of Fas$^{lpr/lpr}$ mice along autoimmune disease progression. Also, IHC on Fas$^{lpr/lpr}$ spleen sections showed OPN expression in granulocytes and other myeloid cells in granulomas and the perivascular zone of the red pulp. As for B cell-expressed OPN, also in this case the staining is suggestive of an intracellular localization.

Remarkably, the immune cell subsets, of either lymphoid or myeloid lineage, populating the spleen of OPN-Fas$^{lpr/lpr}$ mice, express factors important for B cell survival and proliferation at higher level than OPN-competent counterparts. Specifically, CD169+F480+ marginal macrophages from OPN-deficient animals, regardless the naïve or autoimmune conditions, expressed significantly more *Tnfsf13b* (BAFF) than OPN-competent counterpart, and Gr1^{hi} granulocytic cells showed a similar trend. Additionally, CD8+ T cells, Gr1^{hi} granulocytes and classical dendritic cells from OPN-/-Fas$^{lpr/lpr}$ mice showed a higher expression of *Il6* than Fas$^{lpr/lpr}$ animals.

These data suggest that the OPN-/-Fas$^{lpr/lpr}$ splenic microenvironment, providing additional supporting factors for B cell proliferation/survival, may contribute to the exacerbated ABC-DLBCL development observed in these animals.

In line with a possible role of the surrounding microenvironment in our lymphomatous

phenotype, changes occurred in the splenic immune cell subsets between $Fas^{lpr/lpr}$ and OPN-/-$Fas^{lpr/lpr}$ mice. CD3+B220+ autoimmune cells and plasmacytoid dendritic cells, the latter known to have important roles in autoimmune disorders, were up-regulated in OPN-competent autoimmune mice, characterized for a more severe autoimmunity. On the other hand, myeloid cells (CD11b+), and more specifically the Gr-1^{hi} granulocytic and the Ly6C^{hi} monocytic subsets, were expanded in the spleen of OPN-/-$Fas^{lpr/lpr}$ mice. These observations are in agreement with an article showing how myeloid–specific OPN is able to negatively regulate cell cycle and survival of cells of the myeloid lineage during emergency myelopoiesis [119]. Interestingly, the observed expansion of Gr-1^{hi} cells is in line with previous data from our laboratory, showing that tumor-induced myelopoiesis was increased in OPN-deficient versus OPN-competent mice bearing solid tumours [132].

Beside their relative number, the topographic distribution of the different immune populations in a tissue may be even more relevant for their interaction and cross-talk. Indeed, although no significant differences in terms of percentage of T cells were noted by flow cytometry, IHC analysis provided evidences of CD4+ and CD8+ T cells intermingled with the lymphomatous B cells in early and, even more, in late-stage lymphomas. While CD4+ T cells, particularly Follicular Helper T cells, are known to exert a pivotal role in autoimmune disorders [37,38], the presence of CD8+ T cells within the lymphomatous zones was unexpected whereas suggestive of a possible immunogenicity of transformed cells, perhaps capable to induce some kind of immune response, although abortive. On this line, CD8+ T cells in lymphomas from OPN-deficient mice are bigger than in OPN-competent mice and showed a star-shaped morphology, suggestive of an activated state. Flow cytometry analysis however indicated that CD8+ T lymphocytes from OPN-/-$Fas^{lpr/lpr}$ spleen express higher level of the exhaustion marker TIM3 than those from OPN-competent animals. These data suggest that, in the context of the aggressive OPN-/- lymphomas, CD8+ cells are recruited locally and activated, but incapable of an efficient anti-tumour response because the local microenvironment render them exhausted.

The association between low/absent OPN and DLBCL of the ABC type in a translation setting was confirmed by IHC on ABC- versus GC-DLBCL biopsies. Also, *in silico* analysis on publicly available dataset showed a down-regulation of the OPN gene, *SPP1*, in samples from ABC-DLBCL patients in comparison to GC-DLBCL samples.

Interestingly, in the same comparison, *PRDM1* and *STAT3* were significant up-regulated in ABC-DLBCL biopsies, in line with our findings in the mouse model showing higher expression of these proteins in OPN-deficient lymphomas, supporting our hypothesis of an opposite regulation of OPN versus STAT3 and BLIMP1.

In conclusion, our study indicates that B cell-intrinsic iOPN has a protective role from autoimmunity-driven lymphomagenesis contrasting TLR9-MYD88-related programs of proliferation and inflammation. Beside B cell-intrinsic effects, also microenvironment-related OPN, likely the intracellular isoform of the protein expressed by cells of the myeloid lineage, contributes in protecting B cells from transformation, limiting the production of factors critical for B cell proliferation/survival.

7. REFERENCES

1. Fairweather, D., Frisancho-Kiss, S., & Rose, N. R. (2008). Sex differences in autoimmune disease from a pathological perspective. *American Journal of Pathology* (Vol. 173, Issue 3, pp. 600–609). American Society for Investigative Pathology Inc. https://doi.org/10.2353/ajpath.2008.071008

2. Muñoz-Carrillo, J. L., Castro-García, F. P., Chávez-Rubalcaba, F., Chávez-Rubalcaba, I., Martínez-Rodríguez, J. L., & Hernández-Ruiz, M. E. (2018). Immune System Disorders: Hypersensitivity and Autoimmunity. In *Immunoregulatory Aspects of Immunotherapy*. InTech. https://doi.org/10.5772/intechopen.75794

3. Roep, B. O. (2003). The role of T-cells in the pathogenesis of Type 1 diabetes: From cause to cure. *Diabetologia* (Vol. 46, Issue 3, pp. 305–321). Springer Verlag. https://doi.org/10.1007/s00125-003-1089-5

4. Björses, P., Halonen, M., Palvimo, J. J., Kolmer, M., Aaltonen, J., Ellonen, P., Perheentupa, J., Ulmanen, I., & Peltonen, L. (2000). Mutations in the AIRE gene: Effects on subcellular location and transactivation function of the autoimmune polyendocrinopathy-candidiasis - Ectodermal dystrophy protein. *American Journal of Human Genetics*, *66*(2), 378–392. https://doi.org/10.1086/302765

5. Peterson, P., Org, T., & Rebane, A. (2008). Transcriptional regulation by AIRE: Molecular mechanisms of central tolerance. *Nature Reviews Immunology* (Vol. 8, Issue 12, pp. 948–957). https://doi.org/10.1038/nri2450

6. Peterson, P., & Peltonen, L. (2005). Autoimmune polyendocrinopathy syndrome type 1 (APS1) and AIRE gene: New views on molecular basis of autoimmunity. *Journal of Autoimmunity* (Vol. 25, Issue SUPPL., pp. 49–55). https://doi.org/10.1016/j.jaut.2005.09.022

7. Sollid, L. M., Pos, W., & Wucherpfennig, K. W. (2014). Molecular mechanisms for contribution of MHC molecules to autoimmune diseases. *Current Opinion in Immunology* (Vol. 31, pp. 24–30). Elsevier Ltd. https://doi.org/10.1016/j.coi.2014.08.005

8. Walport, M. J. (2002). Complement and systemic lupus erythematosus. *Arthritis research* (Vol. 4, pp. S279–S293). https://doi.org/10.1186/ar586

9. Zhernakova, A., Withoff, S., & Wijmenga, C. (2013). Clinical implications of shared genetics and pathogenesis in autoimmune diseases. *Nature Reviews Endocrinology* (Vol. 9, Issue 11, pp. 646–659). https://doi.org/10.1038/nrendo.2013.161

10. Holzelova, E., Vonarbourg, C., Stolzenberg, M.-C., Arkwright, P. D., Selz, F., Prieur, A.-M., Blanche, S., Bartunkova, J., Vilmer, E., Fischer, A., Le Deist, F., & Rieux-Laucat, F. (2004). Autoimmune Lymphoproliferative Syndrome with Somatic Fas Mutations. *New England Journal of Medicine*, *351*(14), 1409–1418. https://doi.org/10.1056/nejmoa040036

11. Wu, J., Wilson, J., He, J., Xiang, L., Schur, P. H., & Mountz, J. D. (1996). Fas ligand mutation in a patient with systemic lupus erythematosus and lymphoproliferative disease. *Journal of Clinical Investigation*, *98*(5), 1107–1113. https://doi.org/10.1172/JCI118892

12. Watanabe-Fukunaga, R., Brannan, C. I., Copeland, N. G., Jenkins, N. A., & Nagata, S. (1992). Lymphoproliferation disorder in mice explained by defects in Fas antigen that mediates apoptosis. *Nature*, *356*(6367), 314–317. https://doi.org/10.1038/356314a0

13. Fradin, D., Le Fur, S., Mille, C., Naoui, N., Groves, C., Zelenika, D., McCarthy, M. I., Lathrop, M., & Bougnères, P. (2012). Association of the CpG methylation pattern of the proximal insulin gene promoter with type 1 diabetes. *PLoS ONE*, *7*(5). https://doi.org/10.1371/journal.pone.0036278

14. Hu, N., Qiu, X., Luo, Y., Yuan, J., Li, Y., Lei, W., Zhang, G., Zhou, Y., Su, Y., & Lu, Q. (2008). Abnormal histone modification patterns in lupus CD4+ T cells. *Journal of Rheumatology*, *35*(5)

15. Bogdanos, D. P., Smyk, D. S., Rigopoulou, E. I., Mytilinaiou, M. G., Heneghan, M. A., Selmi, C., & Eric Gershwin, M. (2012). Twin studies in autoimmune disease: Genetics, gender and environment. *Journal of Autoimmunity* (Vol. 38, Issues 2–3). https://doi.org/10.1016/j.jaut.2011.11.003

16. Cunningham, M. W. (2014). Rheumatic fever, autoimmunity, and molecular mimicry: The streptococcal connection. *International Reviews of Immunology* (Vol. 33, Issue 4). https://doi.org/10.3109/08830185.2014.917411

17. Vanderlugt, C. L., & Miller, S. D. (2002). Epitope spreading in immune-mediated diseases: Implications for immunotherapy. *Nature Reviews Immunology* (Vol. 2, Issue 2). https://doi.org/10.1038/nri724

18. Fujinami, R. S., Von Herrath, M. G., Christen, U., & Whitton, J. L. (2006). Molecular mimicry, bystander activation, or viral persistence: Infections and autoimmune disease. *Clinical Microbiology Reviews* (Vol. 19, Issue 1). https://doi.org/10.1128/CMR.19.1.80-94.2006

19. Afridi, H. I., Kazi, T. G., Talpur, F. N., Naher, S., & Brabazon, D. (2014). Relationship between toxic metals exposure via cigarette smoking and rheumatoid arthritis. *Clinical Laboratory*, *60*(10). https://doi.org/10.7754/Clin.Lab.2014.131117

20. Ekblom-Kullberg, S., Kautiainen, H., Alha, P., Leirisalo-Repo, M., Miettinen, A., & Julkunen, H. (2014). Smoking, disease activity, permanent damage and dsDNA autoantibody production in patients with systemic lupus erythematosus. *Rheumatology International*, *34*(3). https://doi.org/10.1007/s00296-013-2889-7

21. Rau, R. (2014). Glucocorticoid treatment in rheumatoid arthritis. *Expert Opinion on Pharmacotherapy* (Vol. 15, Issue 11). https://doi.org/10.1517/14656566.2014.922955

22. Cipriani, P., Ruscitti, P., Carubbi, F., Liakouli, V., & Giacomelli, R. (2014). Methotrexate: An old new drug in autoimmune disease. *Expert Review of Clinical Immunology* (Vol. 10, Issue 11). https://doi.org/10.1586/1744666X.2014.962996

23. Casetta, I., Iuliano, G., & Filippini, G. (2007). Azathioprine for multiple sclerosis. *Cochrane Database of Systematic Reviews* (Issue 4). https://doi.org/10.1002/14651858.CD003982.pub2

24. Willrich, M. A. V., Murray, D. L., & Snyder, M. R. (2015). Tumor necrosis factor inhibitors: Clinical utility in autoimmune diseases. *Translational Research* (Vol. 165, Issue 2). https://doi.org/10.1016/j.trsl.2014.09.006

25. Agmon-Levin, N., Theodor, E., Segal, R. M., & Shoenfeld, Y. (2013). Vitamin D in systemic and organ-specific autoimmune diseases. *Clinical Reviews in Allergy and Immunology*, *45*(2). https://doi.org/10.1007/s12016-012-8342-y

26. Edwards, J. C. W., Szczepański, L., Szechiński, J., Filipowicz-Sosnowska, A., Emery, P., Close, D. R., Stevens, R. M., & Shaw, T. (2004). Efficacy of B-Cell–Targeted Therapy with Rituximab in Patients with Rheumatoid Arthritis. *New England Journal of Medicine*, *350*(25). https://doi.org/10.1056/nejmoa032534

27. Wang, L., Wang, F. S., & Gershwin, M. E. (2015). Human autoimmune diseases: A comprehensive update. *Journal of Internal Medicine* (Vol. 278, Issue 4). https://doi.org/10.1111/joim.12395

28. Moulton, V. R., & Tsokos, G. C. (2012). Why do women get lupus? *Clinical Immunology* (Vol. 144, Issue 1). https://doi.org/10.1016/j.clim.2012.04.003

29. Lo, M. S. (2016). Monogenic Lupus. *Current Rheumatology Reports* (Vol. 18, Issue 12). https://doi.org/10.1007/s11926-016-0621-9

30. Teruel, M., & Alarcón-Riquelme, M. E. (2016). The genetic basis of systemic lupus erythematosus: What are the risk factors and what have we learned. *Journal of Autoimmunity* (Vol. 74). https://doi.org/10.1016/j.jaut.2016.08.001

31. Rosetti, F., De La Cruz, A., & Crispín, J. C. (2019). Gene-function studies in systemic lupus erythematosus. *Current Opinion in Rheumatology* (Vol. 31, Issue 2). https://doi.org/10.1097/BOR.0000000000000572

32. Zhang, Y., Zhao, M., Sawalha, A. H., Richardson, B., & Lu, Q. (2013). Impaired DNA methylation and its mechanisms in CD4+T cells of systemic lupus erythematosus. *Journal of Autoimmunity* (Vol. 41). https://doi.org/10.1016/j.jaut.2013.01.005

33. Absher, D. M., Li, X., Waite, L. L., Gibson, A., Roberts, K., Edberg, J., Chatham, W. W., & Kimberly, R. P. (2013). Genome-Wide DNA Methylation Analysis of Systemic Lupus Erythematosus Reveals Persistent Hypomethylation of Interferon Genes and Compositional Changes to CD4+ T-cell Populations. *PLoS Genetics*, *9*(8). https://doi.org/10.1371/journal.pgen.1003678

34. Garcia, B. A., Busby, S. A., Shabanowitz, J., Hunt, D. F., & Mishra, N. (2005). Resetting the epigenetic histone code in the MRL-lpr/lpr mouse model of lupus by histone deacetylase inhibition. *Journal of Proteome Research*, *4*(6). https://doi.org/10.1021/pr050188r

35. C.M., H., T., R., & G.C., T. (2011). cAMP-responsive element modulator (CREM)alpha protein signaling mediates epigenetic remodeling of the human interleukin-2 gene: Implications in systemic lupus erythematosus. *Journal of Biological Chemistry* (Vol. 286, Issue 50)

36. Moulton, V. R., Suarez-Fueyo, A., Meidan, E., Li, H., Mizui, M., & Tsokos, G. C. (2017). Pathogenesis of Human Systemic Lupus Erythematosus: A Cellular Perspective. *Trends in Molecular Medicine* (Vol. 23, Issue 7). https://doi.org/10.1016/j.molmed.2017.05.006

37. Kim, S. J., Lee, K., & Diamond, B. (2018). Follicular helper T cells in systemic lupus erythematosus. *Frontiers in Immunology* (Vol. 9, Issue AUG). https://doi.org/10.3389/fimmu.2018.01793

38. Choi, J. Y., Ho, J. H. E., Pasoto, S. G., Bunin, V., Kim, S. T., Carrasco, S., Borba, E. F., Gonçalves, C. R., Costa, P. R., Kallas, E. G., Bonfa, E., & Craft, J. (2015). Circulating follicular helper-like T cells in systemic lupus erythematosus: Association with disease activity. *Arthritis and Rheumatology*, *67*(4). https://doi.org/10.1002/art.39020

39. Iwata, S., & Tanaka, Y. (2016). B-cell subsets, signaling and their roles in secretion of autoantibodies. *Lupus*, *25*(8), 850–856. https://doi.org/10.1177/0961203316643172

40. Teichmann, L. L., Schenten, D., Medzhitov, R., Kashgarian, M., & Shlomchik, M. J. (2013). Signals via the Adaptor MyD88 in B Cells and DCs Make Distinct and

Synergistic Contributions to Immune Activation and Tissue Damage in Lupus. *Immunity*, *38*(3). https://doi.org/10.1016/j.immuni.2012.11.017

41. Kessenbrock, K., Krumbholz, M., Schönermarck, U., Back, W., Gross, W. L., Werb, Z., Gröne, H. J., Brinkmann, V., & Jenne, D. E. (2009). Netting neutrophils in autoimmune small-vessel vasculitis. *Nature Medicine*, *15*(6). https://doi.org/10.1038/nm.1959

42. Marrack, P., Kappler, J., & Mitchell, T. (1999). Type I interferons keep activated T cells alive. *Journal of Experimental Medicine*, *189*(3). https://doi.org/10.1084/jem.189.3.521

43. Xu, H. C., Grusdat, M., Pandyra, A. A., Polz, R., Huang, J., Sharma, P., Deenen, R., Köhrer, K., Rahbar, R., Diefenbach, A., Gibbert, K., Löhning, M., Höcker, L., Waibler, Z., Häussinger, D., Mak, T. W., Ohashi, P. S., Lang, K. S., & Lang, P. A. (2014). Type I Interferon Protects Antiviral CD8+ T Cells from NK Cell Cytotoxicity. *Immunity*, *40*(6). https://doi.org/10.1016/j.immuni.2014.05.004

44. Swanson, C. L., Wilson, T. J., Strauch, P., Colonna, M., Pelanda, R., & Torres, R. M. (2010). Type I IFN enhances follicular B cell contribution to the T cell-independent antibody response. *Journal of Experimental Medicine*, *207*(7). https://doi.org/10.1084/jem.20092695

45. Baechler, E. C., Batliwalla, F. M., Karypis, G., Gaffney, P. M., Ortmann, W. A., Espe, K. J., Shark, K. B., Grande, W. J., Hughes, K. M., Kapur, V., Gregersen, P. K., & Behrens, T. W. (2003). Interferon-inducible gene expression signature in peripheral blood cells of patients with severe lupus. *Proceedings of the National Academy of Sciences of the United States of America*, *100*(5). https://doi.org/10.1073/pnas.0337679100ù

46. Gatto, M., Saccon, F., Zen, M., Bettio, S., Iaccarino, L., Punzi, L., & Doria, A. (2016). Success and failure of biological treatment in systemic lupus erythematosus: A critical analysis. *Journal of Autoimmunity* (Vol. 74). https://doi.org/10.1016/j.jaut.2016.06.014

47. Andrews, B. S., Eisenberg, R. A., Theofilopoulos, A. N., Izui, S., Wilson, C. B., Meconahey, P. J., Murphy, E. D., Roths, J. B., & Dixon, F. J. (1978). Spontaneous

murine lupus-like syndromes: Clinical and immunopathological manifestations in several strains*. *Journal of Experimental Medicine*, *148*(5). https://doi.org/10.1084/jem.148.5.1198

48. Roths, J. B., Murphy, E. D., & Eicher, E. M. (1984). A new mutation, gld, that produces lymphoproliferation and autoimmunity in C3H/hej mice. *Journal of Experimental Medicine*, *159*(1). https://doi.org/10.1084/jem.159.1.1

49. Nagata, S., & Suda, T. (1995). Fas and Fas ligand: lpr and gld mutations. *Immunology Today*, *16*(1). https://doi.org/10.1016/0167-5699(95)80069-7

50. Magerus-Chatinet, A., Neven, B., Stolzenberg, M. C., Daussy, C., Arkwright, P. D., Lanzarotti, N., Schaffner, C., Cluet-Dennetiere, S., Haerynck, F., Michel, G., Bole-Feysot, C., Zarhrate, M., Radford-Weiss, I., Romana, S. P., Picard, C., Fischer, A., & Rieux-Laucat, F. (2011). Onset of autoimmune lymphoproliferative syndrome (ALPS) in humans as a consequence of genetic defect accumulation. *Journal of Clinical Investigation*, *121*(1). https://doi.org/10.1172/JCI43752

51. Liu, J., Karypis, G., Hippen, K. L., Vegoe, A. L., Ruiz, P., Gilkeson, G. S., & Behrens, T. W. (2006). Genomic view of systemic autoimmunity in MRLlpr mice. *Genes and Immunity*, *7*(2). https://doi.org/10.1038/sj.gene.6364286

52. Davidson, W. F., Giese, T., & Fredrickson, T. N. (1998). Spontaneous development of plasmacytoid tumors in mice with defective fas-fas ligand interactions. *Journal of Experimental Medicine*, *187*(11). https://doi.org/10.1084/jem.187.11.1825

53. Leandro, M. J., & Isenberg, D. A. (2001). Rheumatic diseases and malignancy - Is there an association? In *Scandinavian Journal of Rheumatology* (Vol. 30, Issue 4). https://doi.org/10.1080/030097401316909486

54. Smedby, K. E., Vajdic, C. M., Falster, M., Engels, E. A., Martinez-Maza, O., Turner, J., Hjalgrim, H., Vineis, P., Costantini, A. S., Bracci, P. M., Holly, E. A., Willett, E., Spinelli, J. J., Vecchia, C. La, Zheng, T., Becker, N., De Sanjosé, S., Chiu, B. C. H., Maso, L. D., Cozen, W. (2008). Autoimmune disorders and risk of non-Hodgkin lymphoma subtypes: A pooled analysis within the InterLymph Consortium. *Blood*. https://doi.org/10.1182/blood-2007-10-119974

55. Smedby, K. E., Hjalgrim, H., Askling, J., Chang, E. T., Gregersen, H., Porwit-MacDonald, A., Sundström, C., Åkerman, M., Melbye, M., Glimelius, B., & Adami, H. O. (2006). Autoimmune and chronic inflammatory disorders and risk of non-Hodgkin lymphoma by subtype. *Journal of the National Cancer Institute*. https://doi.org/10.1093/jnci/djj004

56.Smedby, K. E., Baecklund, E., & Askling, J. (2006). Malignant lymphomas in autoimmunity and inflammation: A review of risks, risk factors, and lymphoma characteristics. *Cancer Epidemiology Biomarkers and Prevention* (Vol. 15, Issue 11, pp. 2069–2077). https://doi.org/10.1158/1055-9965.EPI-06-0300

57. Wolfe, F., & Michaud, K. (2004). Lymphoma in rheumatoid arthritis: The effect of methotrexate and anti-tumor necrosis factor therapy in 18,572 patients. *Arthritis and Rheumatism*, *50*(6). https://doi.org/10.1002/art.20311

58. Bongartz, T., Sutton, A. J., Sweeting, M. J., Buchan, I., Matteson, E. L., & Montori, V. (2006). Anti-TNF antibody therapy in rheumatoid arthritis and the risk of serious infections and malignancies: Systematic review and meta-analysis of rare harmful effects in randomized controlled trials. *Journal of the American Medical Association* (Vol. 295, Issue 19). https://doi.org/10.1001/jama.295.19.2275

59. Wolfe, F., & Michaud, K. (2007). The effect of methotrexate and anti-tumor necrosis factor therapy on the risk of lymphoma in rheumatoid arthritis in 19,562 patients during 89,710 person-years of observation. *Arthritis and Rheumatism*, *56*(5). https://doi.org/10.1002/art.22579

60. Küppers, R., Klein, U., Hansmann, M.-L., & Rajewsky, K. (1999). Cellular Origin of Human B-Cell Lymphomas. *New England Journal of Medicine*, *341*(20). https://doi.org/10.1056/nejm199911113412007

61. Winkler, T. H., & Martensson, I. L. (2018). The role of the pre-b cell receptor in b cell development, repertoire selection, and tolerance. *Frontiers in Immunology* (Vol. 9, Issue NOV). https://doi.org/10.3389/fimmu.2018.02423

62. Collins, A. M., & Watson, C. T. (2018). Immunoglobulin light chain gene rearrangements, receptor editing and the development of a self-tolerant antibody

repertoire. *Frontiers in Immunology* (Vol. 9, Issue OCT). Frontiers Media S.A. https://doi.org/10.3389/fimmu.2018.02249

63. Natkunam, Y. (2007). The biology of the germinal center. *Hematology / the Education Program of the American Society of Hematology. American Society of Hematology. Education Program*. https://doi.org/10.1182/asheducation-2007.1.210

64. Pasqualucci, L., & Dalla-Favera, R. (2015). The Genetic Landscape of Diffuse Large B-Cell Lymphoma. *Seminars in Hematology* (Vol. 52, Issue 2). https://doi.org/10.1053/j.seminhematol.2015.01.005

65. Mesin, L., Ersching, J., & Victora, G. D. (2016). Germinal Center B Cell Dynamics. In *Immunity* (Vol. 45, Issue 3). https://doi.org/10.1016/j.immuni.2016.09.001

66. Bende, R. J., Smit, L. A., & van Noesel, C. J. M. (2007). Molecular pathways in follicular lymphoma. *Leukemia* (Vol. 21, Issue 1). https://doi.org/10.1038/sj.leu.2404426

67. Schmitz, R., Ceribelli, M., Pittaluga, S., Wright, G., & Staudt, L. M. (2014). Oncogenic mechanisms in Burkitt lymphoma. *Cold Spring Harbor Perspectives in Medicine*, *4*(2). https://doi.org/10.1101/cshperspect.a014282

68. Lenz, G., Nagel, I., Siebert, R., Roschke, A. V., Sanger, W., Wright, G. W., Dave, S. S., Tan, B., Zhao, H., Rosenwald, A., Muller-Hermelink, H. K., Gascoyne, R. D., Campo, E., Jaffe, E. S., Smeland, E. B., Fisher, R. I., Kuehl, W. M., Chan, W. C., & Staudt, L. M. (2007). Aberrant immunoglobulin class switch recombination and switch translocations in activated B cell-like diffuse large B cell lymphoma. *Journal of Experimental Medicine*, *204*(3). https://doi.org/10.1084/jem.20062041

69. Schmitz, R., Wright, G. W., Huang, D. W., Johnson, C. A., Phelan, J. D., Wang, J. Q., Roulland, S., Kasbekar, M., Young, R. M., Shaffer, A. L., Hodson, D. J., Xiao, W., Yu, X., Yang, Y., Zhao, H., Xu, W., Liu, X., Zhou, B., Du, W., … Staudt, L. M. (2018). Genetics and pathogenesis of diffuse large B-Cell lymphoma. *New England Journal of Medicine*. https://doi.org/10.1056/NEJMoa1801445

70. Victora, G. D., Dominguez-Sola, D., Holmes, A. B., Deroubaix, S., Dalla-Favera, R., & Nussenzweig, M. C. (2012). Identification of human germinal center light

and dark zone cells and their relationship to human B-cell lymphomas. *Blood*, *120*(11). https://doi.org/10.1182/blood-2012-03-415380

71. Alizadeh, A. A., Elsen, M. B., Davis, R. E., Ma, C. L., Lossos, I. S., Rosenwald, A., Boldrick, J. C., Sabet, H., Tran, T., Yu, X., Powell, J. I., Yang, L., Marü, G. E., Moore, T., Hudson, J., Lu, L., Lewis, D. B., Tibshirani, R., Sherlock, G., … Staudt, L. M. (2000). Distinct types of diffuse large B-cell lymphoma identified by gene expression profiling. *Nature*. https://doi.org/10.1038/35000501

72. Wright, G., Tan, B., Rosenwald, A., Hurt, E. H., Wiestner, A., & Staudt, L. M. (2003). A gene expression-based method to diagnose clinically distinct subgroups of diffuse large B cell lymphoma. *Proceedings of the National Academy of Sciences of the United States of America*, *100*(17). https://doi.org/10.1073/pnas.1732008100

73. Lin, P., & Medeiros, L. J. (2007). High-grade B-cell lymphoma/leukemia associated with t(14;18) and 8q24/MYC rearrangement: A neoplasm of germinal center immunophenotype with poor prognosis. *Haematologica* (Vol. 92, Issue 10). https://doi.org/10.3324/haematol.11263

74. Reagan, P. M., & Davies, A. (2017). Current treatment of double hit and double expressor lymphoma. *Hematology*. https://doi.org/10.1182/asheducation-2017.1.295

75. Scott, D. W., Mottok, A., Ennishi, D., Wright, G. W., Farinha, P., Ben-Neriah, S., Kridel, R., Barry, G. S., Hother, C., Abrisqueta, P., Boyle, M., Meissner, B., Telenius, A., Savage, K. J., Sehn, L. H., Slack, G. W., Steidl, C., Staudt, L. M., Connors, J. M., … Gascoyne, R. D. (2015). Prognostic significance of diffuse large B-cell lymphoma cell of origin determined by digital gene expression in formalin-fixed paraffin-embedded tissue biopsies. *Journal of Clinical Oncology*, *33*(26). https://doi.org/10.1200/JCO.2014.60.2383

76. Liu, Y., & Barta, S. K. (2019). Diffuse large B-cell lymphoma: 2019 update on diagnosis, risk stratification, and treatment. *American Journal of Hematology* (Vol. 94, Issue 5). https://doi.org/10.1002/ajh.25460

77. Pejša, V., Prka, Ž., Lucijanić, M., Mitrović, Z., Piršić, M., Jakšić, O., Ajduković, R., & Kušeć, R. (2017). Rituximab with dose-adjusted EPOCH as first-line treatment in patients with highly aggressive diffuse large B-cell lymphoma and autologous stem cell transplantation in selected patients. *Croatian Medical Journal*, *58*(1). https://doi.org/10.3325/cmj.2017.58.40

78. Kawasaki, T., & Kawai, T. (2014). Toll-like receptor signaling pathways. *Frontiers in Immunology* (Vol. 5, Issue SEP). https://doi.org/10.3389/fimmu.2014.00461

79. Darlene A. Monlish, Sima T. Bhatt and Laura G. Schuettpelz (2016). The role of Toll-like receptors in hematopoietic malignancies. *Frontiers in Immunology*. doi: 10.3389/ mmu.2016.00390

80. Browne, E. P., & Littman, D. R. (2009). Myd88 is required for an antibody response to retroviral infection. *PLoS Pathogens*, *5*(2). https://doi.org/10.1371/journal.ppat.1000298

81. Ehlers, M., Fukuyama, H., McGaha, T. L., Aderem, A., & Ravetch, J. V. (2006). TLR9/MyD88 signaling is required for class switching to pathogenic IgG2a and 2b autoantibodies in SLE. *Journal of Experimental Medicine*, *203*(3). https://doi.org/10.1084/jem.20052438

82. Christensen, S. R., Shupe, J., Nickerson, K., Kashgarian, M., Flavell, R. A. A., & Shlomchik, M. J. (2006). Toll-like Receptor 7 and TLR9 Dictate Autoantibody Specificity and Have Opposing Inflammatory and Regulatory Roles in a Murine Model of Lupus. *Immunity*, *25*(3). https://doi.org/10.1016/j.immuni.2006.07.013

83. Tilstra, J. S., John, S., Gordon, R. A., Leibler, C., Kashgarian, M., Bastacky, S., Nickerson, K. M., & Shlomchik, M. J. (2020). B cell-intrinsic TLR9 expression is protective in murine lupus. *Journal of Clinical Investigation*, *130*(6). https://doi.org/10.1172/JCI132328

84. Ngo, V. N., Young, R. M., Schmitz, R., Jhavar, S., Xiao, W., Lim, K. H., Kohlhammer, H., Xu, W., Yang, Y., Zhao, H., Shaffer, A. L., Romesser, P., Wright, G., Powell, J., Rosenwald, A., Muller-Hermelink, H. K., Ott, G., Gascoyne, R. D., Connors, J. M., … Staudt, L. M. (2011). Oncogenically active

MYD88 mutations in human lymphoma. *Nature*, *470*(7332). https://doi.org/10.1038/nature09671

85. Munshi, M., Liu, X., Chen, J. G., Xu, L., Tsakmaklis, N., Demos, M. G., Kofides, A., Guerrera, M. L., Jimenez, C., Chan, G. G., Hunter, Z. R., Palomba, M. L., Argyropoulos, K. V., Meid, K., Keezer, A., Gustine, J., Dubeau, T., Castillo, J. J., Patterson, C. J., … Yang, G. (2020). SYK is activated by mutated MYD88 and drives pro-survival signaling in MYD88 driven B-cell lymphomas. *Blood Cancer Journal*, *10*(1). https://doi.org/10.1038/s41408-020-0277-6

86. Kim, S. J. (2015). Immunological function of Blimp-1 in dendritic cells and relevance to autoimmune diseases. *Immunologic Research* (Vol. 63, Issues 1–3). https://doi.org/10.1007/s12026-015-8694-5

87. Shapiro-Shelef, M., Lin, K. I., McHeyzer-Williams, L. J., Liao, J., McHeyzer-Williams, M. G., & Calame, K. (2003). Blimp-1 is required for the formation of immunoglobulin secreting plasma cells and pre-plasma memory B cells. *Immunity*, *19*(4). https://doi.org/10.1016/S1074-7613(03)00267-X

88. Shaffer, A. L., Lin, K. I., Kuo, T. C., Yu, X., Hurt, E. M., Rosenwald, A., Giltnane, J. M., Yang, L., Zhao, H., Calame, K., & Staudt, L. M. (2002). Blimp-1 orchestrates plasma cell differentiation by extinguishing the mature B cell gene expression program. *Immunity*, *17*(1). https://doi.org/10.1016/S1074-7613(02)00335-7ù

89. Pasare, C., & Medzhitov, R. (2005). Control of B-cell responses by Toll-like receptors. *Nature*, *438*(7066). https://doi.org/10.1038/nature04267

90. Johnson, K., Shapiro-Shelef, M., Tunyaplin, C., & Calame, K. (2005). Regulatory events in early and late B-cell differentiation. *Molecular Immunology*, *42*(7). https://doi.org/10.1016/j.molimm.2004.06.039ù

91. Diehl, S. A., Schmidlin, H., Nagasawa, M., van Haren, S. D., Kwakkenbos, M. J., Yasuda, E., Beaumont, T., Scheeren, F. A., & Spits, H. (2008). STAT3-Mediated Up-Regulation of BLIMP1 Is Coordinated with BCL6 Down-Regulation to Control Human Plasma Cell Differentiation. *The Journal of Immunology*, *180*(7). https://doi.org/10.4049/jimmunol.180.7.4805

92. Mandelbaum, J., Bhagat, G., Tang, H., Mo, T., Brahmachary, M., Shen, Q., Chadburn, A., Rajewsky, K., Tarakhovsky, A., Pasqualucci, L., & Dalla-Favera, R. (2010). BLIMP1 Is a Tumor Suppressor Gene Frequently Disrupted in Activated B Cell-like Diffuse Large B Cell Lymphoma. *Cancer Cell*, *18*(6). https://doi.org/10.1016/j.ccr.2010.10.030

93. Xia, Y., Xu-Monette, Z. Y., Tzankov, A., Li, X., Manyam, G. C., Murty, V., Bhagat, G., Zhang, S., Pasqualucci, L., Visco, C., Dybkaer, K., Chiu, A., Orazi, A., Zu, Y., Richards, K. L., Hsi, E. D., Choi, W. W. L., Van Krieken, J. H., Huh, J., … Young, K. H. (2017). Loss of PRDM1/BLIMP-1 function contributes to poor prognosis of activated B-cell-like diffuse large B-cell lymphoma. *Leukemia*, *31*(3). https://doi.org/10.1038/leu.2016.243

94. Garcia, J. F., Roncador, G., García, J. F., Sáez, A. I., Maestre, L., Lucas, E., Montes-Moreno, S., Victoria, R. F., Martínez-Torrecuadrada, J. L., Marafioti, T., Mason, D. Y., & Piris, M. A. (2006). PRDM1/BLIMP-1 expression in multiple B and T-cell lymphoma. *Haematologica*, *91*(4).

95. Liu, Y. Y., Leboeuf, C., Shi, J. Y., Li, J. M., Wang, L., Shen, Y., Garcia, J. F., Shen, Z. X., Chen, Z., Janin, A., Chen, S. J., & Zhao, W. L. (2007). Rituximab plus CHOP (R-CHOP) overcomes PRDM1-associated resistance to chemotherapy in patients with diffuse large B-cell lymphoma. *Blood*, *110*(1). https://doi.org/10.1182/blood-2006-09-049189

96. Wang, K. X., & Denhardt, D. T. (2008). Osteopontin: Role in immune regulation and stress responses. *Cytokine and Growth Factor Reviews* (Vol. 19, Issues 5–6). https://doi.org/10.1016/j.cytogfr.2008.08.001

97. Lamort, A. S., Giopanou, I., Psallidas, I., & Stathopoulos, G. T. (2019). Osteopontin as a Link between Inflammation and Cancer: The Thorax in the Spotlight. *Cells* (Vol. 8, Issue 8). https://doi.org/10.3390/cells8080815

98. Yokosaki, Y., Tanaka, K., Higashikawa, F., Yamashita, K., & Eboshida, A. (2005). Distinct structural requirements for binding of the integrins alphavbeta6, alphavbeta3, alphavbeta5, alpha5beta1 and alpha9beta1 to osteopontin. *Matrix*

Biology : Journal of the International Society for Matrix Biology, *24*(6). https://doi.org/10.1016/j.matbio.2005.05.005

99. Zohar, R., Lee, W., Arora, P., Cheifetz, S., McCulloch, C., & Sodek, J. (1997). Single cell analysis of intracellular osteopontin in osteogenic cultures of fetal rat calvarial cells. *Journal of Cellular Physiology*, *170*(1). https://doi.org/10.1002/(SICI)1097-4652(199701)170:1<88::AIDJCP10>3.0.CO;2-K

100. Shinohara, M. L., Kim, H. J., Kim, J. H., Garcia, V. A., & Cantor, H. (2008). Alternative translation of osteopontin generates intracellular and secreted isoforms that mediate distinct biological activities in dendritic cells. *Proceedings of the National Academy of Sciences of the United States of America*, *105*(20). https://doi.org/10.1073/pnas.0802301105

101. Fan, X., He, C., Jing, W., Zhou, X., Chen, R., Cao, L., Zhu, M., Jia, R., Wang, H., Guo, Y., & Zhao, J. (2015). Intracellular osteopontin inhibits toll-like receptor signaling and impedes liver carcinogenesis. *Cancer Research*. https://doi.org/10.1158/0008-5472.CAN-14-0615

102. Leavenworth, J. W., Verbinnen, B., Yin, J., Huang, H., & Cantor, H. (2015). A p85α-osteopontin axis couples the receptor ICOS to sustained Bcl-6 expression by follicular helper and regulatory T cells. *Nature Immunology*, *16*(1). https://doi.org/10.1038/ni.3050

103. Inoue, M., & Shinohara, M. L. (2011). Intracellular osteopontin (iOPN) and immunity. *Immunologic Research* (Vol. 49, Issues 1–3). https://doi.org/10.1007/s12026-010-8179-5

104. Rice, J., Courter, D. L., Giachelli, C. M., & Scatena, M. (2006). Molecular mediators of αvβ3-induced endothelial cell survival. *Journal of Vascular Research*, *43*(5). https://doi.org/10.1159/000094884

105. Zhao, W., Wang, L., Zhang, M., Wang, P., Zhang, L., Yuan, C., Qi, J., Qiao, Y., Kuo, P. C., & Gao, C. (2011). NF-κB– and AP-1–Mediated DNA Looping Regulates Osteopontin Transcription in Endotoxin-Stimulated Murine

Macrophages. *The Journal of Immunology*, *186*(5). https://doi.org/10.4049/jimmunol.1003626

106. Lin, Y. H., & Yang-Yen, H. F. (2001). The Osteopontin-CD44 Survival Signal Involves Activation of the Phosphatidylinositol 3-Kinase/Akt Signaling Pathway. *Journal of Biological Chemistry*, *276*(49). https://doi.org/10.1074/jbc.M105132200

107. Mohammadi, S., Ghaffari, S. H., Shaiegan, M., Zarif, M. N., Nikbakht, M., Akbari Birgani, S., Alimoghadam, K., & Ghavamzadeh, A. (2016). Acquired expression of osteopontin selectively promotes enrichment of leukemia stem cells through AKT/mTOR/PTEN/β-catenin pathways in AML cells. *Life Sciences*, *152*. https://doi.org/10.1016/j.lfs.2016.04.003

108. Mari L. Shinohara, Linrong Lu, Jing Bu, Miriam B. F. Werneck, Koichi S.Kobayashi, Laurie H. Glimcher, and Harvey Cantor (2006). Osteopontin expression is essential for interferon-α productionby plasmacytoid dendritic cells. Nat Immunology; 7(5): 498–506. doi:10.1038/ni1327

109. Zhao, K., Zhang, M., Zhang, L., Wang, P., Song, G., Liu, B., Wu, H., Yin, Z., & Gao, C. (2016). Intracellular osteopontin stabilizes TRAF3 to positively regulate innate antiviral response. *Scientific Reports*, *6*. https://doi.org/10.1038/srep23771

110. Shevde, L. A., & Samant, R. S. (2014). Role of osteopontin in the pathophysiology of cancer. *Matrix Biology* (Vol. 37). https://doi.org/10.1016/j.matbio.2014.03.001

111. Ramchandani, D., & Weber, G. F. (2013). An osteopontin promoter polymorphism is associated with aggressiveness in breast cancer. *Oncology Reports*, *30*(4). https://doi.org/10.3892/or.2013.2632

112. Ashkar, S., Weber, G. F., Panoutsakopoulou, V., Sanchirico, M. E., Jansson, M., Zawaideh, S., Rittling, S. R., Denhardt, D. T., Glimcher, M. J., & Cantor, H. (2000). Eta-1 (osteopontin): An early component of type-1 (cell-mediated) immunity. *Science*, *287*(5454). https://doi.org/10.1126/science.287.5454.860

113. Nagai, S., Hashimoto, S. I., Yamashita, T., Toyoda, N., Satoh, T., Suzuki, T., & Matsushima, K. (2001). Comprehensive gene expression profile of human

activated Th1- and Th2-polarized cells. *International Immunology*, *13*(3). https://doi.org/10.1093/intimm/13.3.367

114. Shinohara, M. L., Jansson, M., Hwang, E. S., Werneck, M. B. F., Glimcher, L. H., & Cantor, H. (2005). T-bet-dependent expression of osteopontin contributes to T cell polarization. *Proceedings of the National Academy of Sciences of the United States of America*, *102*(47). https://doi.org/10.1073/pnas.0508666102

115. Lampe, M. A., Patarca, R., Iregui, M. V., & Cantor, H. (1991). Polyclonal B cell activation by the Eta-1 cytokine and the development of systemic autoimmune disease. *The Journal of Immunology*, *147*(9), 2902–2906

116. Frenzel, D. F., Borkner, L., Scheurmann, J., Singh, K., Scharffetter-Kochanek, K., & Weiss, J. M. (2015). Osteopontin deficiency affects imiquimod-induced psoriasis-like murine skin inflammation and lymphocyte distribution in skin, draining lymph nodes and spleen. *Experimental Dermatology* (Vol. 24, Issue 4, pp. 305–307). Blackwell Publishing Ltd. https://doi.org/10.1111/exd.12649

117. Guo, B., Tumang, J. R., & Rothstein, T. L. (2009). B cell receptor crosstalk: B cells express osteopontin through the combined action of the alternate and classical BCR signaling pathways. *Molecular Immunology*, *46*(4). https://doi.org/10.1016/j.molimm.2008.07.029

118. Nilsson, S. K., Johnston, H. M., Whitty, G. A., Williams, B., Webb, R. J., Denhardt, D. T., Bertoncello, I., Bendall, L. J., Simmons, P. J., & Haylock, D. N. (2005). Osteopontin, a key component of the hematopoietic stem cell niche and regulator of primitive hematopoietic progenitor cells. *Blood*, *106*(4). https://doi.org/10.1182/blood-2004-11-4422

119. Kanayama, M., Xu, S., Danzaki, K., Gibson, J. R., Inoue, M., Gregory, S. G., & Shinohara, M. L. (2017). Skewing of the population balance of lymphoid and myeloid cells by secreted and intracellular osteopontin. *Nature Immunology*, *18*(9). https://doi.org/10.1038/ni.3791

120. Clemente, N., Raineri, D., Cappellano, G., Boggio, E., Favero, F., Soluri, M. F., Dianzani, C., Comi, C., Dianzani, U., & Chiocchetti, A. (2016). Osteopontin

Bridging Innate and Adaptive Immunity in Autoimmune Diseases. *Journal of Immunology Research*. https://doi.org/10.1155/2016/7675437

121. Wong, C. K., Lit, L. C. W., Tam, L. S., Li, E. K., & Lam, C. W. K. (2005). Elevation of plasma osteopontin concentration is correlated with disease activity in patients with systemic lupus erythematosus. *Rheumatology*. https://doi.org/10.1093/rheumatology/keh558

122. Rullo, O. J., Woo, J. M. P., Parsa, M. F., Hoftman, A. D. C., Maranian, P., Elashoff, D. A., Niewold, T. B., Grossman, J. M., Hahn, B. H., McMahon, M., McCurdy, D. K., & Tsao, B. P. (2013). Plasma levels of osteopontin identify patients at risk for organ damage in systemic lupus erythematosus. *Arthritis Research and Therapy*, *15*(1). https://doi.org/10.1186/ar4150

123. D'Alfonso, S., Barizzone, N., Giordano, M., Chiocchetti, A., Magnani, C., Castelli, L., Indelicato, M., Giacopelli, F., Marchini, M., Scorza, R., Danieli, M. G., Cappelli, M., Migliaresi, S., Bigliardo, B., Sabbadini, M. G., Baldissera, E., Galeazzi, M., Sebastiani, G. D., Minisola, G., … Momigliano-Richiardi, P. (2005). Two single-nucleotide polymorphisms in the 5′ and 3′ ends of the osteopontin gene contribute to susceptibility to systemic lupus erythematosus. *Arthritis and Rheumatism*, *52*(2). https://doi.org/10.1002/art.20808

124. Trivedi, T., Franek, B. S., Green, S. L., Kariuki, S. N., Kumabe, M., Mikolaitis, R. A., Jolly, M., Utset, T. O., & Niewold, T. B. (2011). Osteopontin alleles are associated with clinical characteristics in systemic lupus erythematosus. *Journal of Biomedicine and Biotechnology*, *2011*. https://doi.org/10.1155/2011/802581

125. Kitamura, M., Iwabuchi, K., Kitaichi, N., Kon, S., Kitamei, H., Namba, K., Yoshida, K., Denhardt, D. T., Rittling, S. R., Ohno, S., Uede, T., & Onoé, K. (2007). Osteopontin Aggravates Experimental Autoimmune Uveoretinitis in Mice. *The Journal of Immunology*, *178*(10). https://doi.org/10.4049/jimmunol.178.10.6567

126. Miyazaki, T., Ono, M., Qu, W. M., Zhang, M. C., Mori, S., Nakatsuru, S., Nakamura, Y., Sawasaki, T., Endo, Y., & Nose, M. (2005). Implication of allelic polymorphism of osteopontin in the development of lupus nephritis in MRL/lpr

mice. *European Journal of Immunology*, *35*(5). https://doi.org/10.1002/eji.200425672

127. Chiocchetti, A., Indelicato, M., Bensi, T., Mesturini, R., Giordano, M., Sametti, S., Castelli, L., Bottarel, F., Mazzarino, M. C., Garbarini, L., Giacopelli, F., Valesini, G., Santoro, C., Dianzani, I., Ramenghi, U., & Dianzani, U. (2004). High levels of osteopontin associated with polymorphisms in its gene are a risk factor for development of autoimmunity/lymphoproliferation. *Blood*, *103*(4). https://doi.org/10.1182/blood-2003-05-1748

128. Weber, G. F., & Cantor, H. (2001). Differential roles of osteopontin/Eta-1 in early and late lpr disease. *Clinical and Experimental Immunology*, *126*(3). https://doi.org/10.1046/j.1365-2249.2001.01702

129. Ceccarelli, F., D'Alfonso, S., Perricone, C., Carlomagno, Y., Alessandri, C., Croia, C., Valesini, G. (2012). The role of eight polymorphisms in three candidate genes in determining the susceptibility, phenotype, and response to anti-TNF therapy in patients with rheumatoid arthritis. *Clinical and Experimental Rheumatology*, 30(6), 939–942. http://www.embase.com/search/results?subaction=viewrecord&from=export&id=L368170171

130. Yamamoto, N., Sakai, F., Kon, S., Morimoto, J., Kimura, C., Yamazaki, H., Okazaki, I., Seki, N., Fujii, T., & Uede, T. (2003). Essential role of the cryptic epitope SLAYGLR within osteopontin in a murine model of rheumatoid arthritis. *Journal of Clinical Investigation*, 112(2), 181–188. https://doi.org/10.1172/JCI17778

131. Zhao, H., Chen, Q., Alam, A., Cui, J., Suen, K. C., Soo, A. P., Eguchi, S., Gu, J., & Ma, D. (2018). The role of osteopontin in the progression of solid organ tumour. *Cell Death and Disease* (Vol. 9, Issue 3). https://doi.org/10.1038/s41419-018-0391-6

132. Sangaletti, S., Tripodo, C., Sandri, S., Torselli, I., Vitali, C., Ratti, C., Botti, L., Burocchi, A., Porcasi, R., Tomirotti, A., Colombo, M. P., & Chiodoni, C. (2014).

Osteopontin shapes immunosuppression in the metastatic niche. *Cancer Research*, *74*(17). https://doi.org/10.1158/0008-5472.CAN-13-3334

133. Wei, R., Wong, J. P. C., & Kwok, H. F. (2017). Osteopontin - A promising biomarker for cancer therapy. *Journal of Cancer* (Vol. 8, Issue 12). https://doi.org/10.7150/jca.20480

134. Hao, C., Cui, Y., Owen, S., Li, W., Cheng, S., & Jiang, W. G. (2017). Human osteopontin: Potential clinical applications in cancer (Review). *International Journal of Molecular Medicine* (Vol. 39, Issue 6). https://doi.org/10.3892/ijmm.2017.2964

135. Castello, L. M., Raineri, D., Salmi, L., Clemente, N., Vaschetto, R., Quaglia, M., Garzaro, M., Gentilli, S., Navalesi, P., Cantaluppi, V., Dianzani, U., Aspesi, A., & Chiocchetti, A. (2017). Osteopontin at the Crossroads of Inflammation and Tumor Progression. *Mediators of Inflammation*. https://doi.org/10.1155/2017/4049098

136. Yushi, Q., Li, Z., Von Roemeling, C. A., Doeppler, H., Marlow, L. A., Kim, B. Y. S., Radisky, D. C., Storz, P., Copland, J. A., & Tun, H. W. (2016). Osteopontin is a multi-faceted pro-tumorigenic driver for central nervous system lymphoma. *Oncotarget*, *7*(22), 32156–32171. https://doi.org/10.18632/oncotarget.853710

137. Liersch, R., Gerss, J., Schliemann, C., Bayer, M., Schwöppe, C., Biermann, C., Appelmann, I., Kessler, T., Löwenberg, B., Büchner, T., Hiddemann, W., Müller-Tidow, C., Berdel, W. E., & Mesters, R. (2012). Osteopontin is a prognostic factor for survival of acute myeloid leukemia patients. *Blood*, *119*(22), 5215–5220. https://doi.org/10.1182/blood-2011-11-389692

138. Boyerinas, B., Zafrir, M., Yesilkanal, A. E., Price, T. T., Hyjek, E. M., & Sipkins, D. A. (2013). Adhesion to osteopontin in the bone marrow niche regulates lymphoblastic leukemia cell dormancy. *Blood*, *121*(24). https://doi.org/10.1182/blood-2012-12-475483

139. Morse HC III, Anver MR, Fredrickson TN, Haines DC, Harris AW, Harris NL, et al. Bethesda proposals for classification of lymphoid neoplasms in mice. *Blood* 2002;100:246–58.

140. Martina, M. N., Noel, S., Saxena, A., Rabb, H., Hamad, A. R. A. Double negative (DN) αβ T cells: misperception and overdue recognition. *Immunol Cell Biol*. 2015 Mar;93(3):305-10. doi: 1038/icb.2014.99.

141. Liu, Z., Meng, J., Li, X., Zhu, F., Liu, T., Wu, G., Zhang, L. Identification of Hub Genes and Key Pathways Associated with Two Subtypes of Diffuse Large B-Cell Lymphoma Based on Gene Expression Profiling via Integrated Bioinformatics. *BioMed Research International* Volume 2018, https://doi.org/10.1155/2018/3574534

142. Hardy RR, Hayakawa K. B cell development pathways. *Annu Rev Immunol* 2001;19:595–621.

143. Varano, G., Raffel, S., Sormani, M., Zanardi, F., Lonardi, S., Zasada, C., Perucho, L., Petrocelli, V., Haake, A., Lee, A. K., Bugatti, M., Paul, U., Van Anken E., Pasqualucci, L., Rabadan, R., Siebert, R., Kempa, S., Ponzoni, M., Facchetti, F., Rajewsky K. & Casola S. The B-cell receptor controls fitness of MYC-driven lymphoma cells via GSK3β inhibition. *Nature*, 2017. doi:10.1038/nature22353

144. Menter T. and Tzankov A. Lymphomas and Their Microenvironment: A Multifaceted Relationship. *Pathobiology*, 2019. DOI: 10.1159/000502912

145. Smulski C. R. and Eibel H. BAFF and BAFF-Receptor in B cell selection and survival. *Frontiers in Immunology*, 2018. https://doi.org/10.3389/fimmu.2018.02285

146. Yang, H., Ye, X., Zhang, X., Li, X., Fu, Q., & Tang, Z. (2018). Intracellular osteopontin negatively regulates toll-like receptor 4-mediated inflammatory response via regulating GSK3β and 4EBP1 phosphorylation. *Cytokine*, *108*. https://doi.org/10.1016/j.cyto.2018.03.013